JPET Fast Forward. Published on February 9, 2015 as DOI: 10.1124/jpet.114.222463
This article has not been copyedited and formatted. The final version may differ from this version.

Title page

Pharmacology of basimglurant (RO4917523, RG7090), a unique mGlu5 negative allosteric modulator in clinical development for depression

Lothar Lindemann*, Richard H. Porter, Sebastian H. Scharf, Basil Kuennecke, Andreas Bruns, Markus von Kienlin, Anthony C. Harrison, Axel Paehler, Christoph Funk, Andreas Gloge, Manfred Schneider, Neil J. Parrott, Liudmila Polonchuk, Urs Niederhauser, Stephen R. Morairty, Thomas S. Kilduff, Eric Vieira, Sabine Kolczewski, Juergen Wichmann, Thomas Hartung, Michael Honer, Edilio Borroni, Jean-Luc Moreau, Eric Prinssen, Will Spooren, Joseph G. Wettstein, Georg Jaeschke

Roche Pharmaceutical Research and Early Development, Discovery Neuroscience, Neuroscience, Ophthalmology, and Rare Diseases (NORD) (L.L., S.H.S., B.K., A.B., M.v.K., M.H., E.B., E.P., W.S., J.G.W.), Discovery Chemistry (E.V., S.K., J.W., G.J.), Operations for Neuroscience, Ophthalmology, and Rare Diseases (R.H.P., J.-L.M.), Pharmaceutical Sciences (A.H., A.P., C.F., A.G., M.S., N.P., L.P., U.N.), Small Molecules Process Research and Synthesis (T.H.), Roche Innovation Center Basel, Grenzacherstrasse 124, CH-4070 Basel, Switzerland

Center for Neuroscience, Biosciences Division, SRI International, Menlo Park, California 94025, USA (S.R.M., T.S.K.)

JPET Fast Forward. Published on February 9, 2015 as DOI: 10.1124/jpet.114.222463
This article has not been copyedited and formatted. The final version may differ from this version.

Running title page

Basimglurant – mGlu5 NAM in development for depression

Author for correspondence:

Lothar Lindemann, PhD

Roche Pharmaceutical Research and Early Development

Neuroscience, Ophthalmology & Rare Diseases (NORD)

Discovery Neuroscience

Roche Innovation Center Basel

Grenzacherstrasse 124

4070 Basel

Switzerland

phone: +41 61 6889863

fax: +41 61 6880832

e-mail: lothar.lindemann@roche.com

Number of text pages: 58

Number of tables: 3 (+ 2 in Supplemental Materials)

Number of figures: 10 (+ 2 in Supplemental Materials)

Number of references: 115

Number of words in: **Abstract:** 249

Introduction: 735

Discussion: 1845

Section assignment: Drug Discovery and Translational Medicine

JPET Fast Forward. Published on February 9, 2015 as DOI: 10.1124/jpet.114.222463
This article has not been copyedited and formatted. The final version may differ from this version.

List of Abbreviations

5-HT: 5-hydroxytryptamine (serotonin)

aCSF: Artificial cerebrospinal fluid

ABP688: (3-(6-methyl-pyridin-2-ylethynyl)-cyclohex-2-enone-O-(11)C-methyl-oxime)

AP: Anterio-posterior

ANCOVA: Analysis of covariance

ANOVA: Analysis of variance

B_{max}: Maximum binding potential

Basimglurant: 2-Chloro-4-[1-(4-fluoro-phenyl)-2,5-dimethyl-1H-imidazol-4-ylethynyl]-pyridine

BDNF: Brain-Derived Neurotrophic Factor

Breaths per minute: Bpm

CA: Cornu ammonis

CASL: Continuous arterial spin labeling

cDNA: Complementary DNA

CER: Conditioned emotional response

C_{max}: Maximum plasma concentration

CMS: Chronic mild stress

CTEP: 2-Chloro-4-((2,5-dimethyl-1-(4-(trifluoromethoxy)phenyl)-1H-imidazol-4-yl)ethynyl)pyridine

DA: Dopamine

DAT: Dopamine transporter

DMSO: Dimethylsulfoxid

E-4031: N-[4-[1-[2-(6-Methylpyridin-2-yl)ethyl]piperidine-4-carbonyl]phenyl]

ECT: Electroconvulsive treatment

EDTA: Ethylenediaminetetraacetic acid

EEG: Electroencephalography

EMG: Electromyography

FDR: False discovery rate

Fenobam: N-(3-chlorophenyl)-N'-(4,5-dihydro-1-methyl-4-oxo-1H-imidazole-2-yl)urea

Fluo-4AM: (2S)-2-Amino-4-phosphonobutanoic acid

JPET Fast Forward. Published on February 9, 2015 as DOI: 10.1124/jpet.114.222463
This article has not been copyedited and formatted. The final version may differ from this version.

fMRI: Functional magnetic resonance imaging

FPS: Fear-potentiated startle

FST: Forced swim test

FXS: Fragile X Syndrome

GABA: γ-Aminobutyric acid

GERD: Gastro esophageal reflux disease

GRN-529: 4-difluoromethoxy-3-(pyridine-2-ylethynyl)phenyl)5H-pyrrolo[3,4-b]pyridine-6(7H)-yl methanone

HBSS: Hanks' balanced salt solution

hERG: Human Ether-a-go-go Related Gene

HEPES: 4-(2-hydroxyethyl)-1-piperazineethanesulfonic acid

HPA-axis: Hypothalamic–pituitary–adrenal axis

HPLC: High-performance liquid chromatography

IBC: Isovolume bladder contraction

ICSS: Intracranial self-stimulation

IC_{50}: Half maximal inhibitory concentration

Indatraline: (1R,3S)-3-(3,4-dichlorophenyl)-N-methyl-2,3-dihydro-1H-inden-1-amine

IP: Inositol phosphate

i.p.: Intraperitoneal

K_d: Dissociation constant

K_i: Inhibition constant

K_{on}: Association rate constant

K_{off}: Dissociation rate constant

L-AP4: (2S)-2-Amino-4-phosphonobutanoic acid

LC-MS/MS: Liquid chromatography–mass spectrometry/ mass spectrometry

L-DOPA: L-3,4-Dihydroxyphenylalanin

LMA: Locomotor activity

M1: Primary motor cortex

Mavoglurant (AFQ056): Methyl (3a*R*,4*S*,7a*R*)-4-hydroxy-4-[(3-methylphenyl)ethynyl]octahydro-1*H*-indole-1-carboxylate

MDD. Major depressive disorder

JPET Fast Forward. Published on February 9, 2015 as DOI: 10.1124/jpet.114.222463
This article has not been copyedited and formatted. The final version may differ from this version.

mGlu: Metabotropic glutamate receptor

MPEP: 2-Methyl-6-(phenylethynyl)pyridine

mPFC: Medial prefrontal cortex

MTEP: 3-((2-Methyl-4-thiazolyl)ethynyl)pyridine

NE: Norepinephrine

NAM: Negative allosteric modulator

NADPH: Nicotinamide adenine dinucleotide phosphate

NET: Norepinephrine transporter

NMDA: N-methyl-D-aspartate

NMP: N-methyl-pyrollidone

Nutrient broth: NB

PBS: Phosphate buffered saline

PD-LID: L-DOPA induced dyskineasia in Parkinson's disease

PET: Positron emission tomography

PK: Pharmacokinetic

PMC: Pattern match coefficient

p.o.: Per os

REM: Rapid eye movement

RG7090: RO4917523, basimglurant

RMS: Root mean square

ROI: Region of interest

RO4623831: 2-Chloro-4-[1-(4-fluoro-phenyl)-2-methyl-1H-imidazol-4-ylethynyl]-pyridine

S1: Primary somatosensory cortex

S2: Secondary somatosensory cortex

s.c.: Subcutaneous

SERT: Serotonin transporter

SIH: Stress-induced hyperthermia

SR: Suppression ratio

SSRI: Selective serotonin reuptake inhibitor

$T_{1/2}$: Half life

JPET Fast Forward. Published on February 9, 2015 as DOI: 10.1124/jpet.114.222463
This article has not been copyedited and formatted. The final version may differ from this version.

T_{max}: Time after administration to peak plasma concentration

V: Ventral

VIMR: Volume-Induced-Micturition-Reflex

V_{ss}: Volume of distribution

ZT: Zeitgeber time

JPET Fast Forward. Published on February 9, 2015 as DOI: 10.1124/jpet.114.222463
This article has not been copyedited and formatted. The final version may differ from this version.

Abstract

Major depressive disorder (MDD) is a serious public health burden and a leading cause of disability. Its pharmacotherapy is currently limited to modulators of monoamine neurotransmitters and second generation antipsychotics. Recently, glutamatergic approaches for the treatment of MDD have increasingly received attention, and preclinical research suggests that metabotropic glutamate receptor 5 (mGlu5) inhibitors have antidepressant-like properties. 2-Chloro-4-[1-(4-fluoro-phenyl)-2,5-dimethyl-1H-imidazol-4-ylethynyl]-pyridine (basimglurant) is a novel mGlu5 negative allosteric modulator currently in Phase 2 clinical development for MDD and Fragile X syndrome (FXS). Here, the comprehensive preclinical pharmacological profile of basimglurant is presented with a focus on its therapeutic potential for MDD and drug-like properties. Basimglurant is a potent, selective, and safe mGlu5 inhibitor with good oral bioavailability and long half-life supportive of once-daily administration, good brain penetration, and high *in vivo* potency. It has antidepressant properties which are corroborated by its functional magnetic imaging (fMRI) profile, as well as anxiolytic-like and antinociceptive features. In electroencephalography (EEG) recordings, basimglurant shows wake-promoting effects followed by increased delta power during subsequent non-rapid eye movement (REM) sleep. In microdialysis studies, basimglurant had no effect on monoamine transmitter levels in the frontal cortex and nucleus accumbens except for a moderate increase of accumbal dopamine which is in line with its lack of pharmacological activity on monoamine reuptake transporters. Taken together basimglurant has favorable drug-like properties, a differentiated molecular mechanism of action, and antidepressant-like features which suggest the possibility of also addressing important comorbidities of MDD including anxiety and pain as well as daytime sleepiness and apathy or lethargy.

JPET Fast Forward. Published on February 9, 2015 as DOI: 10.1124/jpet.114.222463
This article has not been copyedited and formatted. The final version may differ from this version.

Introduction

It has been 23 years since the cDNA encoding the first Group 1 metabotropic glutamate receptor (mGlu) was cloned (Houamed et al., 1991; Masu et al., 1991). Thereafter, Gasparini et al. (Gasparini et al., 1999) published 2-Methyl-6-(phenylethynyl)pyridine (MPEP) which would become a key reference compound in the mGlu5 field, followed soon by more structurally different compounds (Jaeschke et al., 2008). Following that were the initial clinical trials with mGlu5 antagonists.

The latest clinical trial results with mGlu5 inhibitors, however, have been mixed. The development of Methyl (3a*R*,4*S*,7a*R*)-4-hydroxy-4-[(3-methylphenyl)ethynyl]octahydro-1*H*-indole-1-carboxylate (mavoglurant) (Vranesic et al., 2014) for the treatment of L-3,4-Dihydroxyphenylalanin (L-DOPA) induced dyskinesia (PD-LID) (Stocchi et al., 2013) has been discontinued in view of its reported insufficient efficacy (Petrov et al., 2014). More recently, also the clinical development of mavoglurant and basimglurant for FXS have been ended as both drugs did not improve the clinical phenotype of patients (FRAXA mavoglurant posting, FRAXA basimglurant posting), an unexpected result in view a strong hypothesis (Krueger and Bear, 2011; Michalon et al., 2012; Scharf et al., 2015). One therapeutic area that has not been explored at length in patients is depression. This is somewhat surprising in light of the preclinical data supporting the notion that mGlu5 antagonists may correct behaviors associated with depression (see below) and that modulation of mGlu5 receptors may promote synaptic growth and plasticity (Kubera et al., 2012; Piers et al., 2012).

Truly novel therapies for major depressive disorder have been difficult to identify. Most of the commonly used antidepressant drugs are biogenic amine inhibitors, some rather specific (e.g., citalopram) and others having multiple actions (e.g., venlafaxine). For some time now, there has been interest in developing therapies for depression based on modulation of glutamatergic tone (Covington et al., 2010; Duman, 2014). In particular, a study published by Zarate et al (Zarate et al., 2006) showed that subanesthetic doses of ketamine, an inhibitor of N-methyl-D-aspartate (NMDA) type ion channels, has a rapid onset of action as measured by decreased scores on the Hamilton Depression Rating Scale in depressed patients deemed treatment-resistant. Ketamine's use is however limited to an experimental treatment in controlled clinical settings in view of its route of administration and safety issues including the potential for drug dependence and the risk of neurotoxicity (Krystal et al., 2013). Approaching glutamatergic tone from another direction,

JPET Fast Forward. Published on February 9, 2015 as DOI: 10.1124/jpet.114.222463
This article has not been copyedited and formatted. The final version may differ from this version.

mainly mGlu5, may skirt the abuse liability issue seen with ketamine and closely related compounds. For example, the prototypical mGlu5 antagonists MPEP and 3-((2-Methyl-4-thiazolyl)ethynyl)pyridine (MTEP) do not have reinforcing properties in rats (Swedberg et al., 2014) and can attenuate cocaine self-administration in monkeys (Platt et al., 2008), respectively. More to the point, mGlu5 antagonists correct behaviors associated with depression (see below).

On the cellular level, mGlu5 is found on neurons mainly in the postsynaptic density (Lujan et al., 1997; Kuwajima et al., 2004), as well as on glial cells (Aronica et al., 2003). In brain, mGlu5 is expressed in multiple brain areas associated with processing of motivation and emotion including the frontal cortex, striatum, hippocampal formation, nucleus accumbens, and amygdala (Shigemoto and Mizuno, 2000). Thus, it was not surprising to see that mGlu5 inhibitors have behavioral effects in rodents in procedures that are used to identify potential antidepressant and related anti-anxiety drugs. For example, MPEP corrected escape behavior in a learned helplessness procedure while increasing levels of brain-derived neurotropic factor (BDNF) in the hippocampus (Liu et al., 2012); BDNF has long been linked with affective behavior and depression (Nestler et al., 2002; Monteggia, 2011). MPEP and MTEP also decreased immobility in a mouse forced swim test (FST), and the effect of MPEP in the FST was not observed in mGlu5 knock-out mice confirming that the antidepressant-like effect was indeed mediated by mGlu5 receptors (Li et al., 2006). Also, MPEP reversed a learning deficit in olfactory bulbectomized rats (Pilc et al., 2002). For anxiety, fenobam had effects similar to diazepam in Geller-Seifter, Vogel conflict, stress-induced hyperthermia and conditioned emotional response procedures in rodents (Porter et al., 2005). Fenobam also had a modest anxiolytic effect in a Phase II clinical trial (Pecknold et al., 1982).

Herein, we report on a new mGlu5 antagonist with excellent drug-like properties. The compound, basimglurant (RG7090, RO4917523), has undergone extensive pharmacological and safety-related profiling studies and is now in clinical development for depression (NCT00809562, NCT01437657). The results of the recently completed clinical studies will be reported in detail elsewhere. In brief, basimglurant was studied in a 9-week study double-blind placebo-controlled study (6-week double-blind treatment, 3-week post-treatment follow-up) in adult patients with DSM-IV-TR MDD (Quiroz et al., 2014). Basimglurant was administrated at two dose levels of 0.5 mg and 1.5 mg q.d. adjunctive to ongoing treatment with SSRI's or SNRI's, and effects of treatment were evaluated using a multitude of assessments including

JPET Fast Forward. Published on February 9, 2015 as DOI: 10.1124/jpet.114.222463
This article has not been copyedited and formatted. The final version may differ from this version.

rating scales sensitive to the effects of antidepressants. Adjunctive basimglurant treatment at 1.5 mg q.d. showed a consistent antidepressant effect across endpoints which warrants further investigation of the compound in depressive disorders.

Described herein is the *in vitro* pharmacological profile of basimglurant, showing that its mechanism of action is through negative allosteric modulation of mGlu5 receptor. Moreover, also illustrated are its general physiological effects *in vivo* and, more specifically, its behavioral actions in animals that, collectively, suggest that basimglurant may be a mechanistically differentiated addition to the repertoire of antidepressant drugs.

JPET Fast Forward. Published on February 9, 2015 as DOI: 10.1124/jpet.114.222463
This article has not been copyedited and formatted. The final version may differ from this version.

Materials and Methods

Materials

Basimglurant, 2-Chloro-4-[1-(4-fluoro-phenyl)-2-methyl-1H-imidazol-4-ylethynyl]-pyridine (RO4623831), MPEP, and the radiolabeled compounds [^{3}H]-basimglurant, [^{14}C]-basimglurant, [^{3}H]-ABP688 were synthesized at F. Hoffmann La-Roche AG. Antidepressants used in this study were purchased from Tocris (Bristol, UK) and Anawa Trading SA (Wangen, Switzerland). The synthesis of basimglurant and RO4623831 is described in Buettelmann et al. (Buettelmann et al., 2005), the synthesis of [^{3}H]-ABP688 is described in Hintermann et al. (Hintermann et al., 2007). All other radioligands, drugs, chemicals, cell culture reagents, and consumables were purchased from commercial sources as described previously (Lindemann et al., 2011). Plasmids used in this study were described previously (Lindemann et al., 2011); in addition, a plasmid encoding human mGlu4 (Genbank accession number NM_000841.3, plasmid backbone pcDNA5/FRT/TO) was used.

Methods

Cell culture, and membrane preparations

Cell culture, transfections, and preparation of membranes from cell culture and tissue material for radioligand binding experiments were conducted as previously described (Lindemann et al., 2011).

In vitro pharmacology and *in vitro* safety

Radioligand binding and selectivity profiling

Radioligand binding for mGlu5 and $GABA_A$ receptors was performed as described previously (Lindemann et al., 2011).

Ca^{2+} mobilization assays

Ca^{2+} mobilization assays were performed essentially as described previously (Lindemann et al., 2011). In brief, cells were seeded at a density of 5 x 10^4 cells/well in poly-D-lysine treated, 96-well, black/clear-bottomed plates. After 24 h, the cells were loaded for 1 h at 37°C with 2.5 µM (2S)-2-Amino-4-

JPET Fast Forward. Published on February 9, 2015 as DOI: 10.1124/jpet.114.222463
This article has not been copyedited and formatted. The final version may differ from this version.

phosphonobutanoic acid (Fluo-4AM) in loading buffer (1x HBSS, 20 mM HEPES). The cells were washed five times with loading buffer to remove excess dye, and intracellular calcium mobilization [Ca^{2+}]i was measured using FLIPR384 (Molecular Devices, Sunnyvale, California, USA) and FDSS7000 (Hamamatsu, Hamamatsu City, Shizuoka Pref., Japan) instruments.

The potency of basimglurant was studied in the presence of an agonist (mGlu1 and mGlu2: glutamate; mGlu5: quisqualate; mGlu4, mGlu8: L-AP4) at a concentration triggering 60-80% of the maximal agonist response which was determined daily in a separate experiment. The antagonists were applied in a serial dilution with 10 different concentrations 30 min before the application of agonists; potential agonist activities of basimglurant were monitored on-line during the 5-30 min pre-incubation period. Responses were measured as peak increase in fluorescence recorded after the addition of basimglurant and of agonist (testing for antagonist activity), minus basal (i.e. fluorescence without addition of agonist), normalized to the maximal stimulatory effect induced by a saturating concentration of the agonist measured on the same plate. Inhibition curves were fitted using XLfit according to the Hill equation $y = 100/(1+(x/ IC_{50})nH)$, where nH = slope factor.

Inositol phosphate accumulation assay

Inositol phosphate (IP) accumulation assays were performed as described previously (Lindemann et al., 2011).

cAMP accumulation assays

cAMP accumulation assays using a cell line stably transfected with a cDNA encoding human mGlu7 were performed as described previously (Lindemann et al., 2011).

Selectivity screening

The selectivity profiling on approximately 100 targets comprised in the ‘Broad Diversity Profile’ at a single concentration of 10 µM, and follow-up profiling in concentration-response on CB_1 and CB_2 cannabinoid receptors and on I_2 imidazoline receptor were conducted at CEREP (Celle l'Evescault, France). Selectivity

JPET Fast Forward. Published on February 9, 2015 as DOI: 10.1124/jpet.114.222463
This article has not been copyedited and formatted. The final version may differ from this version.

profiling on recombinant human mGlu3 and mGlu6 receptors were conducted in concentration-response using a cAMP assay (Bassoni et al., 2012) at DiscoverX (Fremont, California, USA). Profiling on mGlu1, 2, 4, 7, 8 (Lindemann et al., 2011), monoamine reuptake transporters (see below), and $GABA_A$ (Lindemann et al., 2011) were conducted at F. Hoffmann-La Roche AG (Basel, Switzerland). Key experimental conditions for the selectivity profiling of basimglurant are summarized in Supplemental Table S1.

Monoamine reuptake transporter assays

Monoamine reuptake experiments were performed essentially as described previously (Hysek et al., 2012). In brief, HEK293 cells stably transfected with plasmids encoding human norepinephrine- (NET), 5-HT- (SERT), or dopamine (DAT) reuptake transporter were seeded at 3×10^4 cells/well in 96-wells opaque white assay plates. After 24 h at 37°C, cells were washed once with 100 µl assay buffer (Krebs-Ringer bicarbonate buffer, Sigma Aldrich) for 10 min while shaking. Plates were snap-inverted and 50 µl fresh assay buffer was added followed by 50 µl of basimglurant or (1R,3S)-3-(3,4-dichlorophenyl)-N-methyl-2,3-dihydro-1H-inden-1-amine (indatraline; positive control) diluted in assay buffer. Cells were incubated at 37 °C for 30 min and 50 µl of the radioligand solution was added ([^{3}H]-norepinephrine, Anawa trading SA, Wangen, Switzerland; [^{3}H]-5-HT and [^{3}H]-dopamine, PerkinElmer, Waltham, Massachusetts, USA). After incubation at 37°C for 15 min, the assay was terminated by washing the cells twice with assay buffer using a cell washer. Remaining assay buffer was decanted, 250µl of Microsynth 40 (PerkinElmer) was per well, and radioactivity was counted on a Topcount microplate scintillation counter (PerkinElmer). Results were expressed as a percentage of radioactivity detected in the absence of drugs, and IC_{50} values were determined using XLfit software as described above for radioligand competition binding.

Assessment for the potential to form covalent protein adducts

Assessment of the potential to form covalent protein adducts with hepatic proteins was essentially performed as described previously (Fitch et al., 2010). In brief, [^{14}C]-labeled basimglurant (49.2 µCi/µmol) was incubated with microsomal preparations, and radioactivity irreversibly bound to proteins after washing was measured. The incubation media (600 µl) consisted of 100 mM sodium phosphate buffer (pH 7.4), 1 mg/ml microsomal protein (human liver microsomes, Becton Dickinson Bioscience, Allschwil, Switzerland) 10 µM radiolabeled basimglurant and 1 mM NADPH. Control incubations were lacking NADPH. Additional

JPET Fast Forward. Published on February 9, 2015 as DOI: 10.1124/jpet.114.222463
This article has not been copyedited and formatted. The final version may differ from this version.

experiments were conducted in the presence of reduced glutathione (GSH). Incubations were started after by addition of NADPH after which the mixture was incubated at 37°C for 30 min. Experiments were conducted in triplicate.

The incubation was quenched by transferring 500 µl of the mixture into 650 µl of cold acetonitrile on a Multiscreen deep well filterplate (Solvinert hydrophilic PTFE with prefilter; Millipore Billerica, MA, USA) to afford protein precipitation. Recovery of proteins was achieved by centrifugation at 1000 ×g for 20 min at RT. The protein pellet was washed repeatedly with 750 µl of cold methanol containing H_2SO_4 (0.1 %, v/v) followed by centrifugation at 1000 ×g for 10 min at RT until background radioactivity levels were reached in the supernatants (typically 6-8 times). The remaining protein was dissolved in 500 µl of aqueous 1 M NaOH containing I % (w/v) SDS at 60°C for 1 h. A 100 µl aliquot of the protein solution was used for protein determination (DC protein assay, BioRad, Hercules, CA), and the remaining solution was used for measuring the amount of incorporated radioactivity by liquid scintillation counting. Covalent protein binding was expressed as pmol equivalents of [^{14}C]-labeled material bound per mg microsomal protein. Covalent binding to proteins was considered as significant if an increase as compared to the control incubation (lacking NADPH) was greater than 5-fold and exceeding background radioactivity levels. Covalent binding of > I00 pmol [^{14}C]/mg protein was considered as alert for metabolic activation under the assay conditions.

hERG (Human Ether-a-go-go Related Gene) recordings

Recording of hERG currents on the recombinant human hERG channel was performed essentially as described previously (Fleury et al., 2011). In brief, the outward K^+ currents were recorded in a CHO cell line stably expressing recombinant hERG channels cloned from human heart (F. Hoffmann-La Roche Ltd., New York, USA) using a whole-cell configuration of the patch-voltage-clamp technique at 35-37 °C using an EPC-10 triple amplifier (HEKA Elektronik GmbH, Germany) and associated Patch MasterPro software (HEKA Elektronik GmbH, Germany). Cells were held at a resting voltage of -80 mV and were stimulated by a voltage pattern to activate hERG channels and conduct outward IK_{hERG} current (500 ms prepulse to +20 mV followed by a 500 ms test pulse to -40 mV), at a stimulation frequency of 0.1 Hz (6 bpm). After the cells had stabilized for a few minutes and the currents were steady, the amplitude and kinetics of IK_{hERG} were recorded under control conditions (vehicle control) for 3 min. Thereafter, basimglurant was applied at

JPET Fast Forward. Published on February 9, 2015 as DOI: 10.1124/jpet.114.222463
This article has not been copyedited and formatted. The final version may differ from this version.

ascending concentrations for 3 min each followed by a 100 nM solution of the standard IK_{hERG} blocker N-[4-[1-[2-(6-Methylpyridin-2-yl)ethyl]piperidine-4-carbonyl]phenyl] (E-4031) which completely blocks IK_{hERG} and is used as positive control. Experiments were performed in N=3 replicates. If the drug effect on hERG currents were >20% compared to vehicle control then concentration-response curve data were fitted using non-linear regression analysis with FitMaster Pro software (HEKA Elektronik GmbH, Lambrecht, Germany); if the drug effect was <20% compared to vehicle control, the inhibition was expressed as mean ± SD.

Ames mutagenesis test

The Ames mutagenesis test was performed performed essentially as described previously (Muster et al., 2003). In brief, the *Salmonella typhimurium* strains TA1535, TA97, TA98, TA100, and TA102 were obtained from B.N. Ames (University of California, Berkely, USA). S9 rat liver mixtures were prepared freshly for each experiment by mixing 0.1 ml S9 preparation (Molecular Toxicology Inc., Boone, North Carolina, USA), 0.2 ml of a 165 mM KCl solution, 0.2 ml of a 40 mM $MgCl_2$ solution, 0.2 ml of 200 mM sodium phosphate buffered saline pH 7.4, 3.2 mg NADP (Roche Diagnostics, Rotkreuz, Switzerland), and 1.53 mg glucose-6-phosphate (Roche Diagnostics). Bacterial growth media and agar, supplements, and tetracycline were obtained from Sigma (Buchs, Switzerland).

Cultures of the strains were grown overnight at 37°C in a shaking water bath in a Nutrient Broth (NB) liquid medium to which 0.3 µg /ml tetracycline was added for strain TA102 in order to maintain a stable plasmid copy number (Albertini and Gocke, 1988), and the bacterial density was checked photometrical and cultures were diluted in 0.85% NaCl as needed. The sensitivity of the Salmonella typhimurium strains was verified using the following positive controls: NaN_3 with strains TA1535 and TA100, ICR 191 with strain TA97, 2-nitrofluorene with strain TA98, and MMC with strain TA102. Moreover, 2-aminoanthracene was used with all strains with and without metabolic activation to confirm the activity of the S9 mix.

For the testing of basimglurant, test tubes containing 2 ml of 0.7 % agar medium were autoclaved and kept in a pre-warmed water bath at 42 - 45°C, and the following solutions were added: a) 0.2 ml of a histidine/biotin mixture corresponding to 21 µg L-histidine and 24.4 µg biotin, b) 0.1 ml solutions of basimglurant (20 – 2000 µg/plate) and positive controls, c) 0.1 ml of bacterial overnight liquid cultures, d)

JPET Fast Forward. Published on February 9, 2015 as DOI: 10.1124/jpet.114.222463
This article has not been copyedited and formatted. The final version may differ from this version.

0.5 ml of the S9 mixture where metabolic activation was needed, or 0.5 ml 200 mM sodium phosphate buffered saline pH 7.4 where no metabolic activation was needed.

The contents of the tubes were mixed and poured immediately onto Vogel-Bonner minimal agar plates, allowed to solidify, and incubated at 37°C upside down for 2 d. Bacterial colonies were counted electronically using a DOMINO automatic image analysis system (Perceptive Instruments, Haverhill, UK) after inspection of the background lawn for signs of toxicity. The outcome of the test was considered a positive results indicating mutagenicity when a dose-dependent increase in the number of colonies was observed which should reach at least a 2-fold (strains TA1535, TA98) or 1.5-fold (strains TA97, TA100, TA102) increase over background.

In vitro micronucleus test

The *in vitro* micronucleus test was performed as described previously (Kirchner and Zeller, 2010). In brief, L5178Ytk$^{+/-}$ mouse lymphoma cells (Covance Laboratories Ltd., Harrogate, UK) in exponential growth phase in growth medium (RPMI 1640 supplemented with 10% heat inactivated horse serum, Glutamax-I, 100 IU/ml penicillin, 100 µg/ml streptomycin, 100 µg/ml kanamycin) were seeded in 24-well cell culture plates. S9 rat liver mixtures were prepared freshly for each experiment as described (Kirchner and Zeller, 2010) and added at a final concentration of 2% in the treatment medium.

For the micronucleus test without metabolic activation, 0.3×10^6 cells in 700 µl growth medium were seeded per well, and basimglurant as well as positive controls were added in 7 µl as DMSO stock solutions, and cells were incubated for 24 h. For the micronucleus test with metabolic activation, 0.4×10^6 cells in 700 µl growth medium per well were incubated for 3 h at 37°C with 140 µl S9 mix and 8.4 µl of basimglurant and reference compounds DMSO stock solutions. Basimglurant was tested across a range of concentration of up to 28 µg/ml without and 70 µg/ml with metabolic activation. The cells were then washed twice with growth medium in sterile 1.5 ml Eppendorf cups, resuspended in 700 µl growth medium, seeded in 24-well plates and incubated for another 21 h at 37°C. Preparation of slides, and fixation and staining of cells were performed as described previously (Kirchner and Zeller, 2010), and cells were inspected using fluorescence and light microscopy with phase contrast for the occurrence of micronucleation events

JPET Fast Forward. Published on February 9, 2015 as DOI: 10.1124/jpet.114.222463
This article has not been copyedited and formatted. The final version may differ from this version.

indicative of DNA damage and cell cycle alterations. Results were considered positive of clastogenic/aneugenic if the number of micronucleated cells at any given concentration of test drug was elevated >2-fold compared to the vehicle (i.e. solvent) control.

In vivo pharmacology

Animals and drug treatment

All experiments with animals were conducted in accordance with federal and local regulation at the respective study location.

Rodents were maintained on a 12:12 h light-dark cycle with lights on between 6 AM and 8 AM, with free access to chow and tap water, unless specified otherwise. Room temperature (21-26°C) and humidity (30-75%) were kept constant. Rodents used were Sprague Dawley rats (conditioned emotional response: 350 g, male; Vogel conflict drinking test: 190 – 210 g, male; fear-potentiated startle: 225 - 287 g, male; Bennet neuropathic pain procedure: 100 – 250 g female; overactive bladder procedure: 200 – 250 g, female; electroencephalography recordings: 275 – 325 g, male; microdialysis: 250 – 350 g, male, *in vivo* receptor occupancy: 160 g, male), Wistar rats (pharmacokinetic profiles: 230 – 265 g, male; forced swim test, 100 – 130 g, female; chronic mild stress-induced anhedonia: 350 g, male; Chung pain model: 276 – 340 g, male), Fischer rats (fMRI, Fischer F344 rats: ca. 250g, male), NMRI mice (stress-induced hypothermia: ~22 g, male; formalin-induced pain model: 24 – 30 g, male), C57/Bl6J mice (*in vivo* receptor occupancy: 30 g, male). All experiments were performed with adult animals. Animals were group-housed in groups of 2 – 4 (rats) or 10 (mice), except for single-housing in the following procedures: stress-induced hyperthermia, chronic mild stress-induced anhedonia, microdialysis, and EEG. Rodents originated from Harlan/RCC (Füllinsdorf, Switzerland), Elevage Janvier (53940 Le Genest-Saint-Isle, France) or Charles River (San Diego, California, and Margate, UK).

For recordings of pharmacokinetic profiles in non-human primates adult male cynomolgus monkeys (*Maccaca fascicularis*) with a body weight of approximately 7.5 kg were used. The primates were maintained on a 12:12 h light-dark cycle with lights on at 6 AM and free access to food and water unless specified otherwise.

JPET Fast Forward. Published on February 9, 2015 as DOI: 10.1124/jpet.114.222463
This article has not been copyedited and formatted. The final version may differ from this version.

Basimglurant and reference comparator drugs were formulated as microsuspension in 0.9% NaCl / 0.3% Tween-80 prepared and stored as previously described (Lindemann et al., 2011) and administrated by oral gavage (p.o.), or by subcutaneous (s.c.) or intraperitoneal (i.p.) injections unless otherwise indicated.

Recording of pharmacokinetic (PK) profiles

PK in male rats: For intravenous PK, the compound was formulated in N-methyl-pyrollidone (NMP)/saline (30%/70%) as vehicle and administered at a volume of 2 mL/kg. For oral gavage (p.o.) the compound was administered as suspension using gelatine/saline (7.5%/0.62% in water) at an administration volume of 4 mL/kg.

PK in male cynomolgous monkeys: For intravenous PK, the compound was formulated in cyclodextrin solution as vehicle and administered at a volume of 2 mL/kg. For oral gavage (p.o.), the compound was administered in capsule (2 mg in size-2 capsules, i.e. ~0.3 mg/kg) to fasted or fed monkeys in a cross-over design.

Processing of blood samples and preparation of liver microsomes and hepatocyte cultures was as described previously (Valles et al., 1995). Human liver tissue was obtained from hepatic surgical resections at the Hospital Hautepierre (Strasbourg, France) in accordance with the guidelines of the Ethics Committee. Hepatocyte cultures were incubated with basimglurant at a concentration of 1 – 10 µM for 24 h; hepatocyte microsomes were incubated with basimglurant at a concentration of 1 – 10 µM for 1 h.

All samples were analyzed using routine sample preparation techniques followed by LC-MS/MS analysis as described previously (Lindemann et al., 2011). PK parameters for all studies were calculated using non-compartmental analysis.

Receptor occupancy measurements

Receptor occupancy measurements were performed using a tritiated version of (3-(6-methyl-pyridin-2-ylethynyl)-cyclohex-2-enone-O-(11)C-methyl-oxime) (ABP688) (Ametamey et al., 2006; Hintermann et al.,

JPET Fast Forward. Published on February 9, 2015 as DOI: 10.1124/jpet.114.222463
This article has not been copyedited and formatted. The final version may differ from this version.

2007) essentially as described previously (Lindemann et al., 2011). Animals received p.o. doses of either vehicle or basimglurant (0.03 – 3 mg/kg) 60 min prior to a tail vein injection of [^{3}H]-ABP688 (0.3 mCi/kg). After 30 min, animals were sacrificed and plasma as well as brain samples were collected. Samples were processed further for mice (Lindemann et al., 2011) and rats (Michalon et al., 2014b) as described previously.

[^{3}H]-basimglurant *in vivo* binding was performed by i.v. injection of rats with [^{3}H]-basimglurant (0.3 mCi/kg) in the tail vein. Sixty minutes later, rats received either vehicle (0.9% saline / 0.3% Tween-80) or an oral dose of 10 mg/kg RO4623831 ($C_{16}H_{11}N_3FCl$; M_W 311.75; see Supplemental Table S2 for the pharmacological properties of RO4623831). After 60 minutes post dose of RO4623831 animals were sacrificed and brains were processed as for receptor occupancy measurements.

Chronic mild stress (CMS)-induced anhedonia test

The CMS-induced anhedonia test was performed essentially as described previously (Moreau et al., 1996). In brief, following implantation of electrodes unilaterally in the mesolimbic system at the level of the ventral tegmental area of the midbrain (2 mm anterior from lambda, 0.3 mm lateral from the midline suture, and 8.5 mm ventral from the skull surface; electrode tips approximately 0.5 mm apart in the dorsoventral plane). After surgery animals were allowed to recover for 5 d after which they underwent intracranial self-stimulation (ICSS) training. After establishing a consistent ICSS baseline, rats were either subjected to 6 weeks of unpredictable CMS or left undisturbed. From day 21 to day 42, stressed animals received once-daily doses (i.p.) of drugs (basimglurant, fluoxetine) or vehicle. The control group of animals not undergoing CMS received the high dose of basimglurant (3 mg/kg) or vehicle. The anhedonia index was calculated as the per-cent change in ICSS threshold from baseline.

FST

The FST was performed essentially as described previously (Cryan and Lucki, 2000). Rats were placed inside vertical plexiglas cylinders (height: 40 cm; diameter: 17.5 cm) containing 15 cm of water maintained at 23 - 24 °C for 15 min. After 24 h, the rats were placed again in the cylinder and the total duration of immobility was measured during a 5 min period. Rats received repeated administrations of drugs (p.o.) administration 24 h, 16 h and 2 h prior to the testing period.

JPET Fast Forward. Published on February 9, 2015 as DOI: 10.1124/jpet.114.222463
This article has not been copyedited and formatted. The final version may differ from this version.

fMRI in rats

fMRI imaging and data processing was performed essentially as described (Bruns et al., 2009). In brief, Fischer F344 rats received basimglurant and comparator drugs as single doses (p.o.) approximately 1 h prior to the experiment. For fMRI, rats were anaesthetized with isoflurane in oxygen and air (1:5) supplied to the spontaneously breathing animals using a face mask. Isoflurane concentration was adjusted between 1.8 % and 2.4 % to maintain stable respiration rates at 50–60 breaths per minute (bpm). Animals were placed in a cradle and their heads immobilized in a stereotaxic frame. Respiratory rate, body temperature, and O_2 and CO_2 levels in the inhaled and exhaled air were continuously monitored on a PowerLab data acquisition system (ADInstruments, Spechbach, Germany). Body temperature was maintained at 37 °C with a feedback-regulated electric heating blanket. The total time under anaesthesia was 35 minutes.

Magnetic resonance imaging was performed on a 4.7 T / 40 cm Bruker Biospec animal scanner (Bruker BioSpin, Ettlingen, Germany), equipped with a 72 mm bird-cage resonator for excitation and a surface receiver coil (Rapid Biomedical, Rimpar, Germany). On scout images, the most rostral extension of the corpus callosum was used as a landmark for selection of eight coronal image planes at –10.0, –7.8, –5.3, –2.9, –1.6, –0.3, +1.0 and +2.3 mm from bregma (Paxinos G, 1986). All subsequent images were acquired from these planes, with a field of view of 4 cm × 4 cm and a slice thickness of 1 mm. First, a set of RARE T_2-weighted anatomical images (TR/TEeff 1.8 s/39 ms, RARE factor 8, matrix 256 $\times$ 256) (Hennig et al., 1986). Next, a T_1 image series required to quantitatively calibrate perfusion readouts was obtained using an inversion-recovery snapshot FLASH sequence with 8 inversion times (TR/TE 3.4 s/1.4 ms, matrix 128 × 64) (Haase et al., 2011). Finally, perfusion-weighted images were acquired using continuous arterial spin labelling (CASL) (Williams et al., 1992) with centered RARE readout (TR/TE 3.75 s/5.7 ms, RARE-factor 32, matrix 128 × 64, labeling pulse 2.5 s, post-labelling delay 0.4 s). Three consecutive volumes of perfusion images were acquired within 12 minutes.

Images were processed and analyzed using in-house developed software written in IDL (RSI, Boulder, CO, USA) and MATLAB (The MathWorks Inc., Natick, MA, USA) including the open-source software SPM5 (Wellcome Trust Centre for Neuroimaging, London, UK). For spatial normalization, the anatomical images

JPET Fast Forward. Published on February 9, 2015 as DOI: 10.1124/jpet.114.222463
This article has not been copyedited and formatted. The final version may differ from this version.

were co-registered to a rat-brain template by affine and non-linear transformations which were then applied to the all functional images. T1 maps were calculated on a voxel-wise basis by fitting a 3-parameter exponential to the intensities across the 8 inversion times (Deichmann et al., 1999) and were then combined with the related CASL images to obtain quantitative absolute perfusion maps, as described elsewhere (Alsop and Detre, 1996; Bruns et al., 2009). In order to account for possible systemic changes affecting global brain perfusion, and to eliminate part of the inter-individual variability, perfusion maps of each individual were normalized slice-wise to the brain-mean value, which was set to 100 %. Perfusion values were averaged region-wise with reference to an in-house generated digital atlas with regions of interest (ROIs) adapted from the Paxinos & Watson rat-brain atlas (Paxinos G, 1986).

Statistical analysis of perfusion data was performed with JMP (SAS institute Inc., Cary, USA). Normalized perfusion for each dose group was compared region of interest- (ROI)-wise to those of the pertinent control (vehicle) group using Welch's t-test. Differences were considered significant at $p < 0.05$. In order to avoid a severe drop in statistical power, values were not corrected for multiple testing, but instead the false discovery rate (FDR) was estimated per dose group. The estimated number of false positives was on average 1 ±1 (mean ± SD. across dose groups) and never exceeded 3. Data were further characterized in a framework of pro- and antidepressant interventions by calculating the root mean square (RMS) of the perfusion changes across all ROIs and the scale-invariant pattern match coefficients (PMCs, i.e. the dot product between the two neural activity profile vectors, each scaled to unit length) as measures of response strength and similarity between the effect of basimglurant and reference interventions, respectively.

Vogel conflict drinking test

The Vogel Conflict Test was performed as described previously (Lindemann et al., 2011) with p.o. administration of drugs and 1 h pretreatment time.

Stress-induced hypothermia (SIH) test

The SIH test was essentially performed as described previously (Spooren et al., 2002). In brief, body temperature was measured in mice twice 1 min apart (T1 and T2, respectively) using a rectal probe.

JPET Fast Forward. Published on February 9, 2015 as DOI: 10.1124/jpet.114.222463
This article has not been copyedited and formatted. The final version may differ from this version.

Measurement of T1 served as the handling stressor. The difference in body temperature ($\Delta T = T2-T1$) was determined. Drugs were administrated p.o. with 1 h pretreatment time before measuring T1.

Conditioned emotional response (CER)

The CER was performed as described previously (Ballard et al., 2005) with p.o. administration of drugs and 1 h pretreatment time. In brief, Animals were tested, using a Latin-square design, twice weekly with at least a 48 h interval between test sessions. The readout of the test, the so-called suppression ratio (SR), is defined as the ratio of lever presses within the conditioning period to the total lever presses around this time (lever presses 2 min before + lever presses within the 2 min conditioning period).

Fear-potentiated startle (FPS) response procedure

The FPS response procedure was performed as described previously (Busse et al., 2004), with minor modifications. Rats were conditioned to associate a light stimulus with a mild foot shock (0.25 mA for 0.5 s) during two consecutive sessions on two consecutive days. Animals received drugs with p.o. administration and 1 h pretreatment time before the test session on the third day, in which an acoustic stimulus was either paired with the light stimulus or not. The fear-potentiated startle response was calculated by subtracting the mean startle response (unpaired) from the mean startle response (paired).

Formalin-induced pain (paw licking) test

The formalin-induced pain (paw-licking) test was performed at Porsolt & Partners Pharmacology (Le Genest-Saint-Isle, France) as described previously (Lopes et al., 2013), with minor modifications. In brief, mice received an intraplantar injection of 5% formalin (25 µl) into the posterior left paw. In one group of animals, time spent with licking paws was recorded for 5 minutes, beginning immediately after injection of formalin (early phase). In a second cohort of animals receiving identical formalin injection, paw-licking time was recorded beginning 20 minutes after formalin injection (late phase). NMRI mice received drugs or vehicle (p.o.) 1 h before the start of recording paw-licking time.

JPET Fast Forward. Published on February 9, 2015 as DOI: 10.1124/jpet.114.222463
This article has not been copyedited and formatted. The final version may differ from this version.

Chung model of neuropathic pain

The Chung model of neuropathic pain (Ho Kim and Mo Chung, 1992) was performed at Porsolt & Partners Pharmacology (Le Genest-Saint-Isle, France) as described previously (Basile et al., 2007). In brief, rats were anesthetized with sodium pentobarbital and the left L5 and L6 spinal nerves were ligated, followed by 2 weeks of recovery. For the thermal stimulation, a mobile infrared radiant source was focused under the non-lesioned and lesioned hind paws and the paw-withdrawal latency was automatically recorded. Rats received drugs (p.o.) with 1 h pretreatment time before testing.

Bennet model of cold allodynia (chronic sciatic nerve constriction model)

The Bennett model of cold allodynia was performed as described before (Bennett and Xie, 1988; Hunter et al., 1997), with minor modifications. In brief, rats were anesthetized with isoflurane and the sciatic nerve of the right hind limb was mildly constricted with four ligatures that were tied circumferentially around the nerve approximately 1 mm apart. After recovery for ≥4 - 7 days, rats were tested for cold-induced innocuous pain (allodynia) in a testing chamber filled to a depth of 1.5 – 2.0 cm with water at 2-4 °C. After at least 1 h of resting period, rats received drugs and vehicle s.c. with different pretreatment time as follows: Basimglurant (0.1 - 10 mg/kg; 60 min), morphine (1 mg/kg; 30 min), duloxetine (3 mg/kg; 90 min), and vehicle (60 min). The inhibition rate was calculated with the following formula: Inhibition rate = (paw lifts post treatment - mean paw lifts post vehicle treatment)) / (sham pre-treatment –mean pre-treatment vehicle) x 100. The drug-treated group was compared to the vehicle group using a two-sample t test with equal variance assumption. Basimglurant was formulated in H_2O with 10% propylene glycol adjusted to pH 6.0 with 0.1 M HCl, morphine and duloxetine were dissolved H_2O.

Overactive bladder: Measuring threshold volume in the volume-induced-micturition-reflex (VIMR) model

The VIMR was performed in rats as described before (Hu et al., 2009). In brief, the urinary bladder was cannulated under anesthesia in rats and infused with saline to determine the micturition threshold. After establishing a stable baseline, drug or vehicle doses were administrated i.v. 5 minutes prior to the next infusion cycle, thereafter the change in micturition threshold volume was recorded.

JPET Fast Forward. Published on February 9, 2015 as DOI: 10.1124/jpet.114.222463
This article has not been copyedited and formatted. The final version may differ from this version.

Overactive bladder: Contraction frequency in the isovolume bladder contraction (IBC) model

Bladder contraction frequency was measured in rats as described previously (Hu et al., 2009). In brief, the urinary bladder was cannulated under anesthesia in rats and infused with saline to evoke micturition contractions. After stable IBCs were obtained the infusion rate was lowered to 5 µl/min and the system was allowed to stabilize for at least 30 min. Thereafter, vehicle was dosed, followed 10 minutes later with single doses of basimglurant (0.003 - 0.03 mg/kg; i.v.). The frequency of IBCs was recorded for 60 min in total.

EEG recordings

EEG recordings were performed at SRI International, Biosciences Division (Menlo Park, USA) as described previously (Morairty et al., 2008), with minor modifications. In brief, rats were implanted with telemetric devices for continuous recordings of EEG, electromyograph, core body temperature, and locomotor activity (F40-EET, DSI, Inc., St Paul, MN, USA). Animals were acclimated to the handling procedures and given 2 once-daily 1 mL doses of vehicle 7 and 3 d before start of the study. Drugs (basimglurant 0.03 – 0.3 mg/kg, caffeine 10 mg/kg) were formulated in standard vehicle (0.9% saline/0.3% Tween-80). Using a repeated-measure, counter-balanced design, each rat received five subchronic dosing conditions with 9 d of washout between each subchronic treatment condition. For each condition, daily dosing occurred 2 h into the active period for 5 consecutive days (at the start of Zeitgeber Time [ZT] 14). For the caffeine condition, however, vehicle was administered on days 1-4 and caffeine was only administered on the fifth day. Data were recorded and analyzed only for the fifth day of dosing starting at lights off (2 h prior to dosing).

Microdialysis

Microdialysis was performed at Renasci Ltd. (Nottingham, UK) as described previously (Rowley et al., 2014), with minor modifications. In brief, rats were anaesthetized with isoflurane (5% to induce, 2% to maintain) in an O_2/N_2O (1 litre/min each) mixture and dual-probed whereby two microdialysis probes were stereotaxically implanted bilaterally into i) the prefrontal cortex (2 mm tip, coordinates: AP: +3.2 mm; L: +/-2.5 mm relative to bregma; V: -4.0 mm relative to the skull surface) and ii) the nucleus accumbens (2 mm tip, coordinates: AP: +2.2 mm; L: +/-1.5 mm relative to bregma; V: -8.0 mm relative to the skull surface). Following surgery, animals were individually housed in circular chambers (dimensions 450 mm internal diameter, 320 mm wall height) with the microdialysis probes connected to a liquid swivel and a

JPET Fast Forward. Published on February 9, 2015 as DOI: 10.1124/jpet.114.222463
This article has not been copyedited and formatted. The final version may differ from this version.

counter balanced arm to allow unrestricted movement. Rats were allowed a recovery period of at least 16 h with free access to food and water prior to the onset of sample collection. The experiments were performed one day after surgery. Dialysate samples were collected from freely moving rats at 20 min intervals from 80 min prior to 4 h post drug administration (4 basal samples and 12 post drug samples). Animals received p.o. injections of either basimglurant (0.1 or 1 mg/kg), paroxetine (3 or 10 mg/kg), or vehicle.

Detection and subsequent quantification of 5-HT, dopamine (DA) and norepinephrine (NE) in the dialysis samples was based on reverse-phase, ion-pair HPLC coupled with electrochemical detection and involved the use of an ALEXYS monoamine analyzer (Antec Leyden, The Netherlands). The system consisted of two separate analytical columns that shared a dual-loop autosampler allowing for one sample to be simultaneously analyzed by two systems optimized for different neurotransmitters. In this instance one column separated NA (ALF-115, 150 mm x 1 mm internal diameter) whilst the other separated 5-HT and DA (ALF-105, 50 mm x 1 mm internal diameter). Two solvent delivery pumps (LC 110) were used to circulate the respective mobile phases (5-HT/DA: 50 mM phosphoric acid, 8 mM NaCl, 0.1 mM EDTA, 4.6 mM 1-octane sulphonic acid, 20% methanol, pH 6.0; NA: 50 mM phosphoric acid, 8 mM NaCl, 0.1 mM EDTA, 3 mM 1-octane sulphonic acid, 10% methanol, pH 3.25) at a flow rate of 50 µl/min and an Antec in-line degassing unit was used to remove air. Samples (10 µl) were injected onto the columns via an autosampler (AS 110) with a cooling tray set at 4 ºC. Antec DECADE II electrochemical detectors were used and Antec micro VT 03 cells employing a high-density, glassy carbon working electrode (+0.3 V for 5-HT and DA, +0.59 V for NA) combined with an ISAAC reference electrode. The electrode signal was integrated using Antec's Clarity data acquisition system. Individual stock solutions of 5-HT, DA and NA (1.0 mM) were prepared in a mixture of equal quantities of deionized water and 0.1 M perchloric acid (in order to prevent oxidation) and stored at 4 ºC. A working solution containing all three transmitters was prepared daily by dilution in aCSF.

At the end of the study, rats were sacrificed and probe placement was visually confirmed. Data were reported only from animals where probe membranes were correctly positioned.

JPET Fast Forward. Published on February 9, 2015 as DOI: 10.1124/jpet.114.222463
This article has not been copyedited and formatted. The final version may differ from this version.

Data processing and statistical analysis

Data processing was conducted using Excel (Microsoft, Redmond, Seattle, USA), GaphpadPrism (La Jolla, California, USA), and Statistica (Statsoft Inc., Tulsa, USA). One-way ANOVA was performed and either followed by Dunnetts' *post hoc* test (SIH, CER, FPS, FST) or paired t-tests (EEG:REM/non-REM ratio and latency to REM and non-REM onset). For multidimensional data, two-way ANOVA with repeated measures was performed followed by unpaired t-tests (stress-induced anhedonia) or paired t-tests (EEG:REM time, NR time, non-REM delta power, wakefulness and LMA). Microdialysis data were analyzed with ANCOVA followed by Williams' (Williams, 1971; Williams, 1972) tests. The Mann-Whitney U test was used for the Vogel conflict test and the formalin-induced neuropathic pain. Unpaired t-tests were used for the data from the Chung and Bennett models. All models used 2-tailed tests with the exception of the Vogel conflict test and the *post hoc* comparisons of the CER and FPS. For all statistical procedures, the alpha level was set at 0.05.

JPET Fast Forward. Published on February 9, 2015 as DOI: 10.1124/jpet.114.222463
This article has not been copyedited and formatted. The final version may differ from this version.

Results

Discovery of basimglurant

Basimglurant (RO4917523, RG7090; $C_{18}H_{13}ClFN_3$, M_W 325.77) (Fig. 1) was discovered in a medicinal chemistry effort conducted at F. Hoffmann-La Roche AG starting from the results of a small molecular weight compound library high-throughput screen based on a Ca^{2+} mobilization assay with human mGlu5a (Jaeschke et al., 2015). The high-throughput screen identified several mGlu5 antagonists such as MPEP, MTEP, and fenobam (Fig. 1).

In vitro pharmacology, selectivity, and inverse agonist properties of basimglurant

The potency of basimglurant was analyzed by means of radioligand binding and functional *in vitro* assays. [^{3}H]-basimglurant saturation analysis on recombinant human mGlu5 revealed monophasic saturation isotherms with dissociation constant (Kd) of 1.1 nM (Table 1, Fig. 2A). The rate of [^{3}H]-basimglurant association and dissociation on recombinant human mGlu5 *in vitro* at 37°C indicated that equilibrium binding was reached after approximately 2 h at 37°C, and that the dissociation from the target *in vitro* at 37°C was achieved after approximately 5-6 h (Table 1, Supplemental Fig. S1). In competition binding experiments on human recombinant mGlu5, basimglurant fully displaced [^{3}H]-MPEP with Ki = 35.6 nM and [^{3}H]-ABP688 (Ametamey et al., 2006; Ametamey et al., 2007; Hintermann et al., 2007) with Ki = 1.4 nM (Table 1, Fig. 2B). In HEK293 cells stably expressing human mGlu5, basimglurant inhibited quisqualate-induced Ca^{2+} mobilization with IC_{50} = 7.0 nM and [^{3}H]-inositolphosphate accumulation with IC_{50} = 5.9 nM (Table 1, Fig. 2C-D). Basimglurant showed similar potencies in radioligand binding and functional assay on human and rodent mGlu5 receptor orthologues (Table 1).

Basimglurant acted as inverse agonist in IP accumulation assays, inhibiting constitutive receptor activity by approximately 30% with IC_{50} = 38.1 nM (Fig. 2E). Basimglurant further caused a simultaneous right-shift and a reduction of the maximal signal amplitude in IP accumulation assays with recombinant human mGlu5 (Fig. 2F), demonstrating that it acts as negative allosteric modulator.

JPET Fast Forward. Published on February 9, 2015 as DOI: 10.1124/jpet.114.222463
This article has not been copyedited and formatted. The final version may differ from this version.

The selectivity profiling of basimglurant on a panel of 116 radioligand binding and functional assays including all mGlu receptors revealed a more than 1000-fold selectivity for mGlu5 (Table 2, Supplemental Table S1).

Pharmacokinetic and *in vitro* safety features of basimglurant

Following intravenous administration, basimglurant showed low clearance and high volume of distribution resulting in a long half-life in rats as well as non-human primates of 7.5 h and 20 h, respectively (Table 3, Fig. 3). After single oral doses of basimglurant in rats, the compound was well-absorbed with oral bioavailability of about 50%. In cynomolgus monkeys the overall oral PK profiles were similar to the one seen in rats with the same overall oral bioavailability of about 50% in non-fasted animals and approximately 100% in fasted animals.

The total brain/plasma ratio of about 2-3 in rats is in line with the good brain penetration of the drug and the protein binding of basimglurant was consistently high across species in the range of 97% to 99% bound to plasma proteins in rat, cynomolgus and human.

There was no significant retention of radioactivity to human or rat hepatic proteins when [^{14}C]-labeled basimglurant was incubated with rat and human liver microsomes in the presence of NADPH. The assessment of basimglurant in an Ames mutagenicity test showed no mutagenic potential in absence or presence of metabolic activation with rat liver S9 extracts up to a drug concentration of 500 µM. In an *in vitro* micronucleation test with mouse lymphoma cells, basimglurant showed no clastogenic/aneugenic activity up to a concentration of 85 µM. Basimglurant was also tested for its potential to act on hERG. In patch clamp recordings with recombinant human hERG at 37°C in a protein-free buffer system, basimglurant inhibited K^+ currents by 11±7.5 % compared to vehicle controls only at the highest concentration tested (3 µM).

Brain receptor occupancy – exposure relationship of basimglurant in rats and mice

In *in vivo* radioligand binding experiments with a tritiated version of the PET tracer ABP688 (Fig. 4A), basimglurant fully displaced the tracer in mice and rats at a dose of 3 mg/kg (p.o.): 50% [^{3}H]-ABP688

JPET Fast Forward. Published on February 9, 2015 as DOI: 10.1124/jpet.114.222463
This article has not been copyedited and formatted. The final version may differ from this version.

displacement was reached at plasma concentrations of 4.8 ng/ml in rats (Fig. 4B-D) and 3.5 ng/ml in mice (data not shown).

Autoradiography of parasagittal brain sections from rats receiving a bolus i.v. injection of [^{3}H]-basimglurant 60 min prior to sacrifice showed prominent labeling of brain areas including cortex, hippocampus, striatum, amygdala, and nucleus accumbens (Fig. 4E-F) which have been previously described to express mGlu5 (Shigemoto and Mizuno, 2000). The binding of [^{3}H]-basimglurant was almost completely blocked when rats received an oral dose of 10 mg/kg of RO4623831, a related mGlu5 inhibitor, simultaneously with the tracer injection (see Supplemental Table S2 for the properties of RO4623831).

Antidepressant-like properties of basimglurant

The therapeutic potential of basimglurant for the treatment of depression was addressed using a combination of acute and chronic behavioral procedures as well as fMRI in rats. The quantitative effects of drug treatment described in this paragraph are as per cent change from vehicle.

In the anhedonia model, (Moreau et al., 1992; Moreau, 2002; Holderbach et al., 2007; Hill et al., 2012), the self-stimulation behavior of rats implanted with electrodes in the ventral tegmental area was gradually disrupted by the application of unpredictable chronic mild stress (CMS). In vehicle-treated animals, the CMS reduced the self-stimulation over the first 3 weeks, quantitatively expressed in an increased anhedonia index. Repeated once-daily drug treatment (i.p.) over 3 weeks triggered a significant gradual normalization of the anhedonia index for basimglurant at 3 mg/kg (-72%,-53% and -64% for d 35, d 39 and d 42, respectively) and for fluoxetine at 10 mg/kg (-90%,-70% and -97% for d 35, d 39 and d 42, respectively), indicating antidepressant properties of basimglurant (Fig. 5A, Supplemental Table S3A).

Basimglurant was also tested in the rat forced swim test procedure (Porsolt et al., 1978) which is based on the principle that when placed in water, rodents adopt a characteristic immobile posture with only minimal movements needed to stay afloat after an initial period of vigorous activity. A reduction of the time during a test session spent in the immobile posture is considered indicative of the antidepressant potential of a particular drug. Administration (p.o.) of basimglurant caused a significant reduction of the immobility time at

JPET Fast Forward. Published on February 9, 2015 as DOI: 10.1124/jpet.114.222463
This article has not been copyedited and formatted. The final version may differ from this version.

doses of 10 and 30 mg/kg (-19% and -16%, respectively); also the tricyclic antidepressant desipramine at a dose of 100 mg/kg (p.o.) significantly reduced immobility time (-27%) (Fig. 5B, Supplemental Table S3B).

FMRI experiments in rats revealed that basimglurant triggered profound changes in the brain activity pattern, with increased activity in the dorsal striatum and decreased activity in the medial prefrontal cortex, dorsal hippocampus, thalamus, hypothalamus, septum, accumbens, ventral pallidum, and entorhinal piriform cortex (Fig. 6A-B). The results were further characterized in a reference framework of various pharmacological and non-pharmacological interventions by means of overall response strength (RMS) and scale-invariant pattern match coefficient (PMC). The effects triggered by basimglurant (10 and 30 mg/kg; administration route for basimglurant and all reference drugs was p.o.) were comparable to those elicited by the antidepressants duloxetine, reboxetine, imipramine and bupropione, as well as by electroconvulsive treatment (ECT). The similarity of basimglurant's response patterns to these reference treatments as gauged by the PMC was better than 71% (Fig. 6C). Also, the RMS response strength of basimglurant at 1 and 10 mg/kg surpassed that of electroconvulsive treatment (ECT) and that of standard drug treatments at 30 mg/kg (Fig. 6C). Notably, CMS led to a sizable effect opposite to that of standard treatments with an accordingly inverted response in the neuronal activity profile.

Anxiolytic-like properties of basimglurant

The anxiolytic-like properties of basimglurant, fenobam and diazepam were assessed in multiple procedures sensitive to anxiolytic drugs. The quantitative effects of drug treatment (all p.o.) described in this paragraph are as per cent change from vehicle.

In the Vogel conflict drinking test, basimglurant dose-dependently increased drinking time with a minimal effective dose of 0.03 mg/kg (+165%) up to the highest tested dose of 0.3 mg/kg (Fig. 7A, Supplemental Table S4B); fenobam and diazepam also increased drinking time each with a minimal effective dose of 30 mg/kg (+255% and +334%, respectively). In the stress-induced hyperthermia model, basimglurant reduced the stress-induced body temperature increase with a minimal effective dose of 0.01 mg/kg (-48%) up to the highest tested dose of 1 mg/kg (-145%) (Fig. 7B, Supplemental Table S4B); fenobam and diazepam reduced stress-induced temperature increase with minimal effective doses of 10 (-73%) and 0.1 mg/kg (-

JPET Fast Forward. Published on February 9, 2015 as DOI: 10.1124/jpet.114.222463
This article has not been copyedited and formatted. The final version may differ from this version.

52%), respectively. Basimglurant was further examined in the CER procedure, a fear conditioning paradigm (see Materials and Methods). Basimglurant increased the suppression ratio with a minimal effective dose of 0.3 mg/kg (+567%) up to the highest dose tested of 1 mg/kg (+583%) (Fig. 7C, Supplemental Table S4C); also fenobam and diazepam increased the suppression ratio with a minimal effective dose of 10 mg/kg for both drugs (+400% and +483%, respectively). In fear FPS test in rats, basimglurant dose-dependently reduced the startle amplitude with a minimal effective dose of 0.1 mg/kg (-53%) up to the highest tested dose (-94%) (Fig. 7D, Supplemental Table S4D); also fenobam and diazepam were active in this procedure each with a minimal effective dose of 30 mg/kg (-63 and -78%, respectively).

Taken together, basimglurant had robust and consistent anxiolytic-like activity in four procedures sensitive to anxiolytic drugs. Basimglurant was consistently more potent than fenobam and diazepam, with 10 – 100-fold differences in potency based on drug dose.

Effects of basimglurant in models of pain and overactive bladder

Glutamate is an important neurotransmitter in the context of nociception (Dickenson et al., 1997), and mGlu5 is expressed in the spinal cord and dorsal root ganglia (Shigemoto and Mizuno, 2000; Dang et al., 2002) where it has been implicated in neuropathic pain (Hu et al., 2012; Radulovic and Tronson, 2012). On this background, basimglurant was studied for its anti-nociceptive potential. The quantitative effects of drug treatment described in this paragraph are as per cent change from vehicle.

In the formalin-induced pain model, formalin injected into the paw of mice induced paw-licking behavior indicative of pain. The effects of drugs on both the early and late phases of nociception were recorded. In the early phase, basimglurant had no effect at 0.1 mg/kg (p.o.) and caused a partial yet statistically non-significant reduction of paw licking at 1 and 10 mg/kg (-39% and -44%, respectively) while morphine almost completely blocked paw licking (-95%) (Fig. 8A, Supplemental Table S5A). In the late phase, basimglurant had no effect at 0.1 mg/kg and caused an almost complete blocked of paw-licking at 1 mg/kg (-91%, not significant) and 10 mg/kg (-95%) while morphine completely blocked paw licking (100%) (Fig. 8B, Supplemental Table S5B).

JPET Fast Forward. Published on February 9, 2015 as DOI: 10.1124/jpet.114.222463
This article has not been copyedited and formatted. The final version may differ from this version.

In the Chung model, rats underwent unilateral spinal nerve ligations triggering neuropathic pain on the operated but not the intact side of the animal. The time to paw withdrawal after thermal or tactile stimuli was recorded as measure for the sensitivity to induce neuropathic pain. Basimglurant (0.1 – 10 mg/kg, p.o.) had essentially no effect on pain induced by thermal stimuli on the lesioned side while morphine (64 mg/kg p.o.) almost completely restored paw withdrawal latency of the lesioned side to the one of the unlesioned side (Fig. 8C, Supplemental Table S5C). Also, when tested for antinociceptive effects using tactile stimuli, basimglurant had no apparent effects (data not shown).

In the Bennett model of cold allodynia, rats received a surgical constriction of the sciatic nerve triggering an increased sensitivity to cold. Potential analgesic effects of drug treatment were expressed as inhibition rate (see Materials and Methods). Basimglurant (0.1 – 10 mg/kg, s.c.) dose-dependently increased the inhibition rate with a minimal effective dose of 0.3 mg/kg (36.77%) up to the highest tested dose of 10 mg/kg (58.3 %) (Fig. 8D, Supplemental Table S5D). The maximal effect size reached with the highest dose of basimglurant was comparable to the effects of morphine (1 mg/kg; inhibition rate: 64.3%) and duloxetine (3 mg/kg; inhibition rate: 56.3%).

Micturition is a coordinated reflex under the control of pontine and supra-pontine centers (Blok, 2002). Glutamate signaling plays an important role in the modulation of bladder function (Kakizaki et al., 1998; Yoshiyama et al., 1999), and recently mGlu5 NAM's have been implicated as potential modality for the treatment of overactive bladder (Larson et al., 2011). On this background, basimglurant was assessed in the volume-induced-micturition-reflex model in anesthetized rats (Supplemental Fig. S2A). Basimglurant (0.01 – 0.3 mg/kg, i.v.) dose-dependently increased the threshold of bladder filling volume triggering the micturition reflex with a minimal effective dose of 0.03 mg/kg (+27%, mean change from baseline) up to the highest dose tested of 0.3 mg/kg (+166.9) (Supplemental Fig. S2A). In an isovolumetric bladder contraction model, basimglurant (0.003 – 0.03 mg/kg, i.v.) dose-dependently reduced maximum bladder intercontraction intervals with both doses of 0.01 and 0.03 mg/kg achieving a comparable statistically significant maximal effect of -88.5% and -79.9% of the intercontraction interval observed with vehicle (Supplemental Fig. S2B)

JPET Fast Forward. Published on February 9, 2015 as DOI: 10.1124/jpet.114.222463
This article has not been copyedited and formatted. The final version may differ from this version.

EEG profile of basimglurant in rats

In view of the known effects of antidepressant drugs on the EEG and sleep (Mayers and Baldwin, 2005), the effects of basimglurant on the sleep and wake was studied by telemetry in freely-moving rats. Animals received five consecutive once-daily doses of vehicle or basimglurant (0.03 – 0.3 mg/kg, p.o.) two hours into the dark phase (ZT 14; the active period in rats), and EEG and EMG were continuously recorded for 22 h after the fifth dose; the comparator caffeine (10 mg/kg p.o.) was given acutely on the day of the recordings (Fig. 9A). Basimglurant dose-dependently reduced the ratio of rapid eye movement (REM) to non-REM sleep (i.e., the ratio of cumulative time spent in REM and non-REM sleep) during the dark phase (ZT 14-24) at 0.1 and 0.3 mg/kg without affecting the REM/non-REM ratio during the subsequent light phase (ZT 0-12) (Fig. 9B, Supplemental Table S6A). Basimglurant reduced the time spent in REM at 0.1 and 0.3 mg/kg (up to -100% and -97%, respectively; Fig. 9C) and non-REM at 0.1 and 0.3 mg/kg (up to -94% and -83%, respectively; Fig. 9D). In addition, basimglurant increased the latency to the onset of both REM (up to +351%) and non-REM (up to +226%) sleep (Fig. 9E, Supplemental Table S6B) and produced a wake-promoting effect at 0.1 and 0.3 mg/kg (up to 115% and 136%, respectively; Fig. 9F) without eliciting subsequent hypersomnolence. During non-REM sleep, basimglurant caused a pronounced increase in delta power during the dark phase at all three dose levels (up to +307% at 0.3 mg/kg) that was still detectable in the subsequent light phase (Fig. 9G). The moderate increase in locomotor activity during the dark phase in animals receiving basimglurant (up to +200% at 0.3 mg/kg; Fig. 9H) is consistent with the wake-promoting effects of the drug. Caffeine showed the expected effects, i.e., increased wakefulness (Fig. 9G) and locomotor activity (Fig. 9H) during the first half of the dark period (ZT 14-20), no effect on the REM/non-REM ratio (Fig. 9B), transient decrease (ZT 14-20) and subsequent increase (ZT 20-24) of both REM (Fig. 9C) and non-REM (Fig. 9D) sleep during the dark phase, no effects on delta power (Fig. 9E), and increased latency to REM and non-REM sleep onset (Fig. 9F).

Effects of basimglurant on monoamine neurotroansmitter levels in rats

Monoamine neurotransmitters and their modulation play a critical role in the pathophysiology and treatment of mood disorders (Kupfer et al., 2012; Hamon and Blier, 2013). Consequently, the effects of basimglurant and paroxetine on the levels of 5-HT, DA, and NE in the frontal cortex as well as 5-HT and dopamine in the nucleus accumbens were studied by dual-probe microdialysis in freely moving rats. After recording of

JPET Fast Forward. Published on February 9, 2015 as DOI: 10.1124/jpet.114.222463
This article has not been copyedited and formatted. The final version may differ from this version.

baseline transmitter levels for 1 h, animals received basimglurant (0.1 and 1.0 mg/kg, p.o.) or paroxetine (3.0 and 10.0 mg/kg, p.o.) after which the neurotransmitter levels were sampled for 4 h.

In the frontal cortex, basimglurant had little or no effect on the levels of 5-HT (Fig. 10A, Supplemental Table S7), DA (Fig. 10B, Supplemental Table S7), and NE (Fig. 10C, Supplemental Table S7) whereas paroxetine (10 mg/kg, p.o.) triggered a 2-fold increase in 5-HT levels (Fig. 10A, Supplemental Table S7). Aside from a small effect at 20 min, paroxetine had no consistent effect on DA. In addition, paroxetine (10 mg/kg, p.o.) reduced NE during the 40 – 180 min post-dose period with a maximum effect size of -29% compared to vehicle at 160 min post dose.

In the nucleus accumbens, basimglurant had no significant effect on 5-HT (Fig. 10D, Supplemental Table S7) with the exception of a transient reduction by -54% compared to vehicle observed at 200 min post dose. However, basimglurant caused a consistent, dose-dependent increase in DA (Fig. 10E, Supplemental Table S7), reaching significance at a dose of 1.0 mg/kg with a maximum effect size of +102% compared to baseline at 140 min post-dose. Paroxetine had no significant effects on extracellular 5-HT concentrations in the nucleus accumbens (Fig. 10D, Supplemental Table S7). Paroxetine caused transient elevations in DA levels at 10 mg/kg (Fig. 10E, Supplemental Table S7) reaching significance at 100 – 140 and 180 min post-dose with a maximum effect size at 140 min of +66% compared to vehicle.

JPET Fast Forward. Published on February 9, 2015 as DOI: 10.1124/jpet.114.222463
This article has not been copyedited and formatted. The final version may differ from this version.

Discussion

The mGlu5 receptor has been intensively studied as a drug target for a range of neuropsychiatric conditions including, depression, anxiety, Fragile X syndrome (FXS), autism, Parkinson's disease, and pain (Gasparini et al., 2008; Jaeschke et al., 2008). Pharmacological tools such as MPEP (Gasparini et al., 1999), MTEP (Cosford et al., 2002), fenobam (Pecknold et al., 1982; Porter et al., 2005), and 2-Chloro-4-((2,5-dimethyl-1-(4-(trifluoromethoxy)phenyl)-1H-imidazol-4-yl)ethynyl)pyridine (CTEP) (Lindemann et al., 2011) were instrumental for understanding the target biology and evaluating the therapeutic potential of mGlu5 inhibitors in the context of disease. The pharmacology and drug-like features of basimglurant described here made it possible to take this research one step further into Phase II clinical trials for FXS and MDD.

Basimglurant was found to act as potent and selective mGlu5 NAM with inverse agonist properties and negligible species differences between human and rodent mGlu5 receptor ortholgues. With respect to *in vitro* safety features, basimglurant had no relevant inhibitory activity on hERG channels, no propensity to form covalent protein adducts, no mutagenic potential in the Ames test, and no clastogenic/aneugenic activity in the *in vitro* micronucleus test. With respect to its pharmacokinetic properties basimglurant had low *in vitro* metabolic clearance by rat, cynomolgus, and human hepatocytes; these *in vitro* findings are in line with the observed low *in vivo* clearance of the drug. The large distribution volume in combination with low clearance results in long half-lives of 7.5 h in rats and ca. 20 h in monkey after oral administration, suggesting a once-daily dosing regimen in human. The high brain/plasma ratio in rat and the potent *in vivo* displacement of [^{3}H]-ABP688 receptor occupancy studies in rodents indicate good brain penetration and high *in vivo* potency of basimglurant. Taken together, the high *in vitro* and *in vivo* potency combined with the high selectivity for mGlu5, lack of *in vitro* safety liabilities, excellent oral bioavailability and long half-life constitute favorable drug-like properties for basimglurant.

Basimglurant showed robust antidepressant-like activity in the CMS-induced anhedonia procedure. These results are particularly relevant as the CMS method is considered a disease model for depression with good face-validity (Moreau, 2002; Nestler and Hyman, 2010) reflecting several key aspects of the human condition including a reduced hedonic drive, altered sleep/wake pattern, and endocrine changes in the HPA axis (Moreau et al., 1995; Grippo et al., 2005). The dose-dependent reduction of immobility time by

JPET Fast Forward. Published on February 9, 2015 as DOI: 10.1124/jpet.114.222463
This article has not been copyedited and formatted. The final version may differ from this version.

basimglurant in the forced swim test, a screening procedure used for the profiling of antidepressants (Nestler and Hyman, 2010), is in agreement of what has been reported for other mGlu5 NAM's (Liu et al., 2012; Hughes et al., 2013). Moreover, fMRI recordings revealed insights into the brain regions engaged in basimglurant's *in vivo* effects: many of the brain regions with altered neural activity upon basimglurant treatment have been recognized as critical parts of the neurocircuitry in depression (Russo and Nestler, 2013). The match between the changes of brain activity pattern induced by basimglurant on the one hand, and a broad range of antidepressant drugs and ECT on the other hand fit well to the antidepressant-like pharmacology of basimglurant.

In addition to its antidepressant-like properties, basimglurant had consistent anxiolytic-like activity with comparable efficacy and higher potency than fenobam and diazepam across methods used to detect anxiolytic-like activity. Furthermore, basimglurant showed antinociceptive activity in the formalin pain and cold allodynia procedures. Basimglurant also normalized urine bladder function in rodent models of overactive bladder, confirming previous work with other mGlu5 NAM's (Crock et al., 2012) and suggesting the possibility of benefits in the context of visceral pain. Taken together these results indicate that basimglurant has the potential to address two important co-morbidities of depression, namely anxiety and somatic pain.

The mechanistic underpinning of basimglurant's *in vivo* pharmacology was further explored by EEG and measures of the drug's effect on monoamine neurotransmitter levels by microdialysis in rats. EEG recordings revealed that repeated once-daily administration of basimglurant decreased the REM/non-REM ratio during the active period, and increased wakefulness and subsequent non-REM delta power. These observations are in agreement with EEG data reported for single-dose studies in rats with mavoglurant and -difluoromethoxy-3-(pyridine-2-ylethynyl)phenyl)5H-pyrrolo[3,4-b]pyridine-6(7H)-yl methanone (GRN-529) (Hughes et al., 2013). Disturbances of the sleep-wake pattern and EEG activity are a hallmark of MDD, contributing to daytime sleepiness as well as apathy and lethargy (Ahmadi et al., 2010). Several classes of clinically used antidepressants shift the REM/non-REM ratio in a similar way as observed with basimglurant (Beitinger and Fulda, 2010; Staner et al., 2010), lending further support to basimglurant's antidepressant-like profile(O'Donnel and Shelton, 2011). The increase in the delta frequency spectrum suggests increased sleep pressure during the active phase and improved sleep quality during the subsequent inactive period

JPET Fast Forward. Published on February 9, 2015 as DOI: 10.1124/jpet.114.222463
This article has not been copyedited and formatted. The final version may differ from this version.

(Tobler and Borbely, 1986; Borbely and Tobler, 2011). Of note, no indications of sleep deprivation were detected during the subchronic basimglurant treatment. The wake-promoting features of basimglurant which occur in a consolidated manner hold potential benefits in addressing daytime sleepiness, lethargy and apathy characteristic of MDD. The effects of mGlu5 inhibition on the EEG profile in rat have been studied previously employing a range of compounds including MPEP, MTEP, GRN-529, and mavoglurant (Cavas et al., 2013; Harvey et al., 2013; Ahnaou et al., 2014). These studies collectively showed a significant increase of REM following drug administration. Further, both Harvey et al. (2013) and Ahnaou et al. (2014) reported an increase of time spent in wakefulness and increased sleep consolidation. In contrast to our results, however, Ahnaou et al. (2014) reported a rebound in REM during the dark period following administration of MTEP; nonetheless Ahnaou et al. (2014) concluded that mGlu5 inhibition has overall sleep consolidating effects which they speculate might indirectly have beneficial effects on cognitive and memory performance. The source of the discrepancies between our observations with basimglurant and the reported effects for MTEP are unclear and could be based on methodological differences, including single drug doses for the published studies compared to subchronic drug administration for basimglurant, drug administration during light period for the published studies as opposed to during dark phase for basimglurant, and substantially shorter half-life reported for MPEP and mavoglurant (Vranesic et al., 2014) as well as MTEP (Lindemann et al., 2011) compared to basimglurant.

Microdialysis studies revealed that basimglurant had no significant effects on DA, 5-HT, and NE in the frontal cortex and nucleus accumbens with the exception of moderate DA elevations in the nucleus accumbens. Contributions of direct monoamine reuptake transporter inhibition to the accumbal DA elevation can be excluded in view of basimglurant's lack of activity on these transporters. Previous studies showed that MPEP had no effect on DA levels in the nucleus accumbens, while it blocked nicotine-evoked accumbal DA release (Tronci and Balfour, 2011) and dampened amphetamine-triggered DA outflow in the striatum (Tokunaga et al., 2009). The discrepancy between the current study and the previous report on accumbal DA levels might be due to the higher *in vivo* potency and longer half-life of basimglurant compared to MTEP. The microdialysis results demonstrate that the anxiolytic- and antidepressant-like activity of basimglurant is neurochemically distinct from current antidepressants, which cause a pronounced modulation of extracellular monoamine levels.

JPET Fast Forward. Published on February 9, 2015 as DOI: 10.1124/jpet.114.222463
This article has not been copyedited and formatted. The final version may differ from this version.

The work on novel glutamatergic antidepressant drug candidates also investigates ligands to other mGlu receptors, most notably mGlu2/3 antagonists (Sanacora et al., 2012; Krystal et al., 2013; Celanire et al., 2015). Literature and our own work suggests that mGlu2/3 inhibitors have procognitive properties in a range of preclinical models of short- and long-term memory, executive function, as well as impulse control (Higgins et al., 2004; Spinelli et al., 2005; Marek, 2010; Goeldner et al., 2013), which makes them interesting candidates to address cognitive deficits in MDD (Goeldner et al., 2013). For mGlu5 the situation is different, as studies conducted in wild-type animals suggest that mGlu5 NAM's in general have no procognitive properties (Petersen et al., 2002; Ballard et al., 2005; Ahnaou et al., 2014), while some reports suggest that a high level of mGlu5 receptor inhibition can cause cognitive impairment, at least in the context of certain diseases (Hsieh et al., 2012). In a disease context outside of MDD, in FXS and autism, however, procognitive effects of mGlu5 inhibition have been reported (Michalon et al., 2014a; Seese et al., 2014). It currently remains an open question if the effective reduction of depressive symptoms, and of apathy/lethargy and lack of motivation e.g. by an mGlu5 inhibitor could result in an improved cognitive functioning in MDD patients. Cognitive deficits in MDD in general have received little attention to date which is in part due to the fact that commonly used rating scales such as MADRS and QIDS don't capture cognitive function very well. The picture is further complicated by the discrepancy between self-reported and objectively measured cognitive deficits in depressed patients, and by an apparent disconnect between the severity of depressive symptoms and cognitive functioning (Goeldner et al., 2013). Here the possible interplay especially between attention and executive function on the one side and symptoms of apathy/lethargy and motivation in depression on the other side warrants further investigation.

When comparing the profile of basimglurant to conventional antidepressants, similar antidepressant-like activity in the rodent behavioral procedures employed in the current studies were found including CMS-induced anhedonia and the forced swim test, as well as in the rat fMRI profile are found. Basimglurant showed consistent anxiolytic-like properties in four different rodent procedures sensitive to anxiolytic drugs such as benzodiazepines. By comparison, conventional antidepressants are reported to be mostly inactive in rodent behavioral models of anxiety (Bespalov et al., 2010) while they are effectively used clinically for the treatment of various forms of anxiety, often transiently combined with other anxiolytic drugs such as benzodiazepines during the initial phase of antidepressant treatment (O'Donnel and Shelton, 2011). Basimglurant shows antinociceptive properties in some procedures, and conventional antidepressants such

JPET Fast Forward. Published on February 9, 2015 as DOI: 10.1124/jpet.114.222463
This article has not been copyedited and formatted. The final version may differ from this version.

as duloxetine also show antinociceptive properties in preclinical models of pain (e.g. Bennett model of cold allodynia, Fig. 8D). Several classes of antidepressants including tryciclic antidepressants, SSRI's, SNRI's and SSRI/SNRI's are indeed used clinically for the treatment of pain (Dharmshaktu et al., 2012; Mika et al., 2013). With respect to sleep and sleepiness, conventional antidepressants typically don't show wake-promoting properties, and sedation is a major area of side effects for many antidepressant drugs (O'Donnel and Shelton, 2011). Basimglurant on the other hand showed sustained wake-promoting properties which occured on a consolidated fashion without induction of rebound somnolence. In light of the complexity of MDD symptoms it is conceivable that the pharmacotherapy of choice might differ considerably depending on the combinations of symptoms presented by the individual patient. It is expected that the outcome of the recently concluded MARIGOLD trial in depression (Quiroz et al., 2014) and future clinical research will reveal how basimglurant compares clinically to antidepressant drugs currently in use.

Collectively the preclinical profile presented here demonstrates that basimglurant is a potent and selective mGlu5 NAM with excellent drug-like properties supportive of once-daily dosing. The *in vivo* pharmacology including its antidepressant- and anxiolytic-like properties combined with the antinociceptive and wake-promoting activity make basimglurant a promising, mechanistically differentiated antidepressant drug candidate with the potential to address important comorbidities of MDD including anxiety and pain, as well as daytime sleepiness and apathy or lethargy.

JPET Fast Forward. Published on February 9, 2015 as DOI: 10.1124/jpet.114.222463
This article has not been copyedited and formatted. The final version may differ from this version.

Acknowledgements

For their excellent contributions and technical assistance we thank Catherine Diener and Christophe Fischer (*in vitro* pharmacology); Daniel Rüher, Antonio Ricci, and Daniel Tännler (chemical synthesis of basimglurant); Roland Degen, Karina Müller, and Mathias Müller ([^{3}H]- and [^{14}C]-basimglurant, and [^{3}H]-ABP688 radiosynthesis); Patricia Glaentzlin and Céline Sutter (*in vivo* binding); Marius Hoener, Sylvie Chabos, Daniele Buchy, Paricher Malherbe, Anne Marcuz, Christoph Ullmer, Anja Osterwald, Silvia Gatti, Monique Dellenbach, and Jennifer Beck (contributions to the *in vitro* selectivity profiling); Roland Mory, Patrick Mortas, Martine Maco, Marie Haman, Roger Wyler, Brigitte Algeyer, Severine Bandinelli, Francoise Kahn, Sean Durkin, and Audrey Genet (behavioral pharmacology); Stephanie Schöppenthau and Thomas Bilser (fMRI imaging and image processing); Thomas Thelly and Regina Moog (formulations); Stefan Kirchner (*in vitro* micronucleation test); Quan-Ming Zhu, and Anthony Ford and their colleagues (Bennet model of cold allodynia; models of overactive bladder); Vincent Castagne, Karelle Davoust, and Paul Moser and their colleagues at Porsolt & Partners Pharmacology, France (formalin-induced pain procedure; Chung model of neuropathic pain); Helen Rowley, Sharon Chetam, and Richard Brammer and their colleagues at Renasci Ltd., UK (microdialysis). We further thank Luca Santarelli, Anirvan Ghosh, and Paulo Fontoura for their continued invaluable support of the project.

JPET Fast Forward. Published on February 9, 2015 as DOI: 10.1124/jpet.114.222463
This article has not been copyedited and formatted. The final version may differ from this version.

Authorship contributions

Participated in research design: L.L., R.P. J.G.W., B.K., M.S., S.R.M., T.S.K., S.K., E.B., U.N., J.-L.M., E.P., W.S., G.J.

Conducted experiments: L.L., R.P., B.K., A.C.H., A.P., C.F., A.G., L.P., U.N., S.R.M., E.V., S.K., T.H., M.H., E.B., J.-L.M., W.S., G.J.

Performed data analysis: L.L., R.P., S.H.S., B.K., A.B., A.C.H., A.P., C.F., M.S., N.J.P., L.P., U.N., S.R.M., T.S.K., E.B., J.-L.M., W.S.

Wrote or contributed to the writing of the manuscript: L.L., S.H.S., B.K., A.B., M.v.K., M.S., T.S.K., W.S., J.G.W., G.J.

Contributed new tools or reagents: S.R.M., T.S.K., S.K., J.W., T.H., G.J.

JPET Fast Forward. Published on February 9, 2015 as DOI: 10.1124/jpet.114.222463
This article has not been copyedited and formatted. The final version may differ from this version.

References

Ahmadi N, Saleh P and Shapiro CM (2010) The association between sleep disorders and depression: Implications for treatment, in *Sleep and Mental Illness* (S.R. Pandi Perumal MK ed) pp 165-172, Cambridge University Press, New York.

Ahnaou A, Langlois X, Steckler T, Bartolome-Nebreda JM and Drinkenburg WH (2014) Negative versus positive allosteric modulation of metabotropic glutamate receptors (mGluR5): indices for potential pro-cognitive drug properties based on EEG network oscillations and sleep-wake organization in rats. *Psychopharmacology*.

Albertini S and Gocke E (1988) Plasmid copy number and mutant frequencies in S. typhimurium TA102. *Environ Mol Mutagen* **12**:353-363.

Alsop DC and Detre JA (1996) Reduced transit-time sensitivity in noninvasive magnetic resonance imaging of human cerebral blood flow. *J Cereb Blood Flow Metab* **16**:1236-1249.

Ametamey SM, Kessler LJ, Honer M, Wyss MT, Buck A, Hintermann S, Auberson YP, Gasparini F and Schubiger PA (2006) Radiosynthesis and preclinical evaluation of 11C-ABP688 as a probe for imaging the metabotropic glutamate receptor subtype 5. *J Nucl Med* **47**:698-705.

Ametamey SM, Treyer V, Streffer J, Wyss MT, Schmidt M, Blagoev M, Hintermann S, Auberson Y, Gasparini F, Fischer UC and Buck A (2007) Human PET studies of metabotropic glutamate receptor subtype 5 with 11C-ABP688. *J Nucl Med* **48**:247-252.

Aronica E, Gorter JA, Ijlst-Keizers H, Rozemuller AJ, Yankaya B, Leenstra S and Troost D (2003) Expression and functional role of mGluR3 and mGluR5 in human astrocytes and glioma cells: opposite regulation of glutamate transporter proteins. *Eur J Neurosci* **17**:2106-2118.

Ballard TM, Woolley ML, Prinssen E, Huwyler J, Porter R and Spooren W (2005) The effect of the mGlu5 receptor antagonist MPEP in rodent tests of anxiety and cognition: a comparison. *Psychopharmacology* **179**:218-229.

Basile AS, Janowsky A, Golembiowska K, Kowalska M, Tam E, Benveniste M, Popik P, Nikiforuk A, Krawczyk M, Nowak G, Krieter PA, Lippa AS, Skolnick P and Koustova E (2007) Characterization of the Antinociceptive Actions of Bicifadine in Models of Acute, Persistent, and Chronic Pain. *Journal of Pharmacology and Experimental Therapeutics* **321**:1208-1225.

Bassoni DL, Jafri Q, Sastry S, Mathrubutham M and Wehrman TS (2012) Characterization of G-protein coupled receptor modulators using homogeneous cAMP assays. *Methods Mol Biol* **897**:171-180.

Beitinger ME and Fulda S (2010) Long-term effects of antidepressants on sleep, in *Sleep and Mental Illness* (S.R. Pandi Perumal MK ed) pp 183-201, Cambridge University Press, New York.

Bennett GJ and Xie YK (1988) A peripheral mononeuropathy in rat that produces disorders of pain sensation like those seen in man. *PAIN* **33**:87-107.

Bespalov AY, van Gaalen MM and Gross G (2010) Antidepressant Treatment in Anxiety Disorder, in *Behavioral Neurobiology of Anxiety and Its Treatment* (Stein MB and Steckler T eds) pp 361-390, Springer, New York.

Blok BF (2002) Central pathways controlling micturition and urinary continence. *Urology* **59**:13-17.

Borbely AA and Tobler I (2011) Manifestations and functional implications of sleep homeostasis. *Handb Clin Neurol* **98**:205-213.

Bruns A, Kunnecke B, Risterucci C, Moreau JL and von Kienlin M (2009) Validation of cerebral blood perfusion imaging as a modality for quantitative pharmacological MRI in rats. *Magn Reson Med* **61**:1451-1458.

Buettelmann B, Ceccarelli SM, Jaeschke G, Kolczewski S, Porter RHP, Vieira E, Ford APDW and Zhong Y (2005) Imidazole derivatives in *US 2005/0143375 A1* (EPO ed) p 19, F. HOFFMANN-LA ROCHE AG, US.

Busse CS, Brodkin J, Tattersall D, Anderson JJ, Warren N, Tehrani L, Bristow LJ, Varney MA and Cosford ND (2004) The behavioral profile of the potent and selective mGlu5 receptor antagonist 3-[(2-methyl-1,3-thiazol-4-yl)ethynyl]pyridine (MTEP) in rodent models of anxiety. *Neuropsychopharmacology* **29**:1971-1979.

Cavas M, Scesa G and Navarro JF (2013) Effects of MPEP, a selective metabotropic glutamate mGlu5 ligand, on sleep and wakefulness in the rat. *Prog Neuropsychopharmacol Biol Psychiatry* **40**:18-25.

Celanire S, Sebhat I, Wichmann J, Mayer S, Schann S and Gatti S (2015) Novel metabotropic glutamate receptor 2/3 antagonists and their therapeutic applications: a patent review (2005 - present). *Expert Opin Ther Pat* **25**:69-90.

Cosford NDP, Tehrani L, Roppe J, Schweiger E, Smith ND, Anderson J, Bristow L, Brodkin J, Jiang X, McDonald I, Rao S, Washburn M and Varney MA (2002) 3-[(2-Methyl-1,3-thiazol-4-yl)ethynyl]- pyridine: □ A Potent and Highly Selective Metabotropic Glutamate Subtype 5 Receptor Antagonist with Anxiolytic Activity. *Journal of medicinal chemistry* **46**:204-206.

Covington HE, 3rd, Vialou V and Nestler EJ (2010) From synapse to nucleus: novel targets for treating depression. *Neuropharmacology* **58**:683-693.

Crock LW, Stemler KM, Song DG, Abbosh P, Vogt SK, Qiu CS, Lai HH, Mysorekar IU and Gereau RWt (2012) Metabotropic glutamate receptor 5 (mGluR5) regulates bladder nociception. *Mol Pain* **8**:20.

Cryan JF and Lucki I (2000) Antidepressant-like behavioral effects mediated by 5-Hydroxytryptamine(2C) receptors. *J Pharmacol Exp Ther* **295**:1120-1126.

Dang K, Naeem S, Walker K, Bowery NG and Urban L (2002) Interaction of group I mGlu and NMDA receptor agonists within the dorsal horn of the spinal cord of the juvenile rat. *British journal of pharmacology* **136**:248-254.

Deichmann R, Hahn D and Haase A (1999) Fast T1 mapping on a whole-body scanner. *Magn Reson Med* **42**:206-209.

Dharmshaktu P, Tayal V and Kalra BS (2012) Efficacy of antidepressants as analgesics: a review. *J Clin Pharmacol* **52**:6-17.

Dickenson AH, Chapman V and Green GM (1997) The pharmacology of excitatory and inhibitory amino acid-mediated events in the transmission and modulation of pain in the spinal cord. *Gen Pharmacol* **28**:633-638.

Duman RS (2014) Neurobiology of stress, depression, and rapid acting antidepressants: remodeling synaptic connections. *Depress Anxiety* **31**:291-296.

Fitch WL, Chen Y, Liu L, Paehler A and Young M (2010) Application of Modern Drug Metabolism Structure Determination Tools and Assays to the In vitro Metabolism of Imiloxan. *Drug Metab Lett* **4**:77-87.

Fleury A, Lave T, Jonsson F, Schmitt M, Hirkaler G, Polonchuk L and Breidenbach A (2011) A pharmacokinetic-pharmacodynamic model for cardiovascular safety assessment of R1551. *J Pharmacol Toxicol Methods* **63**:123-133.

Gasparini F, Bilbe G, Gomez-Mancilla B and Spooren W (2008) mGluR5 antagonists: discovery, characterization and drug development. *Curr Opin Drug Discov Devel* **11**:655-665.

Gasparini F, Lingenhohl K, Stoehr N, Flor PJ, Heinrich M, Vranesic I, Biollaz M, Allgeier H, Heckendorn R, Urwyler S, Varney MA, Johnson EC, Hess SD, Rao SP, Sacaan AI, Santori EM, Velicelebi G and Kuhn R (1999) 2-Methyl-6-(phenylethynyl)-pyridine (MPEP), a potent, selective and systemically active mGlu5 receptor antagonist. *Neuropharmacology* **38**:1493-1503.

Goeldner C, Ballard TM, Knoflach F, Wichmann J, Gatti S and Umbricht D (2013) Cognitive impairment in major depression and the mGlu2 receptor as a therapeutic target. *Neuropharmacology* **64**:337-346.

Grippo AJ, Francis J, Beltz TG, Felder RB and Johnson AK (2005) Neuroendocrine and cytokine profile of chronic mild stress-induced anhedonia. *Physiol Behav* **84**:697-706.

Haase A, Frahm J, Matthaei D, Hanicke W and Merboldt KD (2011) FLASH imaging: rapid NMR imaging using low flip-angle pulses. 1986. *J Magn Reson* **213**:533-541.

Hamon M and Blier P (2013) Monoamine neurocircuitry in depression and strategies for new treatments. *Prog Neuropsychopharmacol Biol Psychiatry* **45**:54-63.

Harvey BD, Siok CJ, Kiss T, Volfson D, Grimwood S, Shaffer CL and Hajos M (2013) Neurophysiological signals as potential translatable biomarkers for modulation of metabotropic glutamate 5 receptors. *Neuropharmacology* **75**:19-30.

Hennig J, Nauerth A and Friedburg H (1986) RARE imaging: a fast imaging method for clinical MR. *Magn Reson Med* **3**:823-833.

Higgins GA, Ballard TM, Kew JN, Richards JG, Kemp JA, Adam G, Woltering T, Nakanishi S and Mutel V (2004) Pharmacological manipulation of mGlu2 receptors influences cognitive performance in the rodent. *Neuropharmacology* **46**:907-917.

Hill MN, Hellemans KG, Verma P, Gorzalka BB and Weinberg J (2012) Neurobiology of chronic mild stress: parallels to major depression. *Neurosci Biobehav Rev* **36**:2085-2117.

Hintermann S, Vranesic I, Allgeier H, Brulisauer A, Hoyer D, Lemaire M, Moenius T, Urwyler S, Whitebread S, Gasparini F and Auberson YP (2007) ABP688, a novel selective and high affinity ligand for the labeling of mGlu5 receptors: identification, in vitro pharmacology, pharmacokinetic and biodistribution studies. *Bioorg Med Chem* **15**:903-914.

Ho Kim S and Mo Chung J (1992) An experimental model for peripheral neuropathy produced by segmental spinal nerve ligation in the rat. *PAIN* **50**:355-363.

Holderbach R, Clark K, Moreau JL, Bischofberger J and Normann C (2007) Enhanced long-term synaptic depression in an animal model of depression. *Biol Psychiatry* **62**:92-100.

Houamed KM, Kuijper JL, Gilbert TL, Haldeman BA, O'Hara PJ, Mulvihill ER, Almers W and Hagen FS (1991) Cloning, expression, and gene structure of a G protein-coupled glutamate receptor from rat brain. *Science* **252**:1318-1321.

Hsieh MH, Ho SC, Yeh KY, Pawlak CR, Chang HM, Ho YJ, Lai TJ and Wu FY (2012) Blockade of metabotropic glutamate receptors inhibits cognition and neurodegeneration in an MPTP-induced Parkinson's disease rat model. *Pharmacol Biochem Behav* **102**:64-71.

Hu JH, Yang L, Kammermeier PJ, Moore CG, Brakeman PR, Tu J, Yu S, Petralia RS, Li Z, Zhang PW, Park JM, Dong X, Xiao B and Worley PF (2012) Preso1 dynamically regulates group I metabotropic glutamate receptors. *Nat Neurosci* **15**:836-844.

Hu Y, Dong L, Sun B, Guillon MA, Burbach LR, Nunn PA, Liu X, Vilenski O, Ford APDW, Zhong Y and Rong W (2009) The role of metabotropic glutamate receptor mGlu5 in control of micturition and bladder nociception. *Neurosci Lett* **450**:12-17.

Hughes ZA, Neal SJ, Smith DL, Sukoff Rizzo SJ, Pulicicchio CM, Lotarski S, Lu S, Dwyer JM, Brennan J, Olsen M, Bender CN, Kouranova E, Andree TH, Harrison JE, Whiteside GT, Springer D, O'Neil SV, Leonard SK, Schechter LE, Dunlop J, Rosenzweig-Lipson S and Ring RH (2013) Negative allosteric modulation of metabotropic glutamate receptor 5 results in broad spectrum activity relevant to treatment resistant depression. *Neuropharmacology* **66**:202-214.

Hunter JC, Gogas KR, Hedley LR, Jacobson LO, Kassotakis L, Thompson J and Fontana DJ (1997) The effect of novel anti-epileptic drugs in rat experimental models of acute and chronic pain. *Eur J Pharmacol* **324**:153-160.

Hysek CM, Simmler LD, Nicola VG, Vischer N, Donzelli M, Krahenbuhl S, Grouzmann E, Huwyler J, Hoener MC and Liechti ME (2012) Duloxetine inhibits effects of MDMA ("ecstasy") in vitro and in humans in a randomized placebo-controlled laboratory study. *PLoS One* **7**:e36476.

Jaeschke G, Kolczewski S, Spooren W, Vieira E, Bitter-Stoll N, Boissin P, Borroni E, Buttelmann B, Ceccarelli S, Clemann N, David B, Funk C, Guba W, Harrison A, Hartung T, Honer M, Huwyler J, Kuratli M, Niederhauser U, Pahler A, Peters JU, Petersen A, Prinssen E, Ricci A, Rueher D, Rueher M, Schneider M, Spurr P, Stoll T, Tannler D, Wichmann J, Porter RH, Wettstein JG and Lindemann L (2015) Metabotropic Glutamate Receptor 5 Negative Allosteric Modulators: Discovery of 2-Chloro-4-[1-(4-fluorophenyl)-2,5-dimethyl-1H-imidazol-4-ylethynyl]pyridine (Basimglurant, RO4917523), a Promising Novel Medicine for Psychiatric Diseases. *Journal of medicinal chemistry*.

Jaeschke G, Wettstein JG, Nordquist RE and Spooren W (2008) mGlu5 receptor antagonists and their therapeutic potential. *Expert Opin Ther Pat* **18**:123-142.

Kakizaki H, Yoshiyama M, Roppolo JR, Booth AM and De Groat WC (1998) Role of spinal glutamatergic transmission in the ascending limb of the micturition reflex pathway in the rat. *J Pharmacol Exp Ther* **285**:22-27.

Kirchner S and Zeller A (2010) Comparison of different cytotoxicity measures for the in vitro micronucleus test (MNVit) in L5178Y tk(+/-) cells: Summary of 4 compounds (Mitomycin C, Cyclophosphamide, Colchicine and Diethylstilboestrol) with clastogenic and aneugenic mode of action. *Mutat Res* **702**:193-198.

Krueger DD and Bear MF (2011) Toward fulfilling the promise of molecular medicine in fragile X syndrome. *Annu Rev Med* **62**:411-429.

Krystal JH, Sanacora G and Duman RS (2013) Rapid-acting glutamatergic antidepressants: the path to ketamine and beyond. *Biol Psychiatry* **73**:1133-1141.

Kubera C, Hernandez AL, Heng V and Bordey A (2012) Transient mGlu5R inhibition enhances the survival of granule cell precursors in the neonatal cerebellum. *Neuroscience* **219**:271-279.

Kupfer DJ, Frank E and Phillips ML (2012) Major depressive disorder: new clinical, neurobiological, and treatment perspectives. *Lancet* **379**:1045-1055.

Kuwajima M, Hall RA, Aiba A and Smith Y (2004) Subcellular and subsynaptic localization of group I metabotropic glutamate receptors in the monkey subthalamic nucleus. *J Comp Neurol* **474**:589-602.

Larson JA, Ogagan PD, Chen G, Shen B, Wang J, Roppolo JR, de Groat WC and Tai C (2011) Involvement of metabotropic glutamate receptor 5 in pudendal inhibition of nociceptive bladder activity in cats. *J Physiol* **589**:5833-5843.

Li X, Need AB, Baez M and Witkin JM (2006) Metabotropic glutamate 5 receptor antagonism is associated with antidepressant-like effects in mice. *J Pharmacol Exp Ther* **319**:254-259.

Lindemann L, Jaeschke G, Michalon A, Vieira E, Honer M, Spooren W, Porter R, Hartung T, Kolczewski S, Buttelmann B, Flament C, Diener C, Fischer C, Gatti S, Prinssen EP, Parrott N, Hoffmann G and Wettstein JG (2011) CTEP: a novel, potent, long-acting, and orally bioavailable metabotropic glutamate receptor 5 inhibitor. *J Pharmacol Exp Ther* **339**:474-486.

Liu CY, Jiang XX, Zhu YH and Wei DN (2012) Metabotropic glutamate receptor 5 antagonist 2-methyl-6-(phenylethynyl)pyridine produces antidepressant effects in rats: role of brain-derived neurotrophic factor. *Neuroscience* **223**:219-224.

Lopes SC, da Silva AV, Arruda BR, Morais TC, Rios JB, Trevisan MT, Rao VS and Santos FA (2013) Peripheral antinociceptive action of mangiferin in mouse models of experimental pain: role of endogenous opioids, K(ATP)-channels and adenosine. *Pharmacol Biochem Behav* **110**:19-26.

Lujan R, Roberts JD, Shigemoto R, Ohishi H and Somogyi P (1997) Differential plasma membrane distribution of metabotropic glutamate receptors mGluR1 alpha, mGluR2 and mGluR5, relative to neurotransmitter release sites. *J Chem Neuroanat* **13**:219-241.

Marek GJ (2010) Metabotropic glutamate2/3 (mGlu2/3) receptors, schizophrenia and cognition. *European journal of pharmacology* **639**:81-90.

Masu M, Tanabe Y, Tsuchida K, Shigemoto R and Nakanishi S (1991) Sequence and expression of a metabotropic glutamate receptor. *Nature* **349**:760-765.

Mayers AG and Baldwin DS (2005) Antidepressants and their effect on sleep. *Hum Psychopharmacol* **20**:533-559.

Michalon A, Bruns A, Risterucci C, Honer M, Ballard TM, Ozmen L, Jaeschke G, Wettstein JG, von Kienlin M, Kunnecke B and Lindemann L (2014a) Chronic metabotropic glutamate receptor 5 inhibition corrects local alterations of brain activity and improves cognitive performance in fragile X mice. *Biol Psychiatry* **75**:189-197.

Michalon A, Bruns A, Risterucci C, Honer M, Ballard TM, Ozmen L, Jaeschke G, Wettstein JG, von Kienlin M, Künnecke B and Lindemann L (2014b) Chronic Metabotropic Glutamate Receptor 5 Inhibition Corrects Local Alterations of Brain Activity and Improves Cognitive Performance in Fragile X Mice. *Biol Psychiatry* **75**:189-197.

Michalon A, Sidorov M, Ballard TM, Ozmen L, Spooren W, Wettstein JG, Jaeschke G, Bear MF and Lindemann L (2012) Chronic pharmacological mGlu5 inhibition corrects fragile X in adult mice. *Neuron* **74**:49-56.

Mika J, Zychowska M, Makuch W, Rojewska E and Przewlocka B (2013) Neuronal and immunological basis of action of antidepressants in chronic pain - clinical and experimental studies. *Pharmacol Rep* **65**:1611-1621.

Monteggia LM (2011) Toward neurotrophin-based therapeutics. *Am J Psychiatry* **168**:114-116.

Morairty SR, Hedley L, Flores J, Martin R and Kilduff TS (2008) Selective 5HT2A and 5HT6 receptor antagonists promote sleep in rats. *Sleep* **31**:34-44.

Moreau JL (2002) Simulating the anhedonia symptom of depression in animals. *Dialogues Clin Neurosci* **4**:351-360.

Moreau JL, Bos M, Jenck F, Martin JR, Mortas P and Wichmann J (1996) 5HT2C receptor agonists exhibit antidepressant-like properties in the anhedonia model of depression in rats. *Eur Neuropsychopharmacol* **6**:169-175.

Moreau JL, Jenck F, Martin JR, Mortas P and Haefely WE (1992) Antidepressant treatment prevents chronic unpredictable mild stress-induced anhedonia as assessed by ventral tegmentum self-stimulation behavior in rats. *Eur Neuropsychopharmacol* **2**:43-49.

Moreau JL, Scherschlicht R, Jenck F and Martin JR (1995) Chronic mild stress-induced anhedonia model of depression; sleep abnormalities and curative effects of electroshock treatment. *Behav Pharmacol* **6**:682-687.

Muster W, Albertini S and Gocke E (2003) Structure-activity relationship of oxadiazoles and allylic structures in the Ames test: an industry screening approach. *Mutagenesis* **18**:321-329.

Nestler EJ, Barrot M, DiLeone RJ, Eisch AJ, Gold SJ and Monteggia LM (2002) Neurobiology of depression. *Neuron* **34**:13-25.

Nestler EJ and Hyman SE (2010) Animal models of neuropsychiatric disorders. *Nat Neurosci* **13**:1161-1169.

O'Donnel JM and Shelton RC (2011) Drug therapy of depression and anxiety disorders, in *Goodman and Gilman's The Pharmacologiccal Basis of Therapeutics* (Brunteon LL ed) pp 397-416, McGraw-Hill Professional, New York.

Paxinos G WC (1986) *The rat brain in stereotaxic coordinates.* Academic Press, Sydney, Australia.

Pecknold JC, McClure DJ, Appeltauer L, Wrzesinski L and Allan T (1982) Treatment of anxiety using fenobam (a nonbenzodiazepine) in a double-blind standard (diazepam) placebo-controlled study. *J Clin Psychopharmacol* **2**:129-133.

Petersen S, Bomme C, Baastrup C, Kemp A and Christoffersen GR (2002) Differential effects of mGluR1 and mGlur5 antagonism on spatial learning in rats. *Pharmacol Biochem Behav* **73**:381-389.

Petrov D, Pedros I, de Lemos ML, Pallas M, Canudas AM, Lazarowski A, Beas-Zarate C, Auladell C, Folch J and Camins A (2014) Mavoglurant as a treatment for Parkinson's disease. *Expert Opin Inv Drug*:1-15.

Piers TM, Kim DH, Kim BC, Regan P, Whitcomb DJ and Cho K (2012) Translational Concepts of mGluR5 in Synaptic Diseases of the Brain. *Front Pharmacol* **3**:199.

Pilc A, Klodzinska A, Branski P, Nowak G, Palucha A, Szewczyk B, Tatarczynska E, Chojnacka-Wojcik E and Wieronska JM (2002) Multiple MPEP administrations evoke anxiolytic- and antidepressant-like effects in rats. *Neuropharmacology* **43**:181-187.

Platt DM, Rowlett JK and Spealman RD (2008) Attenuation of cocaine self-administration in squirrel monkeys following repeated administration of the mGluR5 antagonist MPEP: comparison with dizocilpine. *Psychopharmacology* **200**:167-176.

Porsolt RD, Anton G, Blavet N and Jalfre M (1978) Behavioural despair in rats: a new model sensitive to antidepressant treatments. *European journal of pharmacology* **47**:379-391.

Porter RH, Jaeschke G, Spooren W, Ballard TM, Buttelmann B, Kolczewski S, Peters JU, Prinssen E, Wichmann J, Vieira E, Muhlemann A, Gatti S, Mutel V and Malherbe P (2005) Fenobam: a clinically validated nonbenzodiazepine anxiolytic is a potent, selective, and noncompetitive mGlu5 receptor antagonist with inverse agonist activity. *J Pharmacol Exp Ther* **315**:711-721.

Quiroz JA, Tamburri P, Deptula D, Banken L, Beyer U, Fontoura P and Santarelli L (2014) The efficacy and safety of basimglurant as adjunctive therapy in major depression; a randomised, double-blind, placebo-controlled study. *European Neuropsychopharmacology* **24**:468.

Radulovic J and Tronson NC (2012) Preso1, mGluR5 and the machinery of pain. *Nat Neurosci* **15**:805-807.

Rowley HL, Kulkarni RS, Gosden J, Brammer RJ, Hackett D and Heal DJ (2014) Differences in the neurochemical and behavioural profiles of lisdexamfetamine methylphenidate and modafinil revealed by simultaneous dual-probe microdialysis and locomotor activity measurements in freely-moving rats. *J Psychopharmacol* **28**:254-269.

Russo SJ and Nestler EJ (2013) The brain reward circuitry in mood disorders. *Nat Rev Neurosci* **14**:609-625.

Sanacora G, Treccani G and Popoli M (2012) Towards a glutamate hypothesis of depression: an emerging frontier of neuropsychopharmacology for mood disorders. *Neuropharmacology* **62**:63-77.

Scharf SH, Jaeschke G, Wettstein JG and Lindemann L (2015) Metabotropic glutamate receptor 5 as drug target for Fragile X syndrome. *Curr Opin Pharmacol* **20C**:124-134.

Seese RR, Maske AR, Lynch G and Gall CM (2014) Long-term memory deficits are associated with elevated synaptic ERK1/2 activation and reversed by mGluR5 antagonism in an animal model of autism. *Neuropsychopharmacology* **39**:1664-1673.

Shigemoto R and Mizuno N (2000) Metabotropic glutamate receptors – immunocytochemical and in situ hybridization analyses., in *Handbook of Chemical Neuroanatomy: Glutamate* (Ottersen OP S-MJ ed) pp 63-98, Elsevier, Amsterdam, The Netherlands.

Spinelli S, Ballard T, Gatti-McArthur S, Richards GJ, Kapps M, Woltering T, Wichmann J, Stadler H, Feldon J and Pryce CR (2005) Effects of the mGluR2/3 agonist LY354740 on computerized tasks of attention and working memory in marmoset monkeys. *Psychopharmacology* **179**:292-302.

Spooren WPJM, Schoeffter P, Gasparini F, Kuhn R and Gentsch C (2002) Pharmacological and endocrinological characterisation of stress-induced hyperthermia in singly housed mice using classical and candidate anxiolytics (LY314582, MPEP and NKP608). *European journal of pharmacology* **435**:161-170.

Staner L, Staner C and Luthringer R (2010) Antidepressant-induced alteration of sleep EEG, in *Sleep and Mental Illness* (S.R. Pandi Perumal MK ed) pp 202-221, Cambridge University Press, New York.

Stocchi F, Rascol O, Destee A, Hattori N, Hauser RA, Lang AE, Poewe W, Stacy M, Tolosa E, Gao H, Nagel J, Merschhemke M, Graf A, Kenney C and Trenkwalder C (2013) AFQ056 in Parkinson patients with levodopa-induced dyskinesia: 13-week, randomized, dose-finding study. *Mov Disord* **28**:1838-1846.

Swedberg MD, Ellgren M and Raboisson P (2014) mGluR5 antagonist-induced psychoactive properties: MTEP drug discrimination, a pharmacologically selective non-NMDA effect with apparent lack of reinforcing properties. *J Pharmacol Exp Ther* **349**:155-164.

Tobler I and Borbely AA (1986) Sleep EEG in the rat as a function of prior waking. *Electroencephalogr Clin Neurophysiol* **64**:74-76.

Tokunaga M, Seneca N, Shin RM, Maeda J, Obayashi S, Okauchi T, Nagai Y, Zhang MR, Nakao R, Ito H, Innis RB, Halldin C, Suzuki K, Higuchi M and Suhara T (2009) Neuroimaging and physiological evidence for involvement of glutamatergic transmission in regulation of the striatal dopaminergic system. *J Neurosci* **29**:1887-1896.

Tronci V and Balfour DJ (2011) The effects of the mGluR5 receptor antagonist 6-methyl-2-(phenylethynyl)-pyridine (MPEP) on the stimulation of dopamine release evoked by nicotine in the rat brain. *Behav Brain Res* **219**:354-357.

Valles B, Schiller CD, Coassolo P, De Sousa G, Wyss R, Jaeck D, Viger-Chougnet A and Rahmani R (1995) Metabolism of mofarotene in hepatocytes and liver microsomes from different species. Comparison with in vivo data and evaluation of the cytochrome P450 isoenzymes involved in human biotransformation. *Drug Metab Dispos* **23**:1051-1057.

Vranesic I, Ofner S, Flor PJ, Bilbe G, Bouhelal R, Enz A, Desrayaud S, McAllister K, Kuhn R and Gasparini F (2014) AFQ056/mavoglurant, a novel clinically effective mGluR5 antagonist: Identification, SAR and pharmacological characterization. *Bioorg Med Chem*.

Williams DA (1971) A test for differences between treatment means when several dose levels are compared with a zero dose control. *Biometrics* **27**:103-117.

Williams DA (1972) The comparison of several dose levels with a zero dose control. *Biometrics* **28**:519-531.

Williams DS, Detre JA, Leigh JS and Koretsky AP (1992) Magnetic resonance imaging of perfusion using spin inversion of arterial water. *Proc Natl Acad Sci U S A* **89**:212-216.

Yoshiyama M, Nezu FM, Yokoyama O, Chancellor MB and de Groat WC (1999) Influence of glutamate receptor antagonists on micturition in rats with spinal cord injury. *Exp Neurol* **159**:250-257.

Zarate CA, Jr., Singh JB, Carlson PJ, Brutsche NE, Ameli R, Luckenbaugh DA, Charney DS and Manji HK (2006) A randomized trial of an N-methyl-D-aspartate antagonist in treatment-resistant major depression. *Arch Gen Psychiatry* **63**:856-864.

JPET Fast Forward. Published on February 9, 2015 as DOI: 10.1124/jpet.114.222463
This article has not been copyedited and formatted. The final version may differ from this version.

Footnotes

Financial disclosure

L.L, G.J, R.H.P., S.S., B.K, A.B., M.v.K., A.H., A.P., C.F., A.G., M.S., N.J.P., L.P., U.N., E.V., S.K., J.W., T.H., M.H., E.B., J.-L.M., E.P., W.S., and J.G.W. are full-time employees of F. Hoffmann-La Roche AG. S.R.M. and T.S.K. have received payments from F. Hoffmann-La Roche AG for the studies presented in this manuscript.

JPET Fast Forward. Published on February 9, 2015 as DOI: 10.1124/jpet.114.222463
This article has not been copyedited and formatted. The final version may differ from this version.

Figure legends

Fig. 1: Chemical structure of basimglurant, CTEP, MPEP, MTEP, and fenobam

Fig. 2: Activity of basimglurant on mGlu5 *in vitro*.

(A) Representative saturation analysis experiment with [^{3}H]-basimglurant on membranes of HEK293 cells transiently transfected with human mGlu5; **(B)** [^{3}H]-MPEP displacement binding of basimglurant on membranes of HEK293 cells transiently transfected with human, mouse, and rat mGlu5; **(C-D)** Inhibition of quisqualate-induced Ca^{2+} mobilization (C) and IP accumulation (D) in monoclonal HEK293 cell lines stably expressing human, mouse, or rat mGlu5; **(E)** Inverse agonism of basimglurant on human mGlu5 demonstrated by suppression of constitutive receptor activity measured by IP accumulation; **(F)** Basimglurant dose-dependently caused a right-shift and a reduction of the maximal signal amplitude of quisqualate concentration-response curves recorded in an IP accumulation assay on human mGlu5.

Data are mean ± SEM of N = 4-44 except for (A) and (F) which are representative single experiments.

Figure 3: Pharmacokinetic profile of basimglurant in rat and cynomolgus.

(A) Pharmacokinetic profile of basimglurant in rat after p.o. administration; **(B)** Pharmacokinetic profile of basimglurant in cynomologus after p.o. administration. Data are mean ± SD; N = 2-4 per species and route.

Fig. 4: Basimglurant [^{3}H]-ABP688 in receptor occupancy studies and [^{3}H]-basimglurant *in vivo* binding in rat.

(A) Outline of the [^{3}H]-ABP688 receptor occupancy experiment with p.o. administration of basimglurant 60 minutes prior to i.v. administration of the tracer followed by sacrifice and further processing of the animals 30 minutes after the tracer injection; **(B)** Relationship between basimglurant plasma exposure (total) and brain mGlu5 receptor occupancy quantified in three brain areas; **(C-D)** Representative autoradiographs of parasagittal brain sections from mice receiving vehicle (C) and the highest dose of basimglurant used in the experiment achieving full tracer displacement (D); **(E-F)** autoradiographs of parasagittal sections of rat brain (E) after a bolus injection of [^{3}H]-basimglurant and (F) of [^{3}H]-basimglurant followed by the administration of the mGlu5 NAM RO4623831 (Supplemental Table S2) at a dose of 10 mg/kg (p.o.).

JPET Fast Forward. Published on February 9, 2015 as DOI: 10.1124/jpet.114.222463
This article has not been copyedited and formatted. The final version may differ from this version.

Fig. 5: Basimglurant activity in the chronic mild stress-induced anhedonia- and the forced swim test.

(A) Chronic treatment of rats undergoing chronic mild stress with basimglurant and fluoxetine over a period of three weeks caused a reduction of the anhedonia index to values recorded prior to the chronic stress procedure. **(B)** Basimglurant and desipramine caused a reduction of the immobility time in the forced swim test in rats. Drug administration route is i.p. (A) and p.o. (B), respectively. Data are mean ± SEM of N = 7-8 animals per group. Statistics: *: $p<0.05$ versus vehicle based on a two-way repeated measures (A) and one-way (B) ANOVA followed by an unpaired t-test (A) and a Dunnett post hoc test (B). See Supplemental Table S3A-B for related numerical information.

Fig. 6: Brain activity pattern triggered by basimglurant in comparison to antidepressants revealed by fMRI.

(A-B) Brain activity pattern as revealed by fMRI upon dosing of basimglurant (1 and 10 mg/kg, p.o.) to Fischer rats displayed as 'bubble' plot in a schematic parasagittal brain section (A) and as 'spider' diagram (B). For reasons of clarity not all brain (sub-)regions displayed in the spider plot are represented in (A). **(C)** Quantitative comparison of the brain activity pattern of basimglurant with those of prototypical antidepressants with different modes-of-action and non-pharmacological interventions expressed as a scale-invariant pattern match coefficient (PMC).The PMC may assume values between 1 and -1. A PMC of 1 reflects full agreement, 0 no agreement and -1 identifies opposing patterns. Basimglurant at 10 mg/kg was taken as a reference. **(D)** Quantitative representation of the effect strength observed by fMRI for the respective interventions. The effect strength is given as root mean square (RMS) of the perfusion changes across 57 brain regions with reference to vehicle treated animals.
Drug administration was p.o. throughout, numbers in the bars (C-D) indicate drug doses administered in mg/kg. ECT: Electro-convulsive treatment; CMS: Chronic mild stress; Statistics: *: $p<0.05$, **: $p<0.01$, ***: $p<0.001$ versus vehicle; normalized perfusion values of each dose group were compared ROI-wise to those of the vehicle group using Welch's t-test in order to account for non-homogeneous variances. CA: Cornu ammonis; M1: Primary motor cortex; mPFC: Medial prefrontal cortex; S1: Primary somatosensory cortex; S2: Secondary somatosensory cortex

JPET Fast Forward. Published on February 9, 2015 as DOI: 10.1124/jpet.114.222463
This article has not been copyedited and formatted. The final version may differ from this version.

Fig. 7: Anxiolytic-like properties of basimglurant, fenobam, and diazepam.

Basimglurant, fenobam, and diazepam showed dose-dependent activities in a battery of rodent procedures sensitive to anxiolytic drugs. The minimal effective doses (i.e. lowest doses achieving a statistically significant effect) in the different tests were as follows:

(A) In the Vogel conflict drinking test, the minimal effective dose was 0.03 mg/kg for basimglurant and 30 mg/kg for fenobam and diazepam;

(B) In the stress-induced hyperthermia procedure, the minimal effective dose was 0.01 mg/kg for basimglurant, 10 mg/kg for fenobam, and 0.1 mg/kg for diazepam;

(C) In the conditioned emotional response procedure, the minimal effective dose was 0.3 mg/kg for basimglurant and 10 mg/kg for fenobam and diazepam;

(D) In the fear potentiated startle procedure, the minimal effective dose was 0.1 mg/kg for basimglurant, and 30 mg/kg for fenobam and diazepam.

Drug administration route is p.o. throughout. Data are mean ± SEM of (A) N = 11, (B) 15-34, (C) 11, and (D) 12-24 animals per group. Statistics: *: $p<0.05$, **: $p<0.01$, ***: $p<0.001$ versus vehicle; (A) Mann Whitney U tests (drug groups compared individually to vehicle), (B) Dunnett multiple comparison test versus vehicle following a one-way ANOVA, (C) ANOVA, followed by post hoc Dunnett's test, (D) Dunnett multiple comparison test versus vehicle following a one-way Anova test. See Supplemental Table S4A-D for related numerical information.

Fig. 8: Analgesic effects of basimglurant in rodent models of neuropathic pain.

(A-B) Formalin-induced neuropathic pain: Basimglurant (0.1 – 10.0 mg/kg, p.o.) dose-dependently inhibited formalin-induced neuropathic pain in the mouse not in (A) the early phase (i.e. basimglurant administrated 60 min before injection of formalin after which recording of paw-licking behavior starts immediately), but in (B) the late phase (i.e. basimglurant administrated 40 min before the formalin injection, recording of paw-licking behavior starts 20 min later). Morphine (64 mg/kg, p.o.) completely blocked formalin-induced neuropathic pain in the early and late phase.

(C) Chung model (spinal nerve ligature): Basimglurant (0.1 – 10.0 mg/kg, p.o.) had no significant effect on neuropathic pain induced by thermal stimulation in rats. Morphine (64 mg/kg, p.o.) almost completely blocked the neuropathic pain induced by thermal stimulation.

(D) Bennett model of cold allodynia: Basimglurant (0.1 – 10.0 mg/kg, s.c.) dose-dependently inhibited cold allodynia in rats. Morphine (1 mg/kg, s.c.) and duloxetine (3 mg/kg, s.c.) effectively blocked paw withdrawal.

Data are mean ± SEM of (A-B) N = 10, (C) N = 8, and (D) N = 12 animals per group. Statistics: *$p<0.05$, ** $p<0.01$ versus vehicle based on (A-B) Mann-Whitney U test versus vehicle, (C) Unpaired Student's t test versus vehicle, and (D) two-sample t test. See Supplemental Table S5A-D for related numerical information.

JPET Fast Forward. Published on February 9, 2015 as DOI: 10.1124/jpet.114.222463
This article has not been copyedited and formatted. The final version may differ from this version.

Fig. 9: EEG recordings in rats following repeated administration of basimglurant.

(A) Outline of the experiment with once-daily p.o. administration of basimglurant 2 h into the dark phase for 5 d, and recording of EEG traces after the fifth dose (the comparator caffeine was administrated as a single dose on day 5); **(B)** Cumulative REM/non-REM ratio calculated separately for the dark period (ZT 14-24) and the light-period (ZT 24-12); **(C-D)** Time spent in REM (C) and non-REM (D) activity over the entire recording period; **(E)** Latency to the first 6 continuous epochs of non-REM and the first 3 continuous epochs of REM sleep; **(F)** Hourly percent time spent in wake state; **(G)** Time course of non-REM delta power over the entire recording period; **(H)** Time course of locomotor activity over the entire recording period.

Drug administration is p.o. throughout. Data are mean ± SEM with N = 8 rats per group. Statistics: *: $p<0.05$ versus vehicle based on a one-way (B, F) and two-way ANOVA (C-E, G-H) followed by a two-tailed *post hoc* paired t-test was used. ZT: Zeitgeber time; ET: Experimental time (i.e. day time); Dark phase (i.e. active period) highlighted by gray shading. See Supplemental Table S6A-B for related numerical information.

Fig. 10: Effects of basimglurant and the SSRI paroxetine on extracellular levels of monoamine transmitters in rats.

Extracellular levels of monoamine neurotransmitters recorded by dual probe microdialysis in freely moving rats in **(A-C)** the frontal cortex (A) 5-HT; (B) dopamine; (C) norepinephrine), and **(D-E)** in the nucleus accumbens (D) 5-HT; (E) dopamine) before and after acute administration of basimglurant (0.1 and 1.0 mg/kg) and paroxetine (3 and 10 mg/kg).

Drug administration is p.o. throughout. Results are adjusted means ± SEM (see Materials and Methods) of N=5-10 per group. Dotted line indicates drug administration at t = 0 min. Statistics: *$p<0.05$, ** $p<0.01$ and *** $p<0.001$ versus vehicle. Data analyzed by ANCOVA with log(baseline) as covariate; multiple comparisons of each treatment to the control group by separate William' test. See Supplemental Table S7 for related numerical information.

Tables

Table 1: Basimglurant *in vitro* activity on recombinant mGlu5 in radioligand binding and functional assays

The potency of basimglurant on mGlu5 determined by [^{3}H]-basimglurant saturation analysis, [^{3}H]-MPEP competition binding, as well as by Ca^{2+} mobilization and IP accumulation assays. Data are mean ± SEM, with N = 4 for saturation isotherms, N = 16-44 for [^{3}H]-MPEP binding, and N = 6-22 for IP accumulation and Ca^{2+} mobilization, respectively.

	Radioligand binding			Functional assays	
	[^{3}H]-Basimglurant saturation isotherms		[^{3}H]-MPEP compet. binding	IP accumulation	Ca^{2+} mobilization
	Kd (nM)	Bmax (pmol/mg protein)	Ki (nM)	IC_{50} (nM)	IC_{50} (nM)
Human	1.11 ± 0.47	11.76 ± 1.06	35.6 ± 8.63	5.85 ± 2.08	7.0 ± 0.65
Mouse	0.42 ± 0.06	1.05 ± 0.13	29.5 ± 3.75	4.98 ± 0.35	8.88 ± 0.48
Rat	0.44 ± 0.03	3.79 ± 0.00	33.2 ± 6.94	5.93 ± 0.49	7.48 ± 0.34

Table 2: Selectivity profile of basimglurant.

Data generated at a single concentration of 10 μM (CEREP, DiscoverX) represent the mean of N = 2, Ki and IC_{50} values generated with a concentration range up to 10 μM basimglurant represent the mean of N = 2-6. Values are expressed as % control (for single concentration measurements) or as Ki or IC_{50} (for dose response measurements). Targets represented by radioligand binding as well as functional assays are marked with *.

Radioligand binding assays	Activity	
	% control	Ki (μM)
Receptors: Low molecular weight ligands		
Adenosine A_1 receptor (h) [a]	12%	
Adenosine A_{2A} receptor (h) [a]	7%	
Adenosine A_3 receptor (h) [a]	28%	
Adrenergic α_1 receptor (N.S.) (r) [a]	41%	
Adrenergic α_2 receptor (non-selective) (r) [a]	5%	
Adrenergic β_1 receptor (h) [a]	14%	
Adrenergic β_2 receptor (h) [a]	N.A.D.	
Cannabinoid receptor 1 (h) [a, *]		> 8.8
Cannabinoid receptor 2 (h) [a, *]		2.9
Dopamine D_1 receptor (h) [a]	14%	
Dopamine D_2 receptor (h) [a]	N.A.D.	
Dopamine D_3 receptor (h) [a]	9%	
Dopamine D_4 receptor (D4.4 variant) (h) [a]	10%	
Histamine H_1 receptor (h) [a]	21%	

Radioligand binding assays	Activity	
	% control	Ki (μM)
Receptors: Low molecular weight ligands (ctd.)		
Histamine H_2 receptor (h) [a]	14%	
Histamine H_3 receptor (r) [a]	11%	
Melanocortin receptor 4 (h) [a]	7%	
Muscarinic receptors (N.S.) (r) [a]	16%	
Muscarinic receptor 1 (h) [a]	12%	
Muscarinic receptor 2 (h) [a]	6%	
Muscarinic receptor 3 (h) [a]	N.A.D.	
Muscarinic receptor 4 (h) [a]	6%	
Muscarinic receptor 5 (h) [a]	7%	
Neurokinin receptor 1 (h) [a]	24%	
Neurokinin receptor 2 (h) [a]	13%	
Neurokinin receptor 3 (h) [a]	N.A.D.	
Opioid receptor (N.S.) (r) [a]	2%	
Purinergic P2X receptor (r) [a]	1%	

Table 2 (ctd.): Selectivity profile of basimglurant

Radioligand binding assays	Activity	
	% control	Ki (μM)
Receptors: Low molecular weight ligands (ctd.)		
Purinergic P2Y receptor (r) [a]	8%	
Serotonin receptor (N.S.) (r) [a]	2%	
Serotonin receptor 5-HT_{1A} (h) [a]	10%	
Serotonin receptor 5-HT_{1B} (r) [a]	34%	
Serotonin receptor 5-HT_{1D} (b) [a]	12%	
Serotonin receptor 5-HT_{2A} (h) [a]	4%	
Serotonin receptor 5-HT_{2B} (h) [a]	25%	
Serotonin receptor 5-HT_{2C} (h) [a]	4%	
Serotonin receptor 5-HT_{3} (h) [a]	9%	
Serotonin receptor 5-HT_{4c} (h) [a]	2%	
Serotonin receptor 5-HT_{5a} (h) [a]	7%	
Serotonin receptor 5-HT_{6} (h) [a]	N.A.D.	
Serotonin receptor 5-HT_{7} (h) [a]	23%	
Sigma receptor (N.S.) (r) [a]	7%	
Sigma receptor 1 (g) [a]	6%	
Sigma receptor 2 (r) [a]	22%	

Radioligand binding assays	Activity	
	% control	Ki (μM)
Receptors: Peptides and lipids		
Androgen receptor (h) [a]	N.A.D.	
Angiotensin receptor 1 (h) [a]	3%	
Angiotensin receptor 2 (h)	5%	
Arginine vasopressin receptor 1a (h) [a]	N.A.D.	
Arginine vasopressin receptor 2 (h) [a]	N.A.D.	
Bradykinin receptor B_1 (h) [a]	1%	
Bradykinin receptor B_2 (h) [a]	5%	
Cholecystokinin receptor type A (h) [a]	N.A.D.	
Cholecystokinin receptor type B (h) [a]	4%	
Corticotropin-releasing factor receptor 1 (r) [a]	N.A.D.	
Endothelin receptor type A (h) [a]	8%	
Endothelin receptor Type B (h) [a]	1%	
Estrogen receptor (non-selective) (h) [a]	N.A.D.	
Glucocorticoid receptor (h) [a]	1%	
Imidazoline I_1 receptor (b) [a]	2%	
Imidazoline I_2 receptor (r) [a]		> 6.7
Leukotriene D_4 receptor (CysLT1) (h) [a]	2%	

Table 2 (ctd.): Selectivity profile of basimglurant

Radioligand binding assays	Activity	
	% control	Ki (μM)
Receptors: Peptides and lipids (ctd.)		
Neuropeptide Y (non-selective) (r) [a]	6%	
Nociceptin receptor (h) [a]	2%	
Progesterone receptor (h) [a]	N.A.D.	
Somatostatin receptor (non-selective) (m) [a]	N.A.D.	
Thyrotropin releasing hormone receptor (r) [a]	6%	
Transporter		
Choline transporter (CHT1) (r) [a]	N.A.D.	
Dopamine transporter (h) [a, *]	31%	
GABA transporter (r) [a]	11%	
Norepinephrine transporter (h) [a, *]	11%	
Serotonin transporter (h) [a, *]	24%	
Ion channels		
Acetylcholine rec., nicotinic (α- BGTX insensitive) (r) [a]	N.A.D.	
AMPA-type glutamate receptor (r) [a]	N.A.D.	
Ca^{2+} channel, L-type (DHP site) (r) [a]	24%	
Ca^{2+} channel, L-type (diltiazem site) (r) [a]	13%	
Ca^{2+} channel, L-type (verapamil site) (r) [a]	2%	

Radioligand binding assays	Activity	
	% control	Ki (μM)
Ion channels (ctd.)		
Ca^{2+} channel, SK type (non-selective) (r) [a]	N.A.D.	
GABA (N.S.) (r) [a]	N.A.D.	
$GABA_A$ (central, flunitrazepam) (r) [a]	N.A.D.	
$GABA_A$ (central, TBPS) (r) [a]	N.A.D.	
$GABA_A$ (central, flumazenil) (r) [b]		> 3.2
$GABA_A$ (central, flumazenil; $\alpha_5\beta_3\gamma_2$) (h) [b]		> 3.2
K^+ channel, ATP sensitive (Kir6.2) (r) [a]	1%	
K^+ channel, voltage gated (α-DTX) (r) [a]	N.A.D.	
Na^+ channel (site 2) (r) [a]	28%	
Kainate glutamate receptor (r) [a]	7%	
NMDA glutamate receptor (r) [a]	N.A.D.	

Table 2 (ctd.): Selectivity profile of basimglurant

Functional assays	Activity	
	% control	IC_{50} (µM)
Acetylcholinesterase (h) [a]	8	
Adenylate cyclase (r) [a]	3	
Cannabinoid receptor 1 (h) [a, #, *]		> 10
Cannabinoid receptor 2 (h) [a, $, *]		1.7
Catechol-O-methyl transferase (COMT) (p) [a]	19	
Dopamine reuptake transporter (h) [b, *]		> 10
GABA transaminase (r) [a]	1	
Guanylate cyclase (b) [a]	1	
Metabotropic glutamate receptor 1 [b]		> 10
Metabotropic glutamate receptor 2 [b]		> 10
Metabotropic glutamate receptor 3 [c]		> 10
Metabotropic glutamate receptor 4 [b]		> 10
Metabotropic glutamate receptor 6 [c]		> 10
Metabotropic glutamate receptor 7 [b]		> 10

Functional assays	Activity	
	% control	IC_{50} (µM)
Metabotropic glutamate receptor 8 [b]		> 10
Monoaminoxidase A (h) [a]	1	
Monoaminoxidase B (h) [a]	12	
Na^+/K^+-ATPase (d) [a]	2	
Norepinephrine reuptake transporter (h) [b]		> 10
Phenylethanolamine N-methyl transferase (PNMT) (h) [a]	2	
Phosphodiesterase 1 (b) [a]	8	
Phosphodiesterase 2 (h) [a]	3	
Phosphodiesterase 3 (h) [a]	6	
Phosphodiesterase 4 (h) [a]	8	
Phosphodiesterase 5 (h) [a]	N.A.D.	
Protein kinase C (r) [a]	29	
Serotonin reuptake transporter (h) [b, *]		> 10
Tyrosine hydroxylase (r) [a]	5	

a: Data generated at CEREP; b: Data generated at F. Hoffmann-La Roche AG; c: Data generated at DiscoverX; N.A.D.: No activity detected; N.S.: non-selective; species designated in brackets after the target name: h: human, b: bovine, d: dog, g: guinea pig, m: mouse, p: porcine, r: rat; [#]: No activity in agonist-, antagonist-, inverse antagonist mode up to 10 µM; [$]: No agonist activity up to 10 µM, inverse agonist activity IC_{50} = 1.7 µM.

JPET Fast Forward. Published on February 9, 2015 as DOI: 10.1124/jpet.114.222463
This article has not been copyedited and formatted. The final version may differ from this version.

Table 3: Pharmacokinetic properties of basimglurant.

Pharmacokinetic properties of basimglurant in male adult rat and male non-human primate (mean of N = 2-4 per species and route), as well as mean plasma protein binding and intrinsic clearance (CL_{int}) in liver microsomes and hepatocytes from rat, non-human primate and human (mean of N ≥ 2 per species).

	rat	cynomolgus (fasted)	cynomolgus (fed)	human
Dose p.o. / i.v. (mg/kg)	3 / 1	0.3 / 1.0		
C_{max} (ng/ml)	240 [a]	76.5 [a]	36.1 [a]	
T_{max} (h)	2.3 [a]	1 [a]	2 [a]	
$T_{1/2}$ (h)	7.5 [a]	~20 [a]		
Clearance (ml/min/kg)	6.0 [b]	9.1 [b]		
V_{SS} (l/kg)	3.7 [b]	5.1 [b]		
Oral bioavailability, F (%)	42 [a, b]	~100% [a, b, c]	54 [a, b]	
Brain/Plasma ratio	1.7 – 2.9 [d]			
Protein binding (%) [e]	97.9	98.0		98.6
CL_{int} in microsomes [f] (µl/min/mg protein @ 1 µM)	10.9	14.1		6.43
CL_{int} in hepatocytes [f] (µl/min/10^6 cells @ 1 µM)	6.55	0.21		0.32

a, b: PK parameters derived following p.o. (a) and i.v. (b) administration; **c**: Estimate because i.v. and p.o. doses were not identical; **d:** Brain/plasma ratios obtained in the dose range of pharmacodynamic and pharmacokinetic studies; **e:** Pooled plasma; **f:** Pooled from male animals or from male and female human donors.

JPET Fast Forward. Published on February 9, 2015 as DOI: 10.1124/jpet.114.222463
This article has not been copyedited and formatted. The final version may differ from this version.

Figure 1

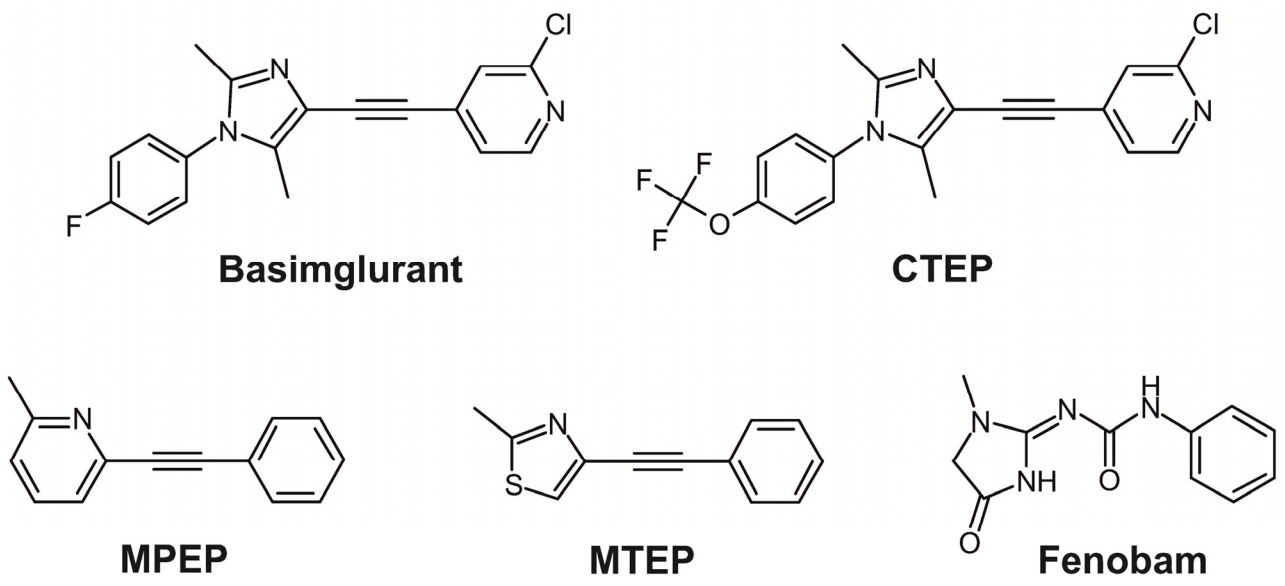

JPET Fast Forward. Published on February 9, 2015 as DOI: 10.1124/jpet.114.222463
This article has not been copyedited and formatted. The final version may differ from this version.

Figure 2

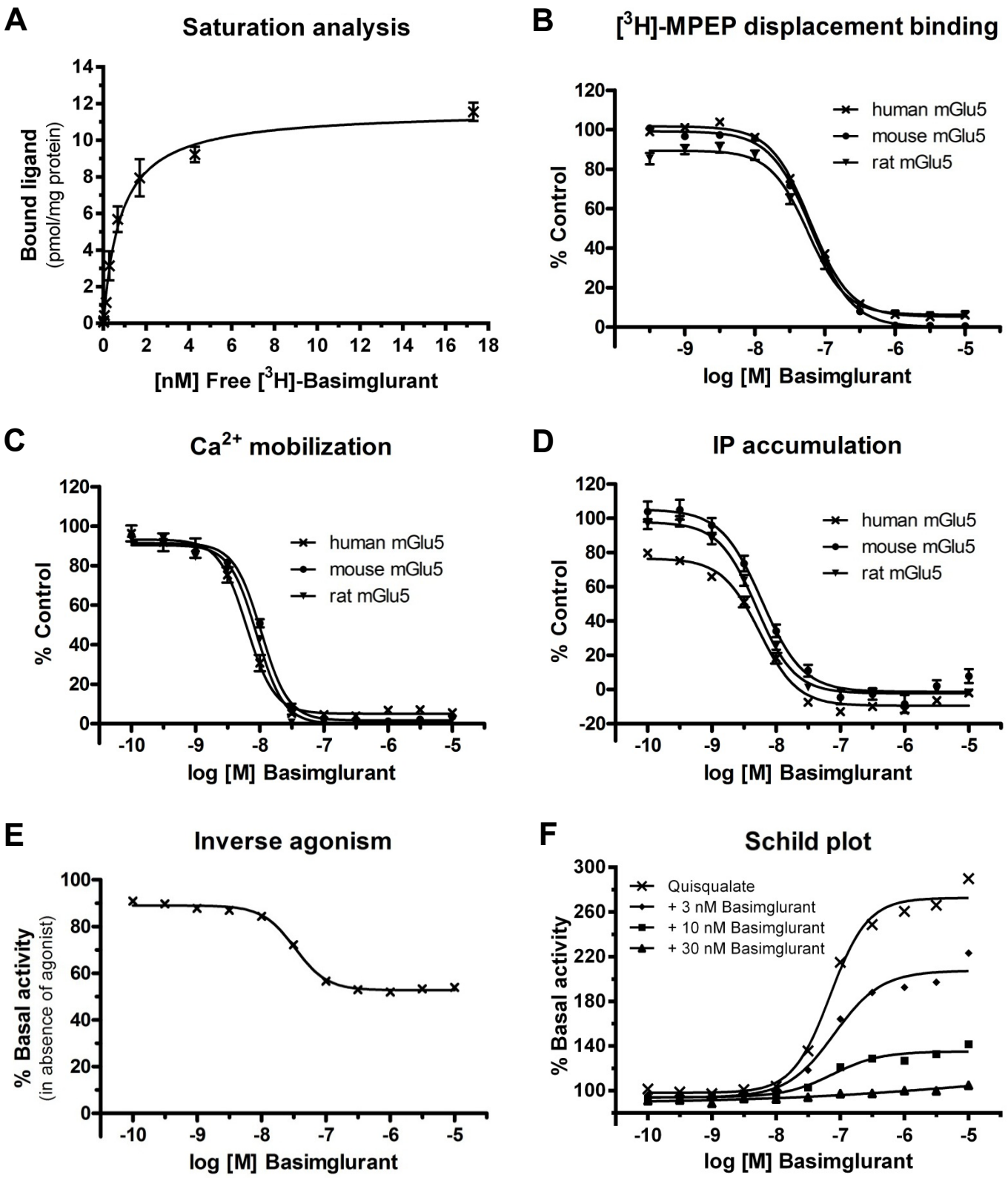

JPET Fast Forward. Published on February 9, 2015 as DOI: 10.1124/jpet.114.222463
This article has not been copyedited and formatted. The final version may differ from this version.

Figure 3

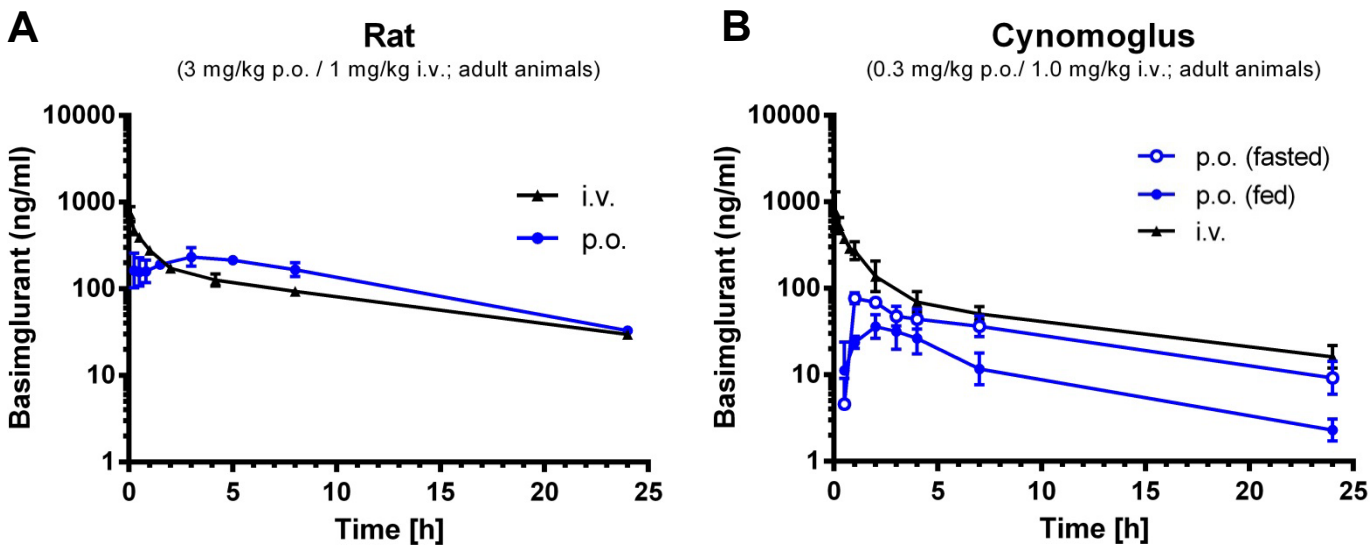

JPET Fast Forward. Published on February 9, 2015 as DOI: 10.1124/jpet.114.222463
This article has not been copyedited and formatted. The final version may differ from this version.

Figure 4

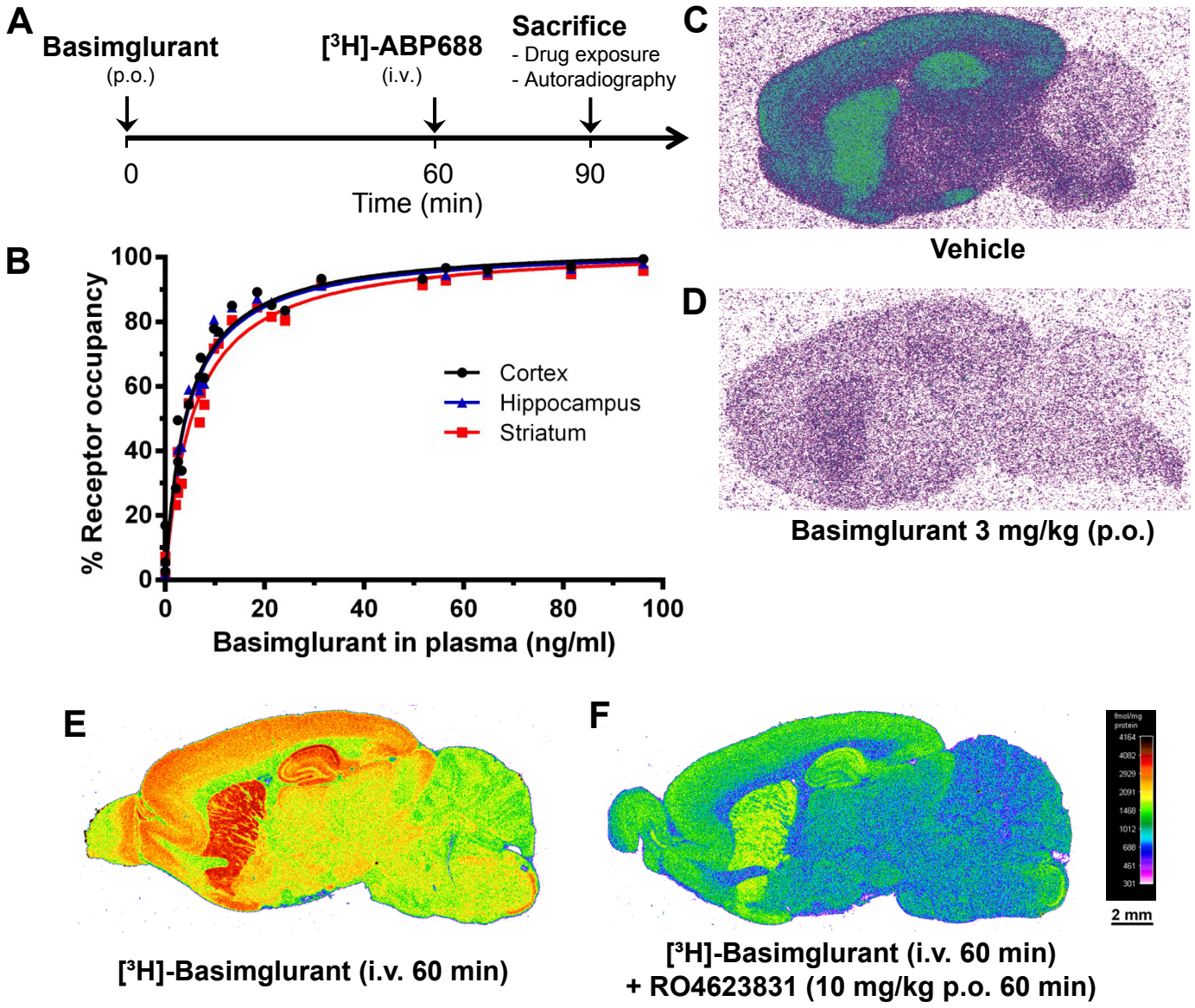

JPET Fast Forward. Published on February 9, 2015 as DOI: 10.1124/jpet.114.222463
This article has not been copyedited and formatted. The final version may differ from this version.

Figure 5

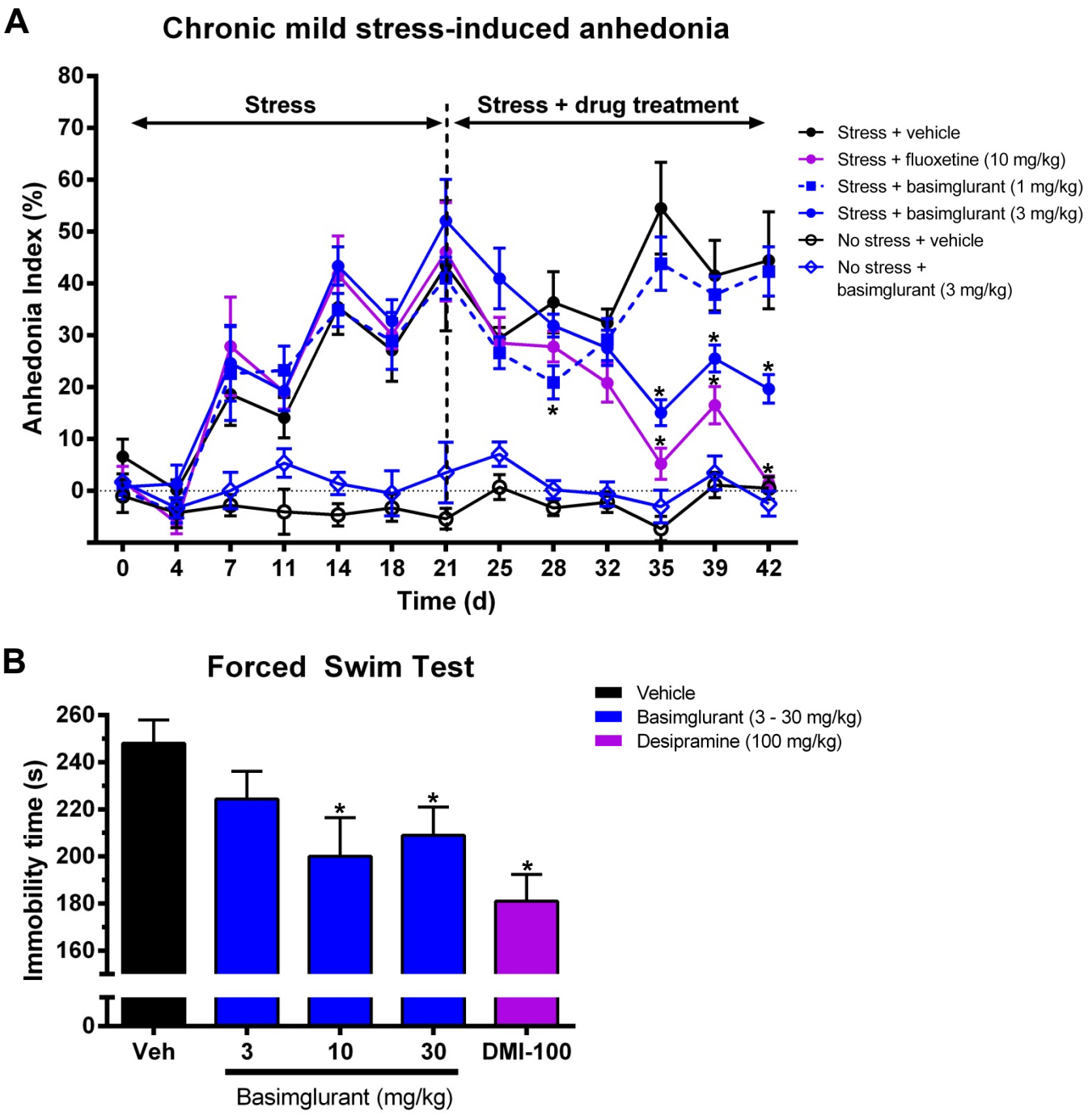

JPET Fast Forward. Published on February 9, 2015 as DOI: 10.1124/jpet.114.222463
This article has not been copyedited and formatted. The final version may differ from this version.

Figure 6

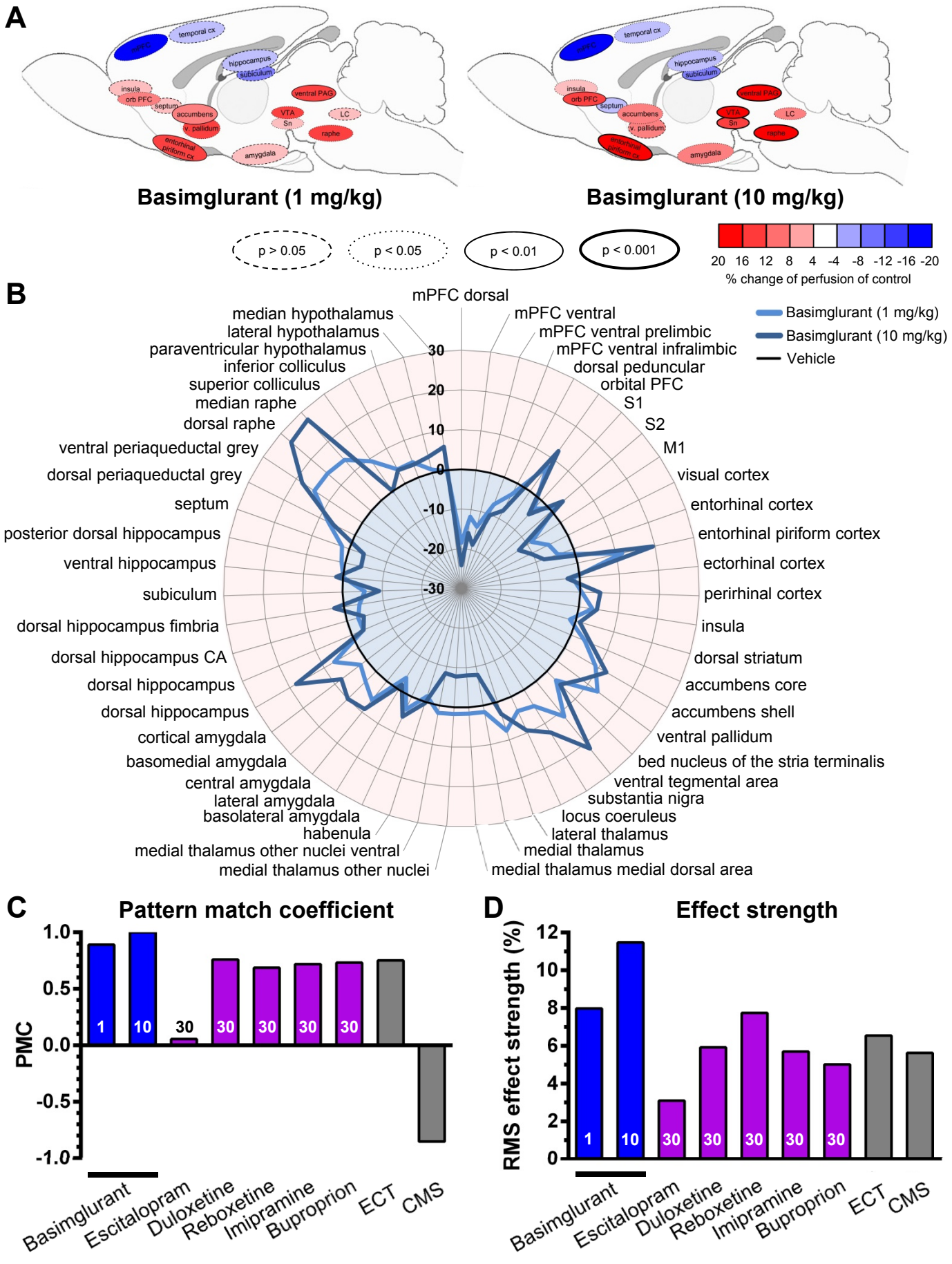

JPET Fast Forward. Published on February 9, 2015 as DOI: 10.1124/jpet.114.222463
This article has not been copyedited and formatted. The final version may differ from this version.

Figure 7

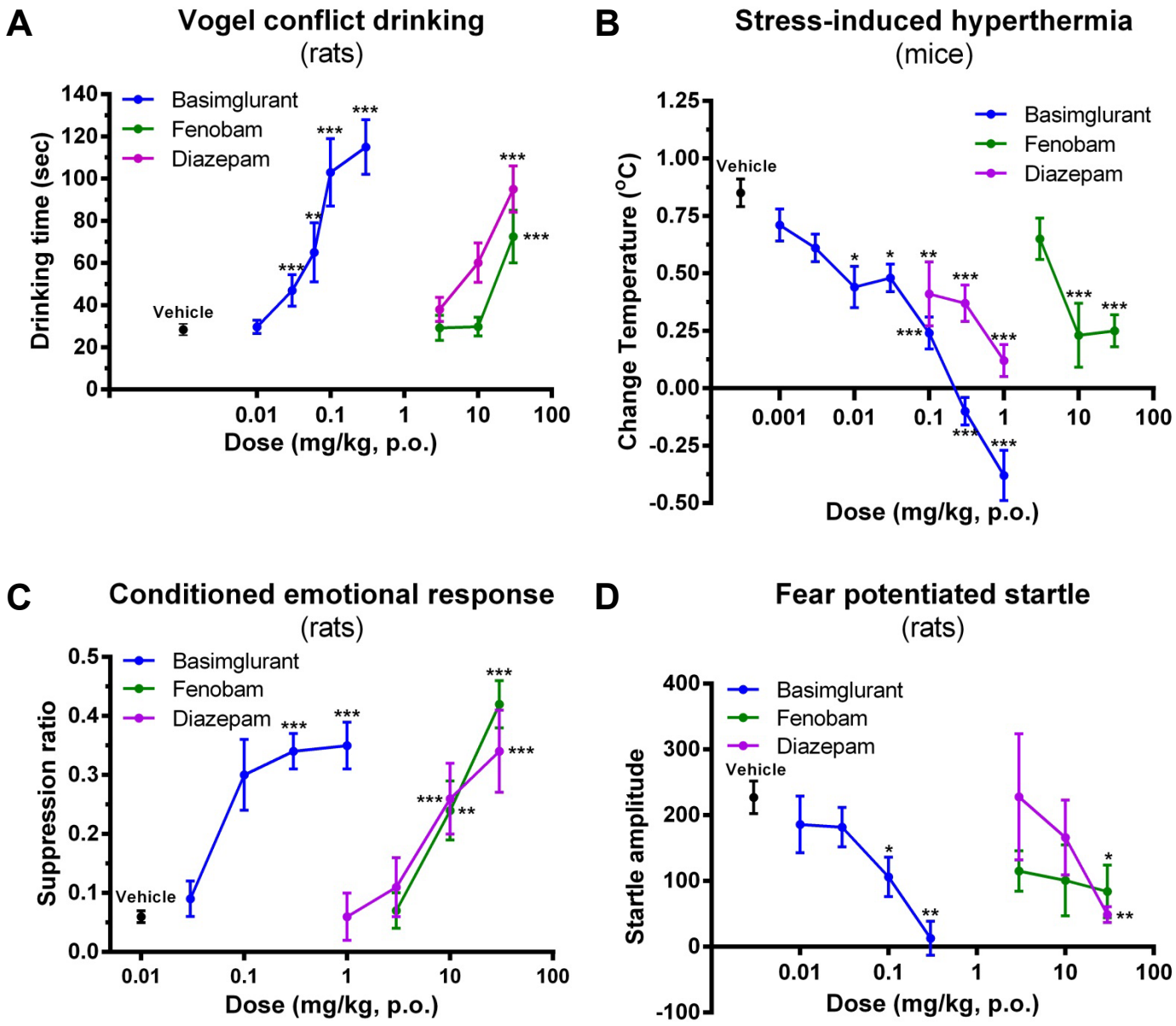

JPET Fast Forward. Published on February 9, 2015 as DOI: 10.1124/jpet.114.222463
This article has not been copyedited and formatted. The final version may differ from this version.

Figure 8

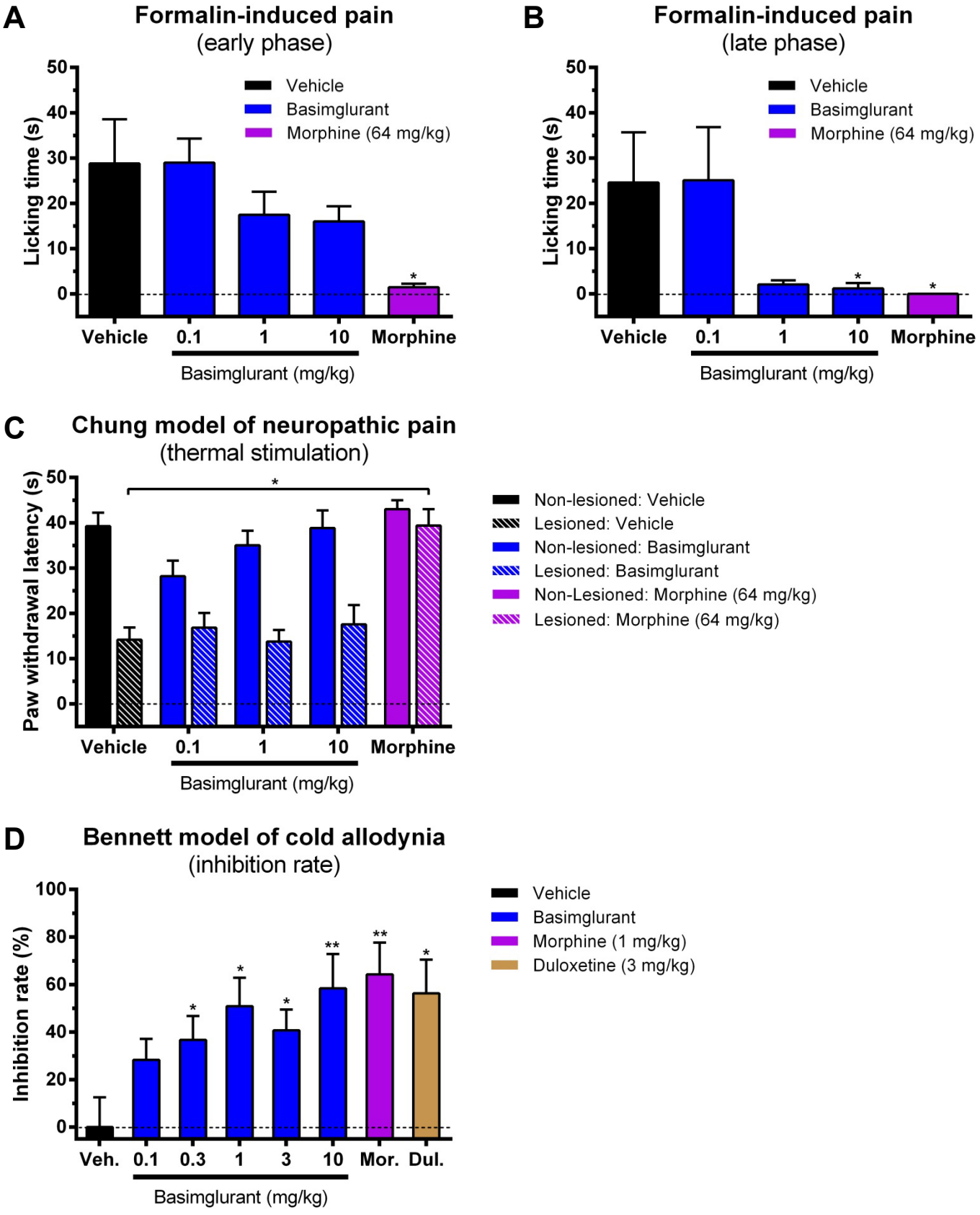

JPET Fast Forward. Published on February 9, 2015 as DOI: 10.1124/jpet.114.222463
This article has not been copyedited and formatted. The final version may differ from this version.

Figure 9

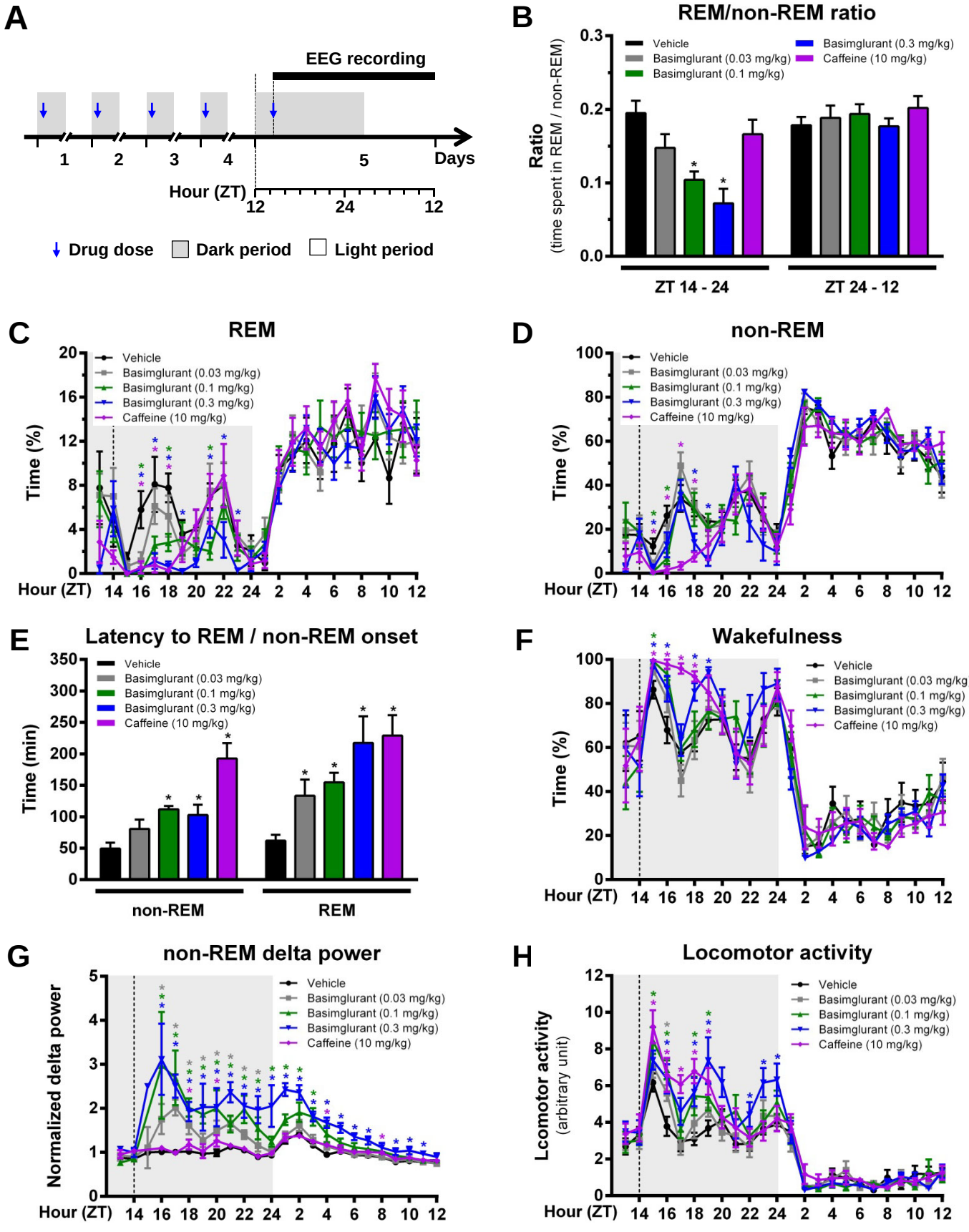

JPET Fast Forward. Published on February 9, 2015 as DOI: 10.1124/jpet.114.222463
This article has not been copyedited and formatted. The final version may differ from this version.

Figure 10

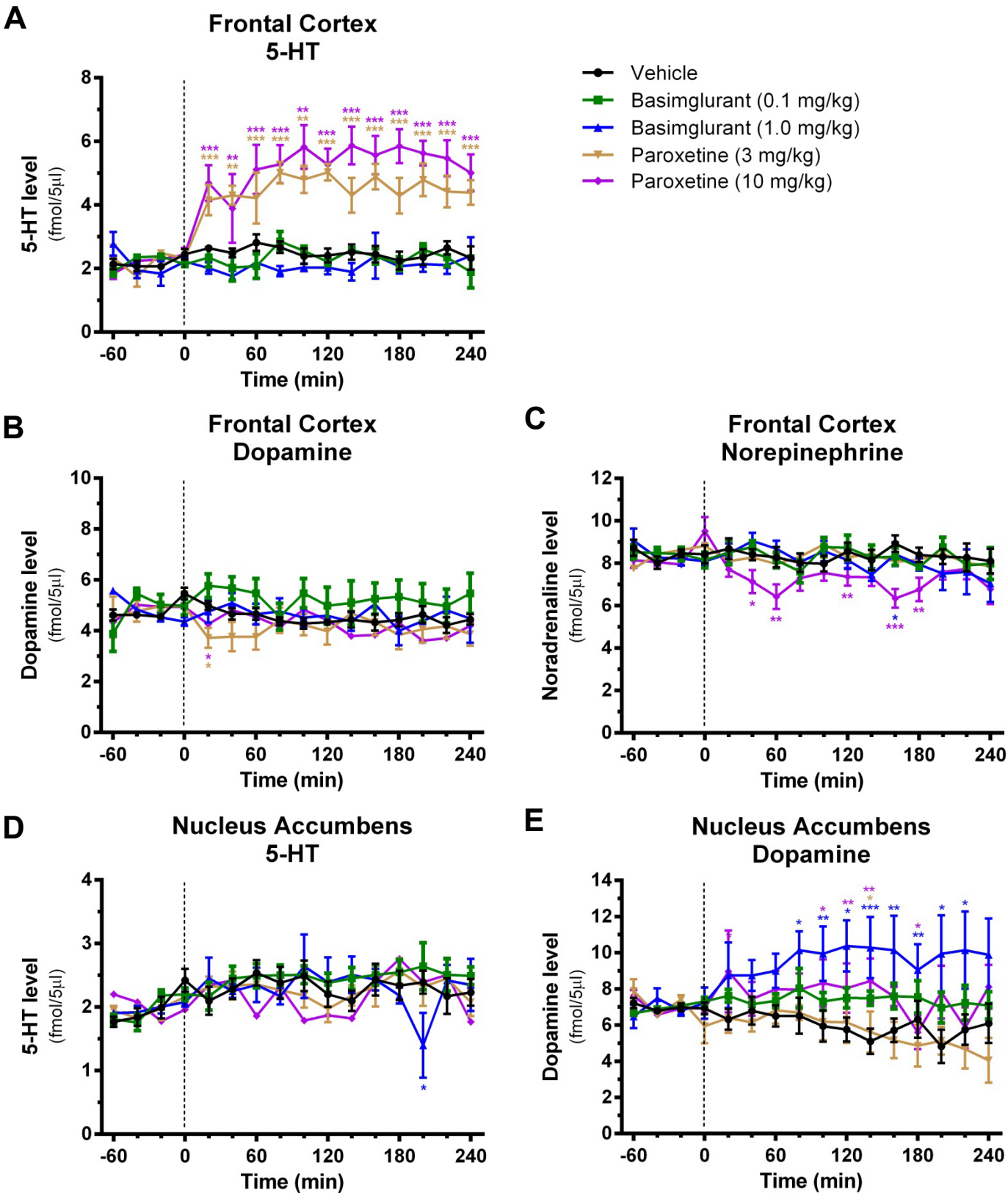

Supplementary Information

Pharmacology of basimglurant (RO4917523, RG7090), a unique mGlu5 negative allosteric modulator in clinical development for depression

Lothar Lindemann*, Richard H. Porter, Sebastian H. Scharf, Basil Kuennecke, Andreas Bruns, Markus von Kienlin, Anthony Harrison, Axel Paehler, Christoph Funk, Andreas Gloge, Manfred Schneider, Neil J. Parrott, Liudmila Polonchuk, Urs Niederhauser, Stephen R. Morairty, Thomas S. Kilduff, Eric Vieira, Sabine Kolczewski, Juergen Wichmann, Thomas Hartung, Michael Honer, Edilio Borroni, Jean-Luc Moreau, Eric Prinssen, Will Spooren, Joseph G. Wettstein, Georg Jaeschke

Roche Pharmaceutical Research and Early Development, Discovery Neuroscience, Neuroscience, Ophthalmology, and Rare Diseases (NORD) (L.L., S.H.S., B.K., A.B., M.v.K., M.H., E.B., E.P., W.S., J.G.W.), Discovery Chemistry (E.V., S.K., J.W., G.J.), Operations for Neuroscience, Ophthalmology, and Rare Diseases (R.H.P., J.-L.M.), Pharmaceutical Sciences (A.H., A.P., C.F., A.G., M.S., N.P., L.P., U.N.), Small Molecules Process Research and Synthesis (T.H.), Roche Innovation Center Basel, Grenzacherstrasse 124, CH-4070 Basel, Switzerland

Center for Neuroscience, Biosciences Division, SRI International, Menlo Park, California 94025, USA

*Corresponding author: lothar.lindemann@roche.com

Table of content

Supplemental Table S1: Assay conditions used for the *in vitro* selectivity profiling of Basimglurant.

a: Data generated at CEREP; b: Data generated at F. Hoffmann-La Roche Ltd.; c: Data generated at DiscoverX; (b): bovine; (g): guinea pig; (h): human; (p): porcine; (r): rat; CHO: Chinese Hamster Ovary cells; HEK293: Human Embryonic Kidney cells; n.a.: not applicable; *: agonist radioligand

Radioligand binding assays	Tracer	Conc.	K_d	Source	Reference
Receptors: Low molecular weight ligands					
Adenosine A_1 receptor (h) [a]	[^{3}H]-DPCPX	1.0 nM	1.5 nM	human recombinant (CHO cells)	(Townsend-Nicholson and Schofield, 1994)
Adenosine A_{2A} receptor (h) [a]	[^{3}H]-CGS 21680*	6 nM	27 nM	human recombinant (HEK293 cells)	(Luthin et al., 1995)
Adenosine A_3 receptor (h) [a]	[^{125}I]-AB-MECA*	0.15 nM	0.22 nM	human recombinant (HEK293 cells)	(Salvatore et al., 1993)
Adrenergic α_1 receptor (non-selective) (r) [a]	[^{3}H]-prazosin	0.25 nM	0.09 nM	rat cerebral cortex	(Greengrass and Bremner, 1979)
Adrenergic α_2 receptor (non-selective) (r) [a]	[^{3}H]-RX 821002	0.5 nM	0.38 nM	rat cerebral cortex	(Uhlen and Wikberg, 1991)
Adrenergic β_1 receptor (h) [a]	[^{3}H]-(-)CGP 12177*	0.15 nM	0.39 nM	human recombinant (HEK293 cells)	(Levin et al., 2002)
Adrenergic β_2 receptor (h) [a]	[^{3}H]-(-)CGP 12177 *	0.15 nM	0.15 nM	human recombinant (Sf9 cells)	(Smith and Teitler, 1999)
Cannabinoid receptor 1 (h) [a]	[^{3}H]-WIN 55212-2*	0.5 nM	3.5 nM	human recombinant (HEK293 cells)	(Matsuda et al., 1990)
Cannabinoid receptor 2 (h) [a]	[^{3}H]-WIN 55212-2*	0.8 nM	1.5 nM	human recombinant (HEK293 cells)	(Munro et al., 1993)
Dopamine D_1 receptor (h) [a]	[^{3}H]-SCH 23390	0.3 nM	0.2 nM	human recombinant (CHO cells)	(Zhou et al., 1990)
Dopamine D_{2S} receptor (h) [a]	[^{3}H]-spiperone	0.3 nM	0.15 nM	human recombinant (CHO cells)	(Grandy et al., 1989)
Dopamine D_3 receptor (h) [a]	[^{3}H]-spiperone	0.3 nM	0.085 nM	human recombinant (CHO cells)	(MacKenzie et al., 1994)
Dopamine D_4 receptor ($D_{4.4}$ variant) (h) [a]	[^{3}H]-spiperone	0.3 nM	0.19 nM	human recombinant (CHO cells)	(Van Tol et al., 1992)
Histamine H_1 receptor (h) [a]	[^{3}H]-pyrilamine	3.0 nM	1.7 nM	human recombinant (HEK293 cells)	(Smit et al., 1996)
Histamine H_2 receptor (h) [a]	[^{125}I]-APT	0.2 nM	2.9 nM	human recombinant (CHO cells)	(Leurs et al., 1994)
Histamine H_3 receptor (r) [a]	[^{3}H]-(R) α-Me-histamine*	1.0 nM	0.32 nM	rat cerebral cortex	(Arrang et al., 1990)
Melanocortin receptor 4 (h) [a]	[^{125}I]-NDP-α-MSH*	0.5 nM	0.54 nM	human recombinant (CHO cells)	(Schioth et al., 1997)
Muscarinic receptors (non-selective) (r) [a]	[^{3}H]-QNB	0.05 nM	0.01 nM	rat cerebral cortex	(Richards, 1990)
Muscarinic receptors 1 (h) [a]	[^{3}H]-pirenzepine	2 nM	13 nM	human recombinant (CHO cells)	(Dorje et al., 1991)
Muscarinic receptors 2 (h) [a]	[^{3}H]-AF-DX 384	2 nM	4.6 nM	human recombinant (CHO cells)	(Dorje et al., 1991)
Muscarinic receptors 3 (h) [a]	[^{3}H]-4-DAMP	0.2 nM	0.5 nM	human recombinant (CHO cells)	(Peralta et al., 1987)
Muscarinic receptors 4 (h) [a]	[^{3}H]-4-DAMP	0.2 nM	0.32 nM	human recombinant (CHO cells)	(Dorje et al., 1991)
Muscarinic receptors 5 (h) [a]	[^{3}H]-4-DAMP	0.2 nM	0.3 nM	human recombinant (CHO cells)	(Dorje et al., 1991)
Neurokinin receptor 1 (h) [a]	[^{125}I]-[Sar^9,Met(O$_2$)^{11}]-SP	0.15 nM	0.6 nM	U-373MG cells	(Heuillet et al., 1993)
Neurokinin receptor 2 (h) [a]	[^{125}I]-NKA	0.1 nM	0.32 nM	human recombinant (CHO cells)	(Aharony et al., 1993)
Neurokinin receptor 3 (h) [a]	[^{3}H]-SR 142801	0.4 nM	0.6 nM	human recombinant (CHO cells)	(Suman-Chauhan et al., 1994)
Opioid receptor (non-selective) (r) [a]	[^{3}H]-naloxone	1.0 nM	0.4 nM	rat cerebral cortex	(Childers et al., 1979)
Purinergic P2X receptor (r) [a]	[^{3}H]-α,β-MeATP*	3.0 nM	2.6 nM	rat urinary bladder	(Bo and Burnstock, 1990)
Prinergic P2Y receptor (r) [a]	[^{35}S]-dATPαS*	10 nM	2.6 nM	rat cerebral cortex	(Simon et al., 1995)
Serotonin receptor (non-selective) (r) [a]	[^{3}H]-serotonin*	2.0 nM	10 nM	rat cerebral cortex	(Peroutka and Snyder, 1979)
Serotonin receptor 5-HT1A (h) [a]	[^{3}H]-8-OH-DPAT*	0.5 nM	2.5 nM	human recombinant (HEK293 cells)	(Mulheron et al., 1994)
Serotonin receptor 5-HT1B (r) [a]	[^{125}I]-CYP (+ 30 mM isoproterenol)	0.1 nM	0.16 nM	rat cerebral cortex	(Hoyer et al., 1985)
Serotonin receptor 5-HT$_{1D}$ (b) [a]	[^{3}H]-serotonin*	2.0 nM	0.5 nM	bovine caudate	(Heuring and Peroutka, 1987)
Serotonin receptor 5-HT$_{2A}$ (h) [a]	[^{125}I]-(±)-DOI*	0.2 nM	0.6 nM	human recombinant (HEK293 cells)	(Bryant et al., 1996)

Supplemental Table S1 (ctd.): Assay conditions used for the *in vitro* selectivity profiling of Basimglurant.

Radioligand binding assays (ctd.)	Tracer	Conc.	K_d	Source	Reference
Receptors: Low molecular weight ligands (ctd.)					
Serotonin receptor 5-HT_{2B} (h) [a]	[^{3}H]-LSD	1.2 nM	2.4 nM	human recombinant (CHO cells)	(Bonhaus et al., 1995)
Serotonin receptor 5-HT_{2C} (h) [a]	[^{125}I]-(±)-DOI*	0.2 nM	0.9 nM	human recombinant (HEK293 cells)	(Bryant et al., 1996)
Serotonin receptor 5-HT_3 (h) [a]	[^{3}H]-BRL 43694	0.5 nM	1.15 nM	human recombinant (HEK293 cells)	(Hope et al., 1996)
Serotonin receptor 5-HT_{4c} (h) [a]	[^{3}H]-GR 113808	0.2 nM	0.2 nM	human recombinant (CHO cells)	(Mialet et al., 2000)
Serotonin receptor 5-HT_{5a} (h) [a]	[^{3}H]-LSD*	1.0 nM	1.5 nM	human recombinant (HEK293 cells)	(Rees et al., 1994)
Serotonin receptor 5-HT_6 (h) [a]	[^{3}H]-LSD*	2.0 nM	1.8 nM	human recombinant (HEK293 cells)	(Monsma et al., 1993)
Serotonin receptor 5-HT_7 (h) [a]	[^{3}H]-LSD*	4.0 nM	2.3 nM	human recombinant (HEK293 cells)	(Shen et al., 1993)
Sigma receptor (non-selective) (r) [a]	[^{3}H]-DTG	8.0 nM	29 nM	rat cerebral cortex	(Shirayama et al., 1993)
Sigma receptor 1 (g) [a]	[^{3}H]-(+)-pentazocine*	2.0 nM	16 nM	guinea pig cerebral cortex	(Bowen et al., 1993)
Sigma receptor 2 (r) [a]	[^{3}H]-DTG (+ 300 nM (+)-pentazocine)*	5 nM	80.84 nM	rat cerebral cortex	(Bowen et al., 1993)
Receptors: Peptides and lipids					
Androgen receptor (h) [a]	[^{3}H]-methyltrienolone*	0.5 nM	2 nM	human, LNCaP cells (cytosol)	(Zava et al., 1979)
Angiotensin receptor 1 (h) [a]	[^{125}I]-[Sar^1,Ile^8]-AT-II	0.05 nM	0.05 nM	human recombinant (CHO cells)	(Bergsma et al., 1992)
Angiotensin receptor 2 (h) [a]	[^{125}I]-CGP 42112A*	0.05 nM	0.02 nM	human recombinant (Hela cells)	(Tsuzuki et al., 1994)
Arginine vasopressin receptor 1a (h) [a]	[^{3}H]-AVP*	0.3 nM	0.5 nM	human recombinant (CHO cells)	(Tahara et al., 1998)
Arginine vasopressin receptor 2 (h) [a]	[^{3}H]-AVP*	0.3 nM	0.76 nM	human recombinant (CHO cells)	(Tahara et al., 1998)
Bradykinin B_1 receptor (h) [a]	[^{3}H]-desArg^{10}-KD*	0.35 nM	0.085 nM	human recombinant (CHO cells)	(Jones et al., 1999)
Bradykinin B_2 receptor (h) [a]	[^{3}H]-bradykinin*	0.2 nM	0.32 nM	human recombinant (CHO cells)	(Pruneau et al., 1998)
Cholecystokinin type A receptor (h) [a]	[^{125}I]-CCK-8*	0.08 nM	0.24 nM	human recombinant (CHO cells)	(Bignon et al., 1999)
Cholecystokinin type B receptor (h) [a]	[^{125}I]-CCK-8*	0.06 nM	0.054 nM	human recombinant (HEK293 cells)	(Lee et al., 1993)
Corticotropin-releasing factor receptor 1 (r) [a]	[^{125}I]-Tyr^0-CRF	0.1 nM	0.12 nM	rat pituitary gland	(Okuyama et al., 1999)
Endothelin receptor type A (h) [a]	[^{125}I]-endothelin-1*	0.03 nM	0.032 nM	human recombinant (CHO cells)	(Buchan et al., 1994)
Endothelin receptor Type B (h) [a]	[^{125}I]-endothelin-1*	0.03 nM	0.04 nM	human recombinant (CHO cells)	(Buchan et al., 1994)
Estrogen receptor (non-selective) (h) [a]	[^{3}H]-estradiol*	1.0 nM	0.07 nM	human, MCF-7 cells (cytosol)	(Sheen et al., 1985)
Glucocorticoid receptor (h) [a]	[^{3}H]-dexamethasone*	1.5 nM	1.5 nM	human, IM-9 cells (cytosol)	(Clark et al., 1996)
Imidazoline I_1 receptor (b) [a]	[^{3}H]-clonidine* (+ 10 µM RX 821002)	15 nM	16 nM	bovine adrenal medulla glands	(Dontenwill et al., 1999)
Imidazoline I_2 receptor (r) [a]	[^{3}H]-idazoxan (+ 1 mM yohimbine)	4 nM	2 nM	rat cerebral cortex	(Brown et al., 1990a)
Leukotriene D_4 receptor (CysLT1) (h) [a]	[^{3}H]-LTD4*	0.3 nM	0.24 nM	human recombinant (CHO cells)	(Martin et al., 2001)
Neuropeptide Y (non-selective) (r) [a]	[^{3}H]-NPY	0.5 nM	0.1 nM	rat cerebral cortex	(Goldstein et al., 1986)
Nociceptin receptor (h) [a]	[^{3}H]-nociceptin*	0.2 nM	0.4 nM	human recombinant (HEK293 cells)	(Ardati et al., 1997)
Progesterone receptor (h) [a]	[^{3}H]-R 5020*	2 nM	1 nM	human, MCF-7 cells (cytosol)	(Eckert and Katzenellenbogen, 1982)
Somatostatin receptor (non-selective) (m) [a]	[^{125}I]-Tyr11-somatostatin*	0.05 nM	0.08 nM	AtT-20-cells	(Brown et al., 1990b)
Thyrotropin releasing hormone receptor (r) [a]	[^{3}H]-Me-TRH*	2 nM	3.9 nM	rat cerebral cortex	(Sharif and Burt, 1983)

Supplemental Table S1 (ctd.): Assay conditions used for the *in vitro* selectivity profiling of Basimglurant.

Radioligand binding assays (ctd.)	Tracer	Conc.	K_d	Source	Reference
Transporter					
Choline transporter (CHT1) (r) [a]	[^{3}H]-hemicholinium-3	3 nM	3.9 nM	rat striatum	(Vickroy et al., 1984)
Dopamine transporter (h) [a]	[^{3}H-]-GBR 12935	0.5 nM	15 nM	human recombinant (CHO cells)	(Pristupa et al., 1994)
GABA transporter (r) [a]	[^{3}H]-GABA (+ 10 µM isoguvacine) (+ 10 µM baclofen)	10 nM	4600 nM	rat cerebral cortex	(Shank et al., 1990)
Norepinephrine transporter (h) [a]	[^{3}H]-nisoxetine	1.0 nM	□ nM	human recombinant (CHO cells)	(Pacholczyk et al., 1991)
Serotonin transporter (h) [a]	[^{3}H]-imipramine	2 nM	1.5 nM	human recombinant (HEK293 cells)	(Tatsumi et al., 1999)
Ion channels					
Acetylcholine receptor, nicotinic (α-BGTX insens.) (r) [a]	[^{3}H]-cytisine*	1.5 nM	1.8 nM	rat cerebral cortex	(Pabreza et al., 1991)
AMPA-type glutamate rec. (r) [a]	[^{3}H]-AMPA*	8 nM	82 nM	rat cerebral cortex	(Murphy et al., 1987)
Ca^{2+} channel, L-type (DHP site) (r) [a]	[^{3}H]-(+)-PN 200-110	0.04 nM	0.02 nM	rat cerebral cortex	(Lee et al., 1984)
Ca^{2+} channel, L-type (diltiazem site) (r) [a]	[^{3}H]-diltiazem	5 nM	52 nM	rat cerebral cortex	(Schoemaker and Langer, 1985)
Ca^{2+} channel, L-type (verapamil site) (r) [a]	[^{3}H]-(-)-D 888	0.5 nM	3 nM	rat cerebral cortex	(Reynolds et al., 1986)
Ca^{2+} channel, SK type (non-selective) (r) [a]	[^{125}I]-apamin	0.004 nM	0.007 nM	rat cerebral cortex	(Hugues et al., 1982)
GABA (non-selective) (r) [a]	[^{3}H]-GABA*	10 nM	15 nM	rat cerebral cortex	(Tsuji et al., 1988)
$GABA_A$ (central, BZD) (r) [a]	[^{3}H]-flunitrazepam*	0.4 nM	2.1 nM	rat cerebral cortex	(Speth et al., 1979)
$GABA_A$ (central, BZD) (r) [a]	[^{3}H]-TBPS	3 nM	14.6 nM	rat cerebral cortex	(Lewin et al., 1989)
$GABA_A$ (central, BZD) (r) [b]	[^{3}H-]-flumazenil	1 nM	1 nM	rat cerebral cortex	See methods and materials
$GABA_A$ (central, BZD; $\alpha_5\beta_3\gamma_2$) (h) [b]	[^{3}H-]-flumazenil	0.49 nM	1 nM	human recombinant (HEK293 cells)	(Ballard et al., 2009)
K^+ channel, ATP sensitive (Kir6.2) (r) [a]	[^{3}H]-glibenclamide	0.1 nM	0.05 nM	rat cerebral cortex	(Angel and Bidet, 1991)
K^+ channel, voltage gated (α-DTX) (r) [a]	[^{125}I]-α-dendrotoxin	0.01 nM	0.04 nM	rat cerebral cortex	(Sorensen and Blaustein, 1989)
Na^+ channel (site 2) (r) [a]	[^{3}H]-batrachotoxinin	10 nM	91 nM	rat cerebral cortex	(Brown, 1986)
Kainate-type glutamate receptor (r) [a]	[^{3}H]-kainic acid*	5 nM	19 nM	rat cerebral cortex	(Monaghan and Cotman, 1982)
NMDA-type glutamate receptor (r) [a]	[^{3}H]-CGP 39653	5 nM	23 nM	rat cerebral cortex	(Sills et al., 1991)
NMDA-type glutamate receptor (PCP) (r) [a]	[^{3}H]-TCP	5.0 nM	66 nM	rat cerebral cortex	(Vignon et al., 1986)

Functional assays	Substrate	Measured product	Source	Reference
Target/Assay				
Acetylcholinesterase (h) [a]	AMTCh (50 µM)	thio-conjugate	human recombinant (HEK293 cells)	(Ellman et al., 1961)
Adenylate cyclase (r) [a]	ATP (0.5 mM) (ctrl.: 300 µM forskolin)	cAMP	rat brain	(Salomon et al., 1974)
Catechol- O-methyl transferase (COMT) (p) [a]	esculetin	scopoletin	porcine liver	(Muller-Enoch et al., 1976)
Dopamine transporter uptake (h) [b]	[^{3}H]-dopamine	n.a.	human recombinant (HEK293 cells)	See methods and materials
Cannabinoid receptor 1 (h) [a]	cAMP accumulation	cAMP	human recombinant (CHO cells)	(Felder et al., 1995; Ross et al., 1999)
Cannabinoid receptor 2 (h) [a]	cAMP accumulation	cAMP	human recombinant (CHO cells)	(Felder et al., 1995; Ross et al., 1999)

Supplemental Table S1 (ctd.): Assay conditions used for the *in vitro* selectivity profiling of Basimglurant.

Functional assays (ctd.)	Substrate	Measured product	Source	Reference
Target/Assay				
GABA transaminase (r) [a]	GABA (9 mM) + α-ketoglutarate (9 mM)	succinic semialdehyde	rat brain	(Loscher, 1981)
Guanylate cyclase (b) [a]	GTP (0.1 mM) (ctrl.: 1 mM Na^+ nitroprusside)	cGMP	bovine lung	(Wolin et al., 1982)
Metabotropic glutamate receptor 1 (h) [b]	Ca^{2+} mobilization	n.a.	human recombinant (HEK293 cells)	(Lindemann et al., 2011)
Metabotropic glutamate receptor 2 (h) [b]	Ca^{2+} mobilization	n.a.	human recombinant (HEK293 cells)	(Lindemann et al., 2011)
Metabotropic glutamate receptor 3 (h) [c]	cAMP accumulation	n.a.	human recombinant (HEK293 cells)	(Bassoni et al., 2012)
Metabotropic glutamate receptor 4 (h) [b]	[^{35}S]-GTPgS binding	n.a.	human recombinant (CHO cells)	(Lindemann et al., 2011)
Metabotropic glutamate receptor 6 (h) [c]	cAMP accumulation	n.a.	human recombinant (HEK293 cells)	(Bassoni et al., 2012)
Metabotropic glutamate receptor 7 (r) [b]	cAMP accumulation	cAMP	rat recombinant (CHO DUKX cells)	(Porter et al., 2005)
Metabotropic glutamate receptor 8 (h) [b]	Ca^{2+} mobilization	n.a.	human recombinant (CHO cells)	(Lindemann et al., 2011)
Monoaminoxidase A (h) [a]	kynuramine (0.15 mM)	4-Ohquinoline	human placenta	(Weyler and Salach, 1985)
Monoaminoxidase B (h) [a]	benzylamine (0.5 mM)	benzaldehyde	human platelets	(Uebelhack et al., 1998)
Na+/K+-ATPase (d) [a]	ATP (2 mM)	phosphate	dog kidney	(Fiske and Subbarow, 1925)
Norepinephrine transporter uptake (h) [b]	[^{3}H]-Norepinephrine	n.a.	human recombinant (HEK293 cells)	See methods and materials
Phenylethanolamine N-methyl transferase (PNMT) (h) [a]	[^{14}C]-SAM (4 µM) + normetanephrine (28 mM)	[^{14}C]-metanephrine	bovine adrenal medulla	(Betito et al., 1993)
Phosphodiesterase 1 (b) [a]	[^{3}H]-cAMP + cAMP (1 µM)	[^{3}H]-5'AMP	bovine brain	(Nicholson et al., 1989)
Phosphodiesterase 2 (h) [a]	[^{3}H]-cAMP + cAMP (1 µM)	[^{3}H]-5'AMP	human, different. U-937 cells	(Torphy et al., 1992)
Phosphodiesterase 3 (h) [a]	[^{3}H]-cAMP + cAMP (0.1 µM)	[^{3}H]-5'AMP	human platelets	(Weishaar et al., 1986)
Phosphodiesterase 4 (h) [a]	[^{3}H]-cAMP + cAMP (1 µM)	[^{3}H]-5'AMP	human, U-937 cells	(Torphy et al., 1992)
Phosphodiesterase 5 (h) [a]	[^{3}H]-cGMP + cGMP (1 µM)	[^{3}H]-5'GMP	human platelets	(Weishaar et al., 1986)
Protein kinase C (r) [a]	ATP + biotinyl-neurogranin 28-43 peptide (60 nM)	phospho-biotinyl-neurogranin 28-43 peptide	rat brain	(Hannun et al., 1985)
Serotonin transporter uptake (h) [b]	[^{3}H]-serotonin	n.a.	human recombinant (HEK293 cells)	See methods and materials
Tyrosine hydroxylase (r) [a]	[^{3}H]-tyrosine (10 µM)	[^{3}H]-H_2O	rat striatum	(Nagatsu et al., 1964)

Supplemental Table S2: Key characteristics of the mGlu5 NAM RO4623831

Chemical structure, as well as *in vitro* potency recorded on recombinant human mGlu5 receptors by means of radioligand binding and Ca^{2+} mobilization assays. *In vitro* pharmacology data are mean ± S.E.M. with N=3 (saturation isotherms), N=4 ([^{3}H]-MPEP binding), and N=8 (Ca^{2+} mobilization). Pharmacokinetic profiles were recorded with N=2 rats per route. N/A: Not available; *: Because of the rapid absorption and the very 'flat' profile over the 20 h recording period, the T_{max} could not be reliably determined.

Structure			
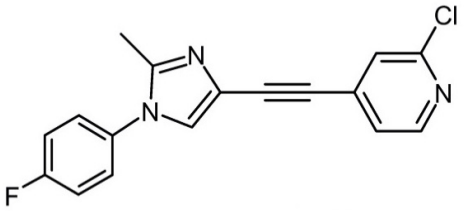			
***In vitro* pharmacology key parameters**			
[^{3}H]-RO4623831 saturation isotherms		**[^{3}H]-MPEP compet. binding**	**Ca^{2+} mobilization**
Kd (nM)	**Bmax (pmol/mg protein)**	**Ki (nM)**	**IC_{50} (nM)**
3.58 ±	5.69 ±	16.17 ± 2.1	26.28 ± 6.0
Pharmacokinetic key parameters (rat)			
Dose p.o. / i.v. (mg/kg)	5 / 2	**Clearance** (ml/min/kg)	2.18
C_{max} (ng/ml)	1480	**V_{SS}** (l/kg)	2.93
T_{max} (h)	N/A*	**Oral bioavailability** (%)	58.6
$T_{1/2}$ (h)	16.2	**Brain/Plasma ratio**	N/A

Supplemental Table S3A: Basimglurant activity in the chronic mild stress-induced anhedonia model

Numerical information related to Figure 5A.

CMS-induced anhedonia	Anhedonia index Absolute (% to training)	Anhedonia index % change to Veh[a]	p value vs Veh[a]
stress + vehicle			
Baseline (d0)	6.6 ± 3.4	100.0 ± 3.4	-
Stress (d21)	43.4 ± 12.6	100.0 ± 12.6	-
Stress + drug (d42)	44.5 ± 9.4	100.0 ± 9.4	-
Stress + basimglurant (1 mg/kg)			
Baseline (d0)	0.1 ± 1.8	-6.6 ± 1.8	n.s.
Stress (d21)	41.0 ± 4.1	-2.4 ± 4.1	n.s.
Stress + drug (d42)	42.3 ± 4.8	-2.2 ± 4.8	n.s.
Stress + basimglurant (3 mg/kg)			
Baseline (d0)	0.8 ± 1.5	-5.9 ± 1.5	n.s.
Stress (d21)	52.1 ± 8.0	+8.7 ± 8.0	n.s.
Stress + drug (d42)	19.7 ± 2.7	-24.8 ± 2.7	$p < 0.05$
Stress + fluoxetine (10 mg/kg)			
Baseline (d0)	1.9 ± 2.8	-4.7 ± 2.8	n.s.
Stress (d21)	46.1 ± 9.5	+2.7 ± 9.5	n.s.
Stress + drug (d42)	1.5 ± 1.4	-42.9 ± 1.4	$p < 0.05$
No stress + vehicle			
Baseline (d0)	-1.0 ± 3.2	100.0 ± 3.2	-
Stress (d21)	-5.4 ± 2.0	100.0 ± 2.0	-
Stress + drug (d42)	0.5 ± 2.2	100.0 ± 2.2	-
No stress + basimglurant (3 mg/kg)			
Baseline (d0)	1.7 ± 1.4	+2.7 ± 1.4	n.s.
Stress (d21)	3.5 ± 5.8	+8.9 ± 5.8	n.s.
Stress + drug (d42)	-2.5 ± 2.4	-3.0 ± 2.4	n.s.

[a]: Stress groups are compared to (stress:vehicle) animals and non-stress groups are compared to (no stress:vehicle) animals. n.s.: Not significant.

Supplemental Table S3B: Basimglurant activity in the forced swim test

Numerical information related to Figure 5B.

	Immobility time absolute (s)	Immobility time % change to Veh	p value vs. Veh
Veh	248 ± 10.0	100 ± 4.0	-
Basimglurant			
3 mg / kg	224.4 ± 11.8	-9.5 ± 4.8	n.s.
10 mg / kg	200.0 ± 16.4	-19.4 ± 6.6	$p < 0.05$
30 mg / kg	209.0 ± 12.0	-15.7 ± 4.8	$p < 0.05$
Desipramine			
(100 mg / kg)	181.0 ± 11.3	-27.0 ± 4.6	$p < 0.05$

Data are mean ± SEM. n.s.: Not significant

Supplemental Table S4A: Basimglurant activity in the Vogel conflict drinking test

Numerical information related to Figure 7A.

	Drinking time absolute (s)	Drinking time % change to Veh	p value vs. Veh
Veh	28.5 ± 2.7	100 ± 9.5	-
Basimglurant			
0.01 mg / kg	29.7 ± 3.2	+4.4 ± 11.2	n.s.
0.03 mg / kg	47.0 ± 7.5	+65.2 ± 26.4	p < 0.001
0.06 mg / kg	65.0 ± 14.0	+128.5 ± 49.2	p < 0.01
0.1 mg / kg	103.0 ± 16.0	+262.0 ± 56.2	p < 0.001
0.3 mg / kg	115.0 ± 13.0	+304.2 ± 45.7	p < 0.001
Fenobam			
3 mg / kg	29.2 ± 6.0	+2.5 ± 21.1	n.s.
10 mg / kg	29.8 ± 4.5	+4.7 ± 15.8	n.s.
30 mg / kg	72.5 ± 12.5	+154.8 ± 43.9	p < 0.001
Diazepam			
3 mg / kg	38.0 ± 5.8	+33.6 ± 20.4	n.s.
10 mg / kg	60.1 ± 9.4	+111.2 ± 33.0	n.s.
30 mg / kg	95.0 ± 11.0	+233.9 ± 38.7	p < 0.001

Data are mean ± SEM. n.s.: Not significant

Supplemental Table S4B: Basimglurant activity in the Stress-induced hyperthermia procedure

Numerical information related to Figure 7B.

SIH	Temp. change absolute (°C)	Temp. change % change to Veh	p value vs. Veh
Veh	0.85 ± 0.06	100 ± 7.1	-
Basimglurant			
0.001 mg / kg	0.71 ± 0.07	-16.5 ± 8.2	n.s.
0.003 mg / kg	0.61 ± 0.06	-28.2 ± 7.1	n.s.
0.01 mg / kg	0.44 ± 0.09	-48.2 ± 10.6	p < 0.05
0.03 mg / kg	0.48 ± 0.06	-43.5 ± 7.1	p < 0.05
0.1 mg / kg	0.24 ± 0.07	-71.8 ± 8.2	p < 0.001
0.3 mg / kg	-0.10 ± 0.06	-111.8 ± 7.1	p < 0.001
1 mg / kg	-0.38 ± 0.11	-144.7 ± 12.9	p < 0.001
Fenobam			
3 mg / kg	0.65 ± 0.09	-23.5 ± 10.6	n.s.
10 mg / kg	0.23 ± 0.14	-72.9 ± 16.5	p < 0.001
30 mg / kg	0.25 ± 0.07	-70.6 ± 8.2	p < 0.001
Diazepam			
0.3 mg / kg	0.41 ± 0.14	-51.8 ± 16.5	p < 0.01
0.1 mg / kg	0.37 ± 0.08	-56.5 ± 9.4	p < 0.001
1 mg / kg	0.12 ± 0.07	-85.9 ± 8.2	p < 0.001

Data are mean ± SEM. n.s.: Not significant

Supplemental Table S4C: Basimglurant activity in the conditioned emotional response procedure

Numerical information related to Figure 7C.

CER	Suppression ratio absolute	Suppression ratio % change to Veh	p value vs. Veh
Veh	0.05 ± 0.02	100 ± 35.7	-
Basimglurant			
0.03 mg / kg	0.13 ± 0.04	+178.4 ± 78.7	n.s.
0.1 mg / kg	0.30 ± 0.06	+545.1 ± 127.6	p < 0.001
0.3 mg / kg	0.37 ± 0.02	+705.9 ± 45.1	p < 0.001
1 mg / kg	0.39 ± 0.03	+741.2 ± 63.1	p < 0.001
Fenobam			
3 mg / kg	0.07 ± 0.03	+51.0 ± 64.7	n.s.
10 mg / kg	0.24 ± 0.05	+417.6 ± 107.8	p < 0.001
30 mg / kg	0.42 ± 0.04	+805.9 ± 86.3	p < 0.001
Diazepam			
1 mg / kg	0.06 ± 0.04	+29.4 ± 86.3	n.s.
3 mg / kg	0.11 ± 0.05	+137.3 ± 107.8	n.s.
10 mg / kg	0.26 ± 0.06	+460.8 ± 129.4	p < 0.001
30 mg / kg	0.34 ± 0.07	+633.3 ± 151.0	p < 0.001

Data are mean ± SEM. n.s.: Not significant

Supplemental Table S4D: Basimglurant activity in the fear potentiated startle procedure

Numerical information related to Figure 7D.

	Startle amplitude absolute	Startle amplitude % change to Veh	p value vs. Veh
Veh	227 ± 25	100.0 ± 11.0	-
Basimglurant			
0.01 mg / kg	186 ± 43	-18.1 ± 18.9	n.s.
0.03 mg / kg	182 ± 30	-19.8 ± 13.2	n.s.
0.1 mg / kg	106 ± 30	-53.3 ± 13.2	p < 0.05
0.3 mg / kg	13 ± 26	-94.3 ± 11.5	p < 0.01
Fenobam			
3 mg / kg	115 ± 31	-49.3 ± 13.7	n.s.
10 mg / kg	101 ± 54	-55.5 ± 23.8	n.s.
30 mg / kg	84 ± 40	-63.0 ± 17.6	p < 0.05
Diazepam			
0.3 mg / kg	228 ± 96	+0.4 ± 42.3	n.s.
0.1 mg / kg	166 ± 57	-26.9 ± 25.1	n.s.
1 mg / kg	49 ± 12	-78.4 ± 5.3	p < 0.01

Data are mean ± SEM. n.s.: Not significant

Supplemental Table S5A: Basimglurant activity in the formalin-induced pain procedure (early phase)

Numerical information related to Figure 8A.

Formalin-induced pain (early phase)	**Licking time** Absolute (s)	**Licking time** % change to Veh	**p value** vs. Veh
Veh	28.8 ± 9.8	100.0 ± 33.9	-
Basimglurant			
0.1 mg / kg	29.0 ± 5.3	+0.7 ± 18.4	n.s.
1 mg / kg	17.5 ± 5.1	-39.2 ± 17.5	n.s.
10 mg / kg	16.0 ± 3.4	-44.4 ± 11.7	n.s.
Morphine			
64 mg / kg	1.5 ± 0.8	-94.8 ± 2.7	$p < 0.05$

Data are mean ± SEM. n.s.: Not significant

Supplemental Table S5B: Basimglurant activity in the formalin-induced pain procedure (late phase)

Numerical information related to Figure 8B.

Formalin-induced pain (late phase)	**Licking time** Absolute (s)	**Licking time** % change to Veh	**p value** vs Veh
Veh	24.6 ± 11.1	100.0 ± 45.1	-
Basimglurant			
0.1 mg / kg	25.1 ± 11.7	+2.0 ± 47.6	n.s.
1 mg / kg	2.1 ± 0.9	-91.5 ± 3.6	n.s.
10 mg / kg	1.2 ± 1.2	-95.1 ± 4.9	$p < 0.05$
Morphine			
64 mg / kg	0.0 ± 0.0	-100.0 ± 0.0	$p < 0.05$

Data are mean ± SEM. n.s.: Not significant

Supplemental Table S5C: Basimglurant activity in the Chung model of neuropathic pain

Numerical information related to Figure 8C.

Chung-model (thermal)	Withdrawal latency Absolute (s)	Withdrawal latency % change to Veh	p value vs Veh
Veh			
Non-lesioned paw	39.3 ± 3.0	100.0 ± 7.6	-
Lesioned paw	14.2 ± 2.7	100.0 ± 19.1	-
Basimglurant (0.1 mg / kg)			
Non-lesioned paw	28.2 ± 3.4	-28.1 ± 8.7	n.s.
Lesioned paw	16.8 ± 3.3	+18.8 ± 23.1	n.s.
Basimglurant (1 mg / kg)			
Non-lesioned paw	35.0 ± 3.2	-10.8 ± 8.2	n.s.
Lesioned paw	13.8 ± 2.6	-2.8 ± 18.0	n.s.
Basimglurant (10 mg / kg)			
Non-lesioned paw	38.8 ± 3.9	-1.1 ± 9.9	n.s.
Lesioned paw	17.6 ± 4.3	+23.9 ± 30.1	n.s.
Morphine (64 mg / kg)			
Non-lesioned paw	43.0 ± 2.0	+9.6 ± 5.1	n.s.
Lesioned paw	39.4 ± 3.6	+177.8 ± 25.6	$p < 0.05$

Data are mean ± SEM. n.s.: Not significant

Supplemental Table S5D: Basimglurant activity in the Bennett model of cold allodynia

Numerical information related to Figure 8D.

Bennet model Cold allodynia	Pre dose paw lifts	Post dose paw lifts	Inhibition rate % change to Veh	p value vs. Veh
Veh	9.8 ± 0.8	10.4 ± 1.2	100.0 ± 12.5	-
Basimglurant				
0.1 mg / kg	9.4 ± 0.7	7.8 ± 0.8	+28.3 ± 8.8	n.s.
0.3 mg / kg	8.2 ± 0.7	7.2 ± 0.9	+36.7 ± 10.1	$p < 0.05$
1 mg / kg	8.3 ± 0.8	6.6 ± 1.0	+50.9 ± 11.9	$p < 0.05$
3 mg / kg	7.0 0.4	5.3 0.6	+40.7 8.7	$p < 0.05$
10 mg / kg	8.1 0.5	5.7 1.2	+58.4 14.4	$p < 0.01$
Morphine				
1 mg / kg	10.6 ± 2.0	4.7 ± 1.3	+64.3 ± 13.4	$p < 0.01$
Duloxetine				
3 mg / kg	7.3 ± 0.5	5.0 ± 1.0	+56.3 ± 14.3	$p < 0.05$

Data are mean ± SEM. n.s.: Not significant

Supplemental Table S6A: Basimglurant effects on REM/non-REM ratio measured by EEG

Numerical information related to Figure 9B.

REM/non-REM ratio	Ratio Absolute	Ratio % change to Veh	p value vs. Veh
Veh			
ZT 14 – 24	0.19 ± 0.02	100.0 ± 8.6	-
ZT 24 – 12	0.18 ± 0.01	100.0 ± 8.6	-
Basimglurant (0.03 mg / kg)			
ZT 14 – 24	0.15 ± 0.02	-24.2 ± 9.5	n.s.
ZT 24 – 12	0.19 ± 0.02	+5.6 ± 9.3	n.s.
Basimglurant (0.1 mg / kg)			
ZT 14 – 24	0.10 ± 0.01	-46.5 ± 5.7	$p < 0.05$
ZT 24 – 12	0.19 ± 0.01	+8.5 ± 7.4	n.s.
Basimglurant (0.3 mg / kg)			
ZT 14 – 24	0.07 ± 0.02	-63.0 ± 10.2	$p < 0.05$
ZT 24 – 12	0.18 ± 0.01	-0.8 ± 6.0	n.s.
Caffeine (10 mg / kg)			
ZT 14 – 24	0.17 ± 0.02	-14.7 ± 10.2	n.s.
ZT 24 – 12	0.20 ± 0.02	+13.2 ± 9.0	n.s.

Data are mean ± SEM. n.s.: Not significant

Supplemental Table S6B: Basimglurant effects latency to REM and non-REM onset measured by EEG

Numerical information related to Figure 9E.

Latency to REM/ non-REM onset	Time to onset Absolute (min)	Time to onset % change to Veh	p value vs. Veh
Veh			
non-REM	49.5 ± 9.3	100.0 ± 18.8	-
REM	62.0 ± 9.2	100.0 ± 14.9	-
Basimglurant (0.03 mg / kg)			
non-REM	80.7 ± 14.8	+63.0 ± 29.8	n.s.
REM	133.4 ± 25.7	+114.9 ± 41.4	$p < 0.05$
Basimglurant (0.1 mg / kg)			
non-REM	111.9 ± 5.1	+126.2 ± 10.2	$p < 0.05$
REM	154.8 ± 15.2	+149.5 ± 24.5	$p < 0.05$
Basimglurant (0.3 mg / kg)			
ZT 14 – 24	102.9 ± 16.1	+108.0 ± 32.5	$p < 0.05$
ZT 24 – 12	217.5 ± 42.2	+250.5 ± 68.1	$p < 0.05$
Caffeine (10 mg / kg)			
ZT 14 – 24	192.5 ± 24.8	+289.1 ± 50.1	$p < 0.05$
ZT 24 – 12	229.1 ± 32.4	+269.3 ± 52.1	$p < 0.05$

Data are mean ± SEM. n.s.: Not significant

Supplemental Table S7: Effects of basimglurant and paroxetine on extracellular levels of monoamine transmitters in rat.

Numerical information related to Figure 10. The maximal/minial effects of each treatment over the recording period are reported.

	T (min)	Absolute level (fmol/5µl)	Ratio % change to Veh	p value vs. Veh
Frontal Cortex				
5-HT				
Basimglurant (0.1 mg / kg)	60	2.08 ± 0.39	-26.2 ± 13.8	n.s.
Basimglurant (1.0 mg / kg)	-60	2.78 ± 0.38	+29.9 ± 17.8	n.s.
Paroxetine (3 mg / kg)	120	5.03 ± 0.26	+108.7 ± 10.8	p < 0.001
Paroxetine (10 mg / kg)	100	5.82 ± 0.69	+143.5 ± 28.9	p < 0.001
Dopamine				
Basimglurant (0.1 mg / kg)	100	5.48 ± 0.58	+27.7 ± 13.5	n.s.
Basimglurant (1.0 mg / kg)	-60	5.58 ± 0.10	+20.8 ± 2.2	n.s.
Paroxetine (3 mg / kg)	20	3.72 ± 0.39	-25.5 ± 7.8	p < 0.05
Paroxetine (10 mg / kg)	20	4.26 ± 0.29	-14.6 ± 5.8	p < 0.001
Norepinephrine				
Basimglurant (0.1 mg / kg)	180	7.83 ± 0.15	-6.8 ± 1.8	n.s.
Basimglurant (1.0 mg / kg)	240	7.06 ± 0.89	-12.9 ± 11.0	n.s.
Paroxetine (3 mg / kg)	100	8.89 ± 0.59	+11.3 ± 7.4	n.s.
Paroxetine (10 mg / kg)	160	6.34 ± 0.45	-28.9 ± 5.0	p < 0.001
Nucleus accumbens				
5-HT				
Basimglurant (0.1 mg / kg)	140	2.45 ± 0.17	+16.5 ± 8.0	n.s.
Basimglurant (1.0 mg / kg)	220	1.40 ± 0.51	-41.4 ± 21.5	p < 0.05
Paroxetine (3 mg / kg)	220	2.45 ± 0.29	+13.1 ± 13.6	n.s.
Paroxetine (10 mg / kg)	100	1.79 ± 0.30	-28.2 ± 12.2	n.s.
Dopamine				
Basimglurant (0.1 mg / kg)	140	7.48 ± 0.40	+46.6 ± 7.9	p < 0.05
Basimglurant (1.0 mg / kg)	200	9.95 ± 2.13	+106.7 ± 44.3	p < 0.05
Paroxetine (3 mg / kg)	240	4.05 ± 1.24	-33.6 ± 20.4	n.s.
Paroxetine (10 mg / kg)	140	8.44 ± 1.24	+65.4 ± 24.4	p < 0.001

Data are adjusted means ± SEM. n.s.: Not significant

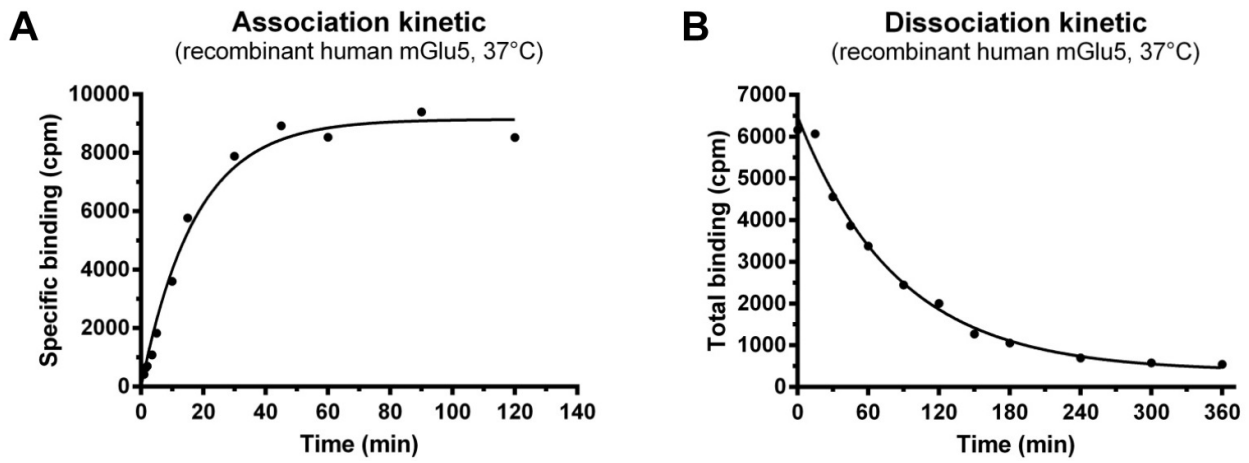

Supplemental Fig. S1: Receptor binding kinetics of [^{3}H]-basimglurant on recombinant human mGlu5.
Representative association (A) and dissociation (B) binding experiment with [^{3}H]-basimglurant on membranes of HEK293 cells transiently transfected with human mGlu5, measured at 37°C.

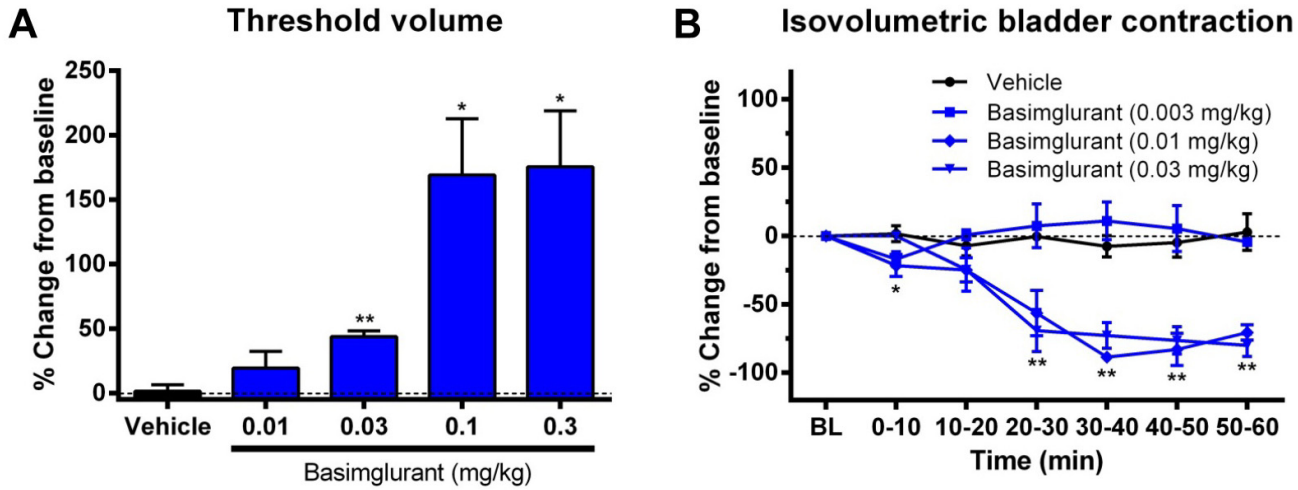

Supplemental Fig. S2: Effects of basimglurant on the micturition effect in rats.
(A) Basimglurant (0.01 – 0.3 mg/kg, i.v.) dose-dependently increased the threshold volume of the bladder of anestheized rats triggering the micturition reflex.
(B) In the isovolumetric bladder contraction model, basimglurant (0.003 – 0.03 mg/kg, i.v.) dose-dependently increased the intercontraction interval.
Data are mean ± SEM with N = 4-5 per group. Statistics: *p<0.05, ** p<0.01 versus vehicle based on one-way ANOVA followed by a pairwise comparison using Dunnet's test.

Supplemental references

Aharony D, Little J, Powell S, Hopkins B, Bundell KR, McPheat WL, Gordon RD, Hassall G, Hockney R, Griffin R and et al. (1993) Pharmacological characterization of cloned human NK-2 (neurokinin A) receptor expressed in a baculovirus/Sf-21 insect cell system. *Mol Pharmacol* **44**:356-363.

Angel I and Bidet S (1991) The binding site for [3H]glibenclamide in the rat cerebral cortex does not recognize K-channel agonists or antagonists other than sulphonylureas. *Fundam Clin Pharmacol* **5**:107-115.

Ardati A, Henningsen RA, Higelin J, Reinscheid RK, Civelli O and Monsma FJ, Jr. (1997) Interaction of [3H]orphanin FQ and 125I-Tyr14-orphanin FQ with the orphanin FQ receptor: kinetics and modulation by cations and guanine nucleotides. *Mol Pharmacol* **51**:816-824.

Arrang JM, Roy J, Morgat JL, Schunack W and Schwartz JC (1990) Histamine H3 receptor binding sites in rat brain membranes: modulations by guanine nucleotides and divalent cations. *European journal of pharmacology* **188**:219-227.

Ballard TM, Knoflach F, Prinssen E, Borroni E, Vivian JA, Basile J, Gasser R, Moreau JL, Wettstein JG, Buettelmann B, Knust H, Thomas AW, Trube G and Hernandez MC (2009) RO4938581, a novel cognitive enhancer acting at GABAA alpha5 subunit-containing receptors. *Psychopharmacology* **202**:207-223.

Bassoni DL, Jafri Q, Sastry S, Mathrubutham M and Wehrman TS (2012) Characterization of G-protein coupled receptor modulators using homogeneous cAMP assays. *Methods Mol Biol* **897**:171-180.

Bergsma DJ, Ellis C, Kumar C, Nuthulaganti P, Kersten H, Elshourbagy N, Griffin E, Stadel JM and Aiyar N (1992) Cloning and characterization of a human angiotensin II type 1 receptor. *Biochem Biophys Res Commun* **183**:989-995.

Betito K, Diorio J and Boksa P (1993) Brief cortisol exposure elevates adrenal phenylethanolamine N-methyltransferase after a necessary lag period. *European journal of pharmacology* **238**:273-282.

Bignon E, Bachy A, Boigegrain R, Brodin R, Cottineau M, Gully D, Herbert JM, Keane P, Labie C, Molimard JC, Olliero D, Oury-Donat F, Petereau C, Prabonnaud V, Rockstroh MP, Schaeffer P, Servant O, Thurneyssen O, Soubrie P, Pascal M, Maffrand JP and Le Fur G (1999) SR146131: a new potent, orally active, and selective nonpeptide cholecystokinin subtype 1 receptor agonist. I. In vitro studies. *J Pharmacol Exp Ther* **289**:742-751.

Bo XN and Burnstock G (1990) High- and low-affinity binding sites for [3H]-alpha, beta-methylene ATP in rat urinary bladder membranes. *British journal of pharmacology* **101**:291-296.

Bonhaus DW, Bach C, DeSouza A, Salazar FH, Matsuoka BD, Zuppan P, Chan HW and Eglen RM (1995) The pharmacology and distribution of human 5-hydroxytryptamine2B (5-HT2B) receptor gene products: comparison with 5-HT2A and 5-HT2C receptors. *British journal of pharmacology* **115**:622-628.

Bowen WD, Tolentino PJ, Kirschner BN, Varghese P, de Costa BR and Rice KC (1993) Sigma receptors and signal transduction: negative modulation of signaling through phosphoinositide-linked receptor systems. *NIDA Res Monogr* **133**:69-93.

Brown CM, MacKinnon AC, McGrath JC, Spedding M and Kilpatrick AT (1990a) Alpha 2-adrenoceptor subtypes and imidazoline-like binding sites in the rat brain. *British journal of pharmacology* **99**:803-809.

Brown GB (1986) 3H-batrachotoxinin-A benzoate binding to voltage-sensitive sodium channels: inhibition by the channel blockers tetrodotoxin and saxitoxin. *J Neurosci* **6**:2064-2070.

Brown PJ, Lee AB, Norman MG, Presky DH and Schonbrunn A (1990b) Identification of somatostatin receptors by covalent labeling with a novel photoreactive somatostatin analog. *J Biol Chem* **265**:17995-18004.

Bryant HU, Nelson DL, Button D, Cole HW, Baez MB, Lucaites VL, Wainscott DB, Whitesitt C, Reel J, Simon R and Koppel GA (1996) A novel class of 5-HT2A receptor antagonists: aryl aminoguanidines. *Life Sci* **59**:1259-1268.

Buchan KW, Alldus C, Christodoulou C, Clark KL, Dykes CW, Sumner MJ, Wallace DM, White DG and Watts IS (1994) Characterization of three non-peptide endothelin receptor ligands using human cloned ETA and ETB receptors. *British journal of pharmacology* **112**:1251-1257.

Childers SR, Creese I, Snowman AM and Synder SH (1979) Opiate receptor binding affected differentially by opiates and opioid peptides. *European journal of pharmacology* **55**:11-18.

Clark AF, Lane D, Wilson K, Miggans ST and McCartney MD (1996) Inhibition of dexamethasone-induced cytoskeletal changes in cultured human trabecular meshwork cells by tetrahydrocortisol. *Invest Ophthalmol Vis Sci* **37**:805-813.

Dontenwill M, Vonthron C, Greney H, Magnier C, Heemskerk F and Bousquet P (1999) Identification of human I1 receptors and their relationship to alpha 2-adrenoceptors. *Ann N Y Acad Sci* **881**:123-134.

Dorje F, Wess J, Lambrecht G, Tacke R, Mutschler E and Brann MR (1991) Antagonist binding profiles of five cloned human muscarinic receptor subtypes. *J Pharmacol Exp Ther* **256**:727-733.

Eckert RL and Katzenellenbogen BS (1982) Effects of estrogens and antiestrogens on estrogen receptor dynamics and the induction of progesterone receptor in MCF-7 human breast cancer cells. *Cancer Res* **42**:139-144.

Ellman GL, Courtney KD, Andres V, Jr. and Feather-Stone RM (1961) A new and rapid colorimetric determination of acetylcholinesterase activity. *Biochem Pharmacol* **7**:88-95.

Felder CC, Joyce KE, Briley EM, Mansouri J, Mackie K, Blond O, Lai Y, Ma AL and Mitchell RL (1995) Comparison of the pharmacology and signal transduction of the human cannabinoid CB1 and CB2 receptors. *Mol Pharmacol* **48**:443-450.

Fiske CH and Subbarow Y (1925) The Colorimetric Determination of Phosphorus. *J Biol Chem* **66**:375 - 400.

Goldstein M, Kusano N, Adler C and Meller E (1986) Characterization of central neuropeptide Y receptor binding sites and possible interactions with alpha 2-adrenoceptors. *Prog Brain Res* **68**:331-335.

Grandy DK, Marchionni MA, Makam H, Stofko RE, Alfano M, Frothingham L, Fischer JB, Burke-Howie KJ, Bunzow JR, Server AC and et al. (1989) Cloning of the cDNA and gene for a human D2 dopamine receptor. *Proc Natl Acad Sci U S A* **86**:9762-9766.

Greengrass P and Bremner R (1979) Binding characteristics of 3H-prazosin to rat brain alpha-adrenergic receptors. *European journal of pharmacology* **55**:323-326.

Hannun YA, Loomis CR and Bell RM (1985) Activation of protein kinase C by Triton X-100 mixed micelles containing diacylglycerol and phosphatidylserine. *J Biol Chem* **260**:10039-10043.

Heuillet E, Menager J, Fardin V, Flamand O, Bock M, Garret C, Crespo A, Fallourd AM and Doble A (1993) Characterization of a human NK1 tachykinin receptor in the astrocytoma cell line U 373 MG. *J Neurochem* **60**:868-876.

Heuring RE and Peroutka SJ (1987) Characterization of a novel 3H-5-hydroxytryptamine binding site subtype in bovine brain membranes. *J Neurosci* **7**:894-903.

Hope AG, Peters JA, Brown AM, Lambert JJ and Blackburn TP (1996) Characterization of a human 5-hydroxytryptamine3 receptor type A (h5-HT3R-AS) subunit stably expressed in HEK 293 cells. *British journal of pharmacology* **118**:1237-1245.

Hoyer D, Engel G and Kalkman HO (1985) Characterization of the 5-HT1B recognition site in rat brain: binding studies with (-)[125I]iodocyanopindolol. *European journal of pharmacology* **118**:1-12.

Hugues M, Duval D, Kitabgi P, Lazdunski M and Vincent JP (1982) Preparation of a pure monoiodo derivative of the bee venom neurotoxin apamin and its binding properties to rat brain synaptosomes. *J Biol Chem* **257**:2762-2769.

Jones C, Phillips E, Davis C, Arbuckle J, Yaqoob M, Burgess GM, Docherty RJ, Webb M, Bevan SJ and McIntyre P (1999) Molecular characterisation of cloned bradykinin B1 receptors from rat and human. *European journal of pharmacology* **374**:423-433.

Lee HR, Roeske WR and Yamamura HI (1984) High affinity specific [3H](+)PN 200-110 binding to dihydropyridine receptors associated with calcium channels in rat cerebral cortex and heart. *Life Sci* **35**:721-732.

Lee YM, Beinborn M, McBride EW, Lu M, Kolakowski LF, Jr. and Kopin AS (1993) The human brain cholecystokinin-B/gastrin receptor. Cloning and characterization. *J Biol Chem* **268**:8164-8169.

Leurs R, Smit MJ, Menge WM and Timmerman H (1994) Pharmacological characterization of the human histamine H2 receptor stably expressed in Chinese hamster ovary cells. *British journal of pharmacology* **112**:847-854.

Levin MC, Marullo S, Muntaner O, Andersson B and Magnusson Y (2002) The myocardium-protective Gly-49 variant of the beta 1-adrenergic receptor exhibits constitutive activity and increased desensitization and down-regulation. *J Biol Chem* **277**:30429-30435.

Lewin AH, de Costa BR, Rice KC and Skolnick P (1989) meta- and para-isothiocyanato-t-butylbicycloorthobenzoate: irreversible ligands of the gamma-aminobutyric acid-regulated chloride ionophore. *Mol Pharmacol* **35**:189-194.

Lindemann L, Jaeschke G, Michalon A, Vieira E, Honer M, Spooren W, Porter R, Hartung T, Kolczewski S, Buttelmann B, Flament C, Diener C, Fischer C, Gatti S, Prinssen EP, Parrott N, Hoffmann G and Wettstein JG (2011) CTEP: a novel, potent, long-acting, and orally bioavailable metabotropic glutamate receptor 5 inhibitor. *J Pharmacol Exp Ther* **339**:474-486.

Loscher W (1981) Effect of inhibitors of GABA aminotransferase on the metabolism of GABA in brain tissue and synaptosomal fractions. *J Neurochem* **36**:1521-1527.

Luthin DR, Olsson RA, Thompson RD, Sawmiller DR and Linden J (1995) Characterization of two affinity states of adenosine A2a receptors with a new radioligand, 2-[2-(4-amino-3-[125I]iodophenyl)ethylamino]adenosine. *Mol Pharmacol* **47**:307-313.

MacKenzie RG, VanLeeuwen D, Pugsley TA, Shih YH, Demattos S, Tang L, Todd RD and O'Malley KL (1994) Characterization of the human dopamine D3 receptor expressed in transfected cell lines. *European journal of pharmacology* **266**:79-85.

Martin V, Sawyer N, Stocco R, Unett D, Lerner MR, Abramovitz M and Funk CD (2001) Molecular cloning and functional characterization of murine cysteinyl-leukotriene 1 (CysLT(1)) receptors. *Biochem Pharmacol* **62**:1193-1200.

Matsuda LA, Lolait SJ, Brownstein MJ, Young AC and Bonner TI (1990) Structure of a cannabinoid receptor and functional expression of the cloned cDNA. *Nature* **346**:561-564.

Mialet J, Berque-Bestel I, Eftekhari P, Gastineau M, Giner M, Dahmoune Y, Donzeau-Gouge P, Hoebeke J, Langlois M, Sicsic S, Fischmeister R and Lezoualc'h F (2000) Isolation of the serotoninergic 5-HT4(e) receptor from human heart and comparative analysis of its pharmacological profile in C6-glial and CHO cell lines. *British journal of pharmacology* **129**:771-781.

Monaghan DT and Cotman CW (1982) The distribution of [3H]kainic acid binding sites in rat CNS as determined by autoradiography. *Brain Res* **252**:91-100.

Monsma FJ, Jr., Shen Y, Ward RP, Hamblin MW and Sibley DR (1993) Cloning and expression of a novel serotonin receptor with high affinity for tricyclic psychotropic drugs. *Mol Pharmacol* **43**:320-327.

Mulheron JG, Casanas SJ, Arthur JM, Garnovskaya MN, Gettys TW and Raymond JR (1994) Human 5-HT1A receptor expressed in insect cells activates endogenous G(o)-like G protein(s). *J Biol Chem* **269**:12954-12962.

Muller-Enoch D, Seidl E and Thomas H (1976) [6.7-Dihydroxycoumarin (Aesculetin) as a substrate for catechol-o-methyltransferase (author's transl)]. *Z Naturforsch C* **31**:280-284.

Munro S, Thomas KL and Abu-Shaar M (1993) Molecular characterization of a peripheral receptor for cannabinoids. *Nature* **365**:61-65.

Murphy DE, Snowhill EW and Williams M (1987) Characterization of quisqualate recognition sites in rat brain tissue using DL-[3H]alpha-amino-3-hydroxy-5-methylisoxazole-4-propionic acid (AMPA) and a filtration assay. *Neurochem Res* **12**:775-781.

Nagatsu T, Levitt M and Udenfriend S (1964) A Rapid and Simple Radioassay for Tyrosine Hydroxylase Activity. *Anal Biochem* **9**:122-126.

Nicholson CD, Jackman SA and Wilke R (1989) The ability of denbufylline to inhibit cyclic nucleotide phosphodiesterase and its affinity for adenosine receptors and the adenosine re-uptake site. *British journal of pharmacology* **97**:889-897.

Okuyama S, Chaki S, Kawashima N, Suzuki Y, Ogawa S, Nakazato A, Kumagai T, Okubo T and Tomisawa K (1999) Receptor binding, behavioral, and electrophysiological profiles of nonpeptide corticotropin-releasing factor subtype 1 receptor antagonists CRA1000 and CRA1001. *J Pharmacol Exp Ther* **289**:926-935.

Pabreza LA, Dhawan S and Kellar KJ (1991) [3H]cytisine binding to nicotinic cholinergic receptors in brain. *Mol Pharmacol* **39**:9-12.

Pacholczyk T, Blakely RD and Amara SG (1991) Expression cloning of a cocaine- and antidepressant-sensitive human noradrenaline transporter. *Nature* **350**:350-354.

Peralta EG, Ashkenazi A, Winslow JW, Smith DH, Ramachandran J and Capon DJ (1987) Distinct primary structures, ligand-binding properties and tissue-specific expression of four human muscarinic acetylcholine receptors. *Embo J* **6**:3923-3929.

Peroutka SJ and Snyder SH (1979) Multiple serotonin receptors: differential binding of [3H]5-hydroxytryptamine, [3H]lysergic acid diethylamide and [3H]spiroperidol. *Mol Pharmacol* **16**:687-699.

Porter RH, Jaeschke G, Spooren W, Ballard TM, Buttelmann B, Kolczewski S, Peters JU, Prinssen E, Wichmann J, Vieira E, Muhlemann A, Gatti S, Mutel V and Malherbe P (2005) Fenobam: a clinically validated nonbenzodiazepine anxiolytic is a potent, selective, and noncompetitive mGlu5 receptor antagonist with inverse agonist activity. *J Pharmacol Exp Ther* **315**:711-721.

Pristupa ZB, Wilson JM, Hoffman BJ, Kish SJ and Niznik HB (1994) Pharmacological heterogeneity of the cloned and native human dopamine transporter: disassociation of [3H]WIN 35,428 and [3H]GBR 12,935 binding. *Mol Pharmacol* **45**:125-135.

Pruneau D, Luccarini JM, Fouchet C, Defrene E, Franck RM, Loillier B, Duclos H, Robert C, Cremers B, Belichard P and Paquet JL (1998) LF 16.0335, a novel potent and selective nonpeptide antagonist of the human bradykinin B2 receptor. *British journal of pharmacology* **125**:365-372.

Rees S, den Daas I, Foord S, Goodson S, Bull D, Kilpatrick G and Lee M (1994) Cloning and characterisation of the human 5-HT5A serotonin receptor. *FEBS Lett* **355**:242-246.

Reynolds IJ, Snowman AM and Snyder SH (1986) (-)-[3H] desmethoxyverapamil labels multiple calcium channel modulator receptors in brain and skeletal muscle membranes: differentiation by temperature and dihydropyridines. *J Pharmacol Exp Ther* **237**:731-738.

Richards MH (1990) Rat hippocampal muscarinic autoreceptors are similar to the M2 (cardiac) subtype: comparison with hippocampal M1, atrial M2 and ileal M3 receptors. *British journal of pharmacology* **99**:753-761.

Ross RA, Brockie HC, Stevenson LA, Murphy VL, Templeton F, Makriyannis A and Pertwee RG (1999) Agonist-inverse agonist characterization at CB1 and CB2 cannabinoid receptors of L759633, L759656, and AM630. *British journal of pharmacology* **126**:665-672.

Salomon Y, Londos C and Rodbell M (1974) A highly sensitive adenylate cyclase assay. *Anal Biochem* **58**:541-548.

Salvatore CA, Jacobson MA, Taylor HE, Linden J and Johnson RG (1993) Molecular cloning and characterization of the human A3 adenosine receptor. *Proc Natl Acad Sci U S A* **90**:10365-10369.

Schioth HB, Muceniece R and Wikberg JE (1997) Characterization of the binding of MSH-B, HB-228, GHRP-6 and 153N-6 to the human melanocortin receptor subtypes. *Neuropeptides* **31**:565-571.

Schoemaker H and Langer SZ (1985) [3H]diltiazem binding to calcium channel antagonists recognition sites in rat cerebral cortex. *European journal of pharmacology* **111**:273-277.

Shank RP, Baldy WJ, Mattucci LC and Villani FJ, Jr. (1990) Ion and temperature effects on the binding of gamma-aminobutyrate to its receptors and the high-affinity transport system. *J Neurochem* **54**:2007-2015.

Sharif NA and Burt DR (1983) Rat brain TRH receptors: kinetics, pharmacology, distribution and ionic effects. *Regul Pept* **7**:399-411.

Sheen YY, Ruh TS, Mangel WF and Katzenellenbogen BS (1985) Antiestrogenic potency and binding characteristics of the triphenylethylene H1285 in MCF-7 human breast cancer cells. *Cancer Res* **45**:4192-4199.

Shen Y, Monsma FJ, Jr., Metcalf MA, Jose PA, Hamblin MW and Sibley DR (1993) Molecular cloning and expression of a 5-hydroxytryptamine7 serotonin receptor subtype. *J Biol Chem* **268**:18200-18204.

Shirayama Y, Nishikawa T, Umino A and Takahashi K (1993) p-chlorophenylalanine-reversible reduction of sigma binding sites by chronic imipramine treatment in rat brain. *European journal of pharmacology* **237**:117-126.

Sills MA, Fagg G, Pozza M, Angst C, Brundish DE, Hurt SD, Wilusz EJ and Williams M (1991) [3H]CGP 39653: a new N-methyl-D-aspartate antagonist radioligand with low nanomolar affinity in rat brain. *European journal of pharmacology* **192**:19-24.

Simon J, Webb TE and Barnard EA (1995) Characterization of a P2Y purinoceptor in the brain. *Pharmacol Toxicol* **76**:302-307.

Smit MJ, Timmerman H, Hijzelendoorn JC, Fukui H and Leurs R (1996) Regulation of the human histamine H1 receptor stably expressed in Chinese hamster ovary cells. *British journal of pharmacology* **117**:1071-1080.

Smith C and Teitler M (1999) Beta-blocker selectivity at cloned human beta 1- and beta 2-adrenergic receptors. *Cardiovasc Drugs Ther* **13**:123-126.

Sorensen RG and Blaustein MP (1989) Rat brain dendrotoxin receptors associated with voltage-gated potassium channels: dendrotoxin binding and receptor solubilization. *Mol Pharmacol* **36**:689-698.

Speth RC, Wastek GJ and Yamamura HI (1979) Benzodiazepine receptors: temperature dependence of [3H]flunitrazepam binding. *Life Sci* **24**:351-357.

Suman-Chauhan N, Grimson P, Guard S, Madden Z, Chung FZ, Watling K, Pinnock R and Woodruff G (1994) Characterisation of [125I][MePhe7]neurokinin B binding to tachykinin NK3 receptors: evidence for interspecies variance. *European journal of pharmacology* **269**:65-72.

Tahara A, Saito M, Sugimoto T, Tomura Y, Wada K, Kusayama T, Tsukada J, Ishii N, Yatsu T, Uchida W and Tanaka A (1998) Pharmacological characterization of the human vasopressin receptor subtypes stably expressed in Chinese hamster ovary cells. *British journal of pharmacology* **125**:1463-1470.

Tatsumi M, Jansen K, Blakely RD and Richelson E (1999) Pharmacological profile of neuroleptics at human monoamine transporters. *European journal of pharmacology* **368**:277-283.

Torphy TJ, Zhou HL and Cieslinski LB (1992) Stimulation of beta adrenoceptors in a human monocyte cell line (U937) up-regulates cyclic AMP-specific phosphodiesterase activity. *J Pharmacol Exp Ther* **263**:1195-1205.

Townsend-Nicholson A and Schofield PR (1994) A threonine residue in the seventh transmembrane domain of the human A1 adenosine receptor mediates specific agonist binding. *J Biol Chem* **269**:2373-2376.

Tsuji A, Sato H, Kume Y, Tamai I, Okezaki E, Nagata O and Kato H (1988) Inhibitory effects of quinolone antibacterial agents on gamma-aminobutyric acid binding to receptor sites in rat brain membranes. *Antimicrob Agents Chemother* **32**:190-194.

Tsuzuki S, Ichiki T, Nakakubo H, Kitami Y, Guo DF, Shirai H and Inagami T (1994) Molecular cloning and expression of the gene encoding human angiotensin II type 2 receptor. *Biochem Biophys Res Commun* **200**:1449-1454.

Uebelhack R, Franke L and Schewe HJ (1998) Inhibition of platelet MAO-B by kava pyrone-enriched extract from Piper methysticum Forster (kava-kava). *Pharmacopsychiatry* **31**:187-192.

Uhlen S and Wikberg JE (1991) Rat spinal cord alpha 2-adrenoceptors are of the alpha 2A-subtype: comparison with alpha 2A- and alpha 2B-adrenoceptors in rat spleen, cerebral cortex and kidney using 3H-RX821002 ligand binding. *Pharmacol Toxicol* **69**:341-350.

Van Tol HH, Wu CM, Guan HC, Ohara K, Bunzow JR, Civelli O, Kennedy J, Seeman P, Niznik HB and Jovanovic V (1992) Multiple dopamine D4 receptor variants in the human population. *Nature* **358**:149-152.

Vickroy TW, Roeske WR and Yamamura HI (1984) Sodium-dependent high-affinity binding of [3H]hemicholinium-3 in the rat brain: a potentially selective marker for presynaptic cholinergic sites. *Life Sci* **35**:2335-2343.

Vignon J, Privat A, Chaudieu I, Thierry A, Kamenka JM and Chicheportiche R (1986) [3H]thienyl-phencyclidine ([3H]TCP) binds to two different sites in rat brain. Localization by autoradiographic and biochemical techniques. *Brain Res* **378**:133-141.

Weishaar RE, Burrows SD, Kobylarz DC, Quade MM and Evans DB (1986) Multiple molecular forms of cyclic nucleotide phosphodiesterase in cardiac and smooth muscle and in platelets. Isolation, characterization, and effects of various reference phosphodiesterase inhibitors and cardiotonic agents. *Biochem Pharmacol* **35**:787-800.

Weyler W and Salach JI (1985) Purification and properties of mitochondrial monoamine oxidase type A from human placenta. *J Biol Chem* **260**:13199-13207.

Wolin MS, Wood KS and Ignarro LJ (1982) Guanylate cyclase from bovine lung. A kinetic analysis of the regulation of the purified soluble enzyme by protoporphyrin IX, heme, and nitrosyl-heme. *J Biol Chem* **257**:13312-13320.

Zava DT, Landrum B, Horwitz KB and McGuire WL (1979) Androgen receptor assay with [3H]methyltrienolone (R1881) in the presence of progesterone receptors. *Endocrinology* **104**:1007-1012.

Zhou QY, Grandy DK, Thambi L, Kushner JA, Van Tol HH, Cone R, Pribnow D, Salon J, Bunzow JR and Civelli O (1990) Cloning and expression of human and rat D1 dopamine receptors. *Nature* **347**:76-80.